

**Concepts for the
Analysis of Very Small Samples
and
Fast Capillary Electrophoresis
Coupled to Mass Spectrometry**



Dissertation zur Erlangung des
Doktorgrades der Naturwissenschaften (Dr. rer. nat.)
der Fakultät Chemie und Pharmazie
der Universität Regensburg

vorgelegt von Marco Grundmann aus Karl-Marx-Stadt (jetzt Chemnitz)

im Jahr 2012

Diese Dissertation entstand in der Zeit von November 2008 bis Mai 2012 am Institut für analytische Chemie, Chemo- und Biosensorik der Fakultät Chemie und Pharmazie der Universität Regensburg.

Die Arbeit wurde angeleitet von Prof. Dr. Frank-Michael Matysik.

Die Arbeit ist in englischer Sprach verfasst. Der deutsche Titel dieser Arbeit lautet „Konzepte für die Analyse sehr kleiner Probemengen und schnelle Kapillarelektrophorese in Kopplung mit der Massenspektrometrie“. Eine Zusammenfassung in deutscher Sprache ist in Kapitel 7 (S. 94 ff.) zu finden.

Das Promotionsgesuch wurde am 25. Mai 2012 eingereicht.

Das Kolloquium fand am 9. Juli 2012 statt.

Dem Prüfungsausschuss saß Prof. Dr. Joachim Wegener vor. Erster Gutachter war Prof. Dr. Frank-Michael Matysik, zweiter Gutachter war Prof. Dr. Otto S. Wolfbeis, dritter Prüfer war Prof. Dr. Günther Bernhardt.

Concepts for the
Analysis of Very Small Samples
and
Fast Capillary Electrophoresis
Coupled to Mass Spectrometry

Doctoral Thesis

by

Marco Grundmann

Ich möchte mich bei all jenen herzlich bedanken, die mich auf meinem Weg zur Promotion unterstützt und gefördert haben.

I would like to thank each and every one of the people involved in helping and supporting me en route to my doctorate.

“Curiously enough, the only thing that went through the mind of the bowl of petunias as it fell was

Oh no, not again.

Many people have speculated that if we knew exactly why the bowl of petunias had thought that we would know a lot more about the nature of the Universe than we do now.”¹

¹ Douglas Adams (1979) *The Hitchhiker’s Guide to the Galaxy*. Arthur Barker, London

Table of Contents

Curriculum Vitae	v
Publications	vi
Peer-reviewed Journal Articles	vi
Other Articles.....	vii
Oral Presentations.....	vii
Poster Presentations	viii
Declaration of Collaborations	ix
Abbreviations	xi
1 Background.....	1
1.1 Capillary Electrophoresis.....	1
1.1.1 Principle of Separation.....	1
1.1.2 Fast CE	3
1.2 Mass Spectrometry	5
1.2.1 Principle of Operation	5
1.2.2 Ionisation.....	6
1.3 Capillary Electrophoresis–Mass Spectrometry.....	8
1.4 Modern Injection Concepts for CE.....	10
1.5 Capillary Batch Injection	11
1.6 Model Systems.....	12
1.6.1 Catecholamines.....	12
1.6.2 Hyaluronan and its Oligomeres	12
1.6.3 Organotin Compounds.....	14
1.6.4 Organoarsenic Compounds.....	14
2 Motivation.....	15
2.1 Why Fast CE–MS?.....	15
2.2 Why Novel Injection Methods?.....	17

3	Experimental	18
3.1	Chemicals and Materials.....	18
3.2	Instrumentation	20
3.3	Software	21
3.4	Methods	22
3.4.1	Sample Collection and Preparation.....	22
3.4.2	Manual Sample Injection Technique	23
3.4.3	Cooling of Separation Capillary	25
3.4.4	Microscopic Investigation of Electrospray	26
3.4.5	Preparation of Capillary Seal.....	28
3.5	CE Method Development.....	29
3.5.1	EOF Marker.....	29
3.6	MS Method Development	31
3.6.1	General Approach	31
3.6.2	ESI Interface.....	31
3.6.3	Ion Optics	31
3.6.4	Mass Trace Selection	32
3.6.5	Mass Calibration.....	32
3.7	Experimental Setup for Capillary Batch Injection.....	34
3.7.1	Initial Tests	34
3.7.2	Main Setup	36
3.8	Control Software for Capillary Batch Injection.....	40
3.8.1	General.....	40
3.8.2	User Interface	40
3.8.3	Program Structure.....	44

4	Fast Capillary Electrophoresis–Mass Spectrometry	46
4.1	Method Development	46
4.1.1	Optimisation of ESI Parameters	46
4.1.2	Fast CE–MS Separations	50
4.1.3	Advantages and Disadvantages of Small ID Capillaries	51
4.1.4	Conclusions	55
4.2	Application to Hyaluronan Oligomers	56
4.2.1	Capillary Length	56
4.2.2	Capillary ID	57
4.2.3	BGE Composition	59
4.2.4	Optimised Method Parameters	60
4.2.5	Application to Hyaluronan Digest Analysis	62
4.2.6	Application to the Analysis of a Complex Sample	63
4.2.7	Conclusions	65
4.3	Application to Organotin Speciation	66
4.3.1	CE–UV Method Development	66
4.3.2	Optimisation of MS Parameters	67
4.3.3	CE–MS Method Development	69
4.3.4	CE–MS Method Evaluation	70
4.3.5	Application to River Water Samples	70
4.3.6	Conclusions	72
4.4	Application to Organoarsenic Speciation	73
4.4.1	Comparison of Aqueous and Non-aqueous BGEs	73
4.4.2	Pressure-assisted (Very) Fast CE–MS	73
4.4.3	BGE Optimisation	74
4.4.4	Conclusions	75

5	Capillary Batch Injection	76
5.1	Initial Tests.....	76
5.1.1	Injection Environment	76
5.1.2	Delivery of Sample Solution	76
5.1.3	Alignment of Capillaries.....	77
5.2	General Considerations for the Injection Process.....	79
5.3	Sequence of Events for an Injection Process.....	81
5.4	Optimisation of Injection Process.....	83
5.5	100% Injection Efficiency	86
5.6	Analytical Characterisation	88
5.7	Very Fast CE–MS.....	89
5.8	Conclusions.....	90
6	Summary	91
6.1	Fast Capillary Electrophoresis–Mass Spectrometry	91
6.2	Small Samples.....	92
7	Zusammenfassung	94
7.1	Schnelle Kapillarelektrophorese–Massenspektrometrie	94
7.2	Kleine Probemengen	95
8	References	97
9	Appendix	102
9.1	Schematics.....	102
9.1.1	Adapter Piece for Cooling of Separation Capillary	102
9.1.2	x,y-Positioner	103
9.2	Complex Hyaluronan Sample.....	106

Curriculum Vitae

Personal Details

Full Name	Marco Grundmann
Date and place of birth	6 th May 1984 in Karl-Marx-Stadt (now Chemnitz)
Nationality	German
Spoken languages	German (native speaker), English (C1: effective operational proficiency)

Education

Degree	Institution	Subjects	Period	Mark
PhD	University of Regensburg	Analytical Chemistry	2008–2012	
Master of Science	University of Leipzig	Chemistry (focus on Analytical Chemistry)	2006–2008	1.5 ("very good")
	Dublin City University, Ireland	Analytical Chemistry, Environmental Science and Health	2006–2007	(part of Masters)
Bachelor of Science	University of Leipzig	Chemistry	2003–2006	2.0 ("good")
Abitur	Johannes-Kepler-Gymnasium Chemnitz	Special subjects: Maths, Chemistry, English	1994–2002	1.8 ("very good")

Scientific Stays Abroad

- Dublin, Ireland: 1 year. Erasmus exchange during Master's Degree.
- Patiala, India: 2 months. Exchange with cooperating research group of Prof. A. K. Malik.

Other Research Experience

- **Research Assistant** with Dr. med. Mario Bauer at the Helmholtz Centre for Environmental Research (UFZ) in Leipzig. Research topic: SPE, MEPS and HPLC-FD method development for stereospecific determination of metabolites of carcinogenic polycyclic aromatic hydrocarbons and their metabolites.
- **Research Assistant** with Prof. Brett Paull at the School of Chemical Sciences of Dublin City University (DCU). Research topic: Development of a new student lab course in pharmaceutical analysis

Publications

Peer-reviewed Journal Articles

Concepts and results reported on in this thesis have also been published in the following peer-reviewed journal articles.

M. Grundmann, F.-M. Matysik (2011) Fast capillary electrophoresis–time-of-flight mass spectrometry using capillaries with inner diameters ranging from 75 to 5 μm . *Anal Bioanal Chem* 400:269–278

M. Grundmann, M. Rothenhöfer, G. Bernhardt, A. Buschauer, F.-M. Matysik (2011) Fast counter-electroosmotic capillary electrophoresis–time-of-flight mass spectrometry of hyaluronan oligosaccharides. *Anal Bioanal Chem* DOI: 10.1007/s00216–011–5254–2

C. Niegel, S.A. Pfeiffer, **M. Grundmann**, U. Arroyo-Abad, J. Mattusch, F.-M. Matysik (2012) Fast separations by capillary electrophoresis hyphenated to electrospray ionisation time-of-flight mass spectrometry as a tool for arsenic speciation analysis. *Analyst* DOI: 10.1039/C2AN15944A

M. Grundmann, F.-M. Matysik (2012) Analyzing Small Samples with High Efficiency: Capillary Batch Injection–Capillary Electrophoresis–Mass Spectrometry. (submitted)

A. K. Malik, **M. Grundmann**, F.-M. Matysik (2012) Development of a fast capillary electrophoresis-time-of-flight mass spectrometry method for the speciation of organotin compounds under separation conditions of high electrical field strengths. (submitted)

M. Rothenhöfer, **M. Grundmann**, G. Bernhardt, F.-M. Matysik A. Buschauer (2012) High performance anion exchange chromatography using pulsed amperometric detection (HPAEC–PAD) for monitoring hyaluronan cleavage by bovine testicular hyaluronidase and hyaluronate lyase from *Streptococcus agalactiae*. (in preparation)

Other Articles

F.-M. Matysik, **M. Grundmann** (2010) Schnelle elektrophoretische Trennungen in kurzen Kapillaren. GIT 3:206

M. Grundmann, F.-M. Matysik (2011) CE ergänzt HPLC: Kapillarelektrophorese-Massenspektrometrie. Nachrichten aus der Chemie 59:1081–1083

Oral Presentations

“CE–ESI–TOF–MS: Fast Separations in Short Capillaries with Small Inner Diameters”

M. Grundmann and F.-M. Matysik.

Presented at the CE-Forum 2010 in Jülich, Germany

“Capillary Electrophoresis Coupled to Time-of-Flight Mass Spectrometry: Fast Separations in Short Capillaries with Small Inner Diameters”

M. Grundmann and F.-M. Matysik.

Presented at the ANAKON 2011 in Zürich, Switzerland

“Injection Efficiency for Capillary Electrophoresis–Mass Spectrometry”

M. Grundmann and F.-M. Matysik.

Presented at the Ph.D. Student Seminar of the GDCh’s AK Separation Science 2012, Hohenroda, Germany. (Awarded 1st price)

“Improving Injection Efficiency in Capillary Electrophoresis: Approaches for Fast CE–MS and (Very) Small Samples”

M. Grundmann and F.-M. Matysik.

Presented at the Chebana Winter School 2012, Barcelona, Spain. (Invited keynote)

Poster Presentations

“Exotic Monoliths for Separation Science and Beyond: Gold nano-layer coated silica monoliths”

M. Grundmann, Z. Walsh, S. Abele, B. S. O’Connell, F.-Q. Nie, B. Paull and M. Macka.

Presented at the HPLC 2007 in Gent, Belgium.

“Characterisation of Mixed Phase Micro-Extraction by Packed Sorbent (MEPS) Materials Based on Sub-micromolar Serotonin Determination in Plasma Using HPLC-Electrochemical Detection”

M. Grundmann and F.-M. Matysik.

Presented at the Analytical Research Forum 2008 in Kingston Upon Hull, UK.

“How Small Can Solid Phase Extraction Go? – Characterisation and Application of Micro-Extraction by Packed Sorbent (MEPS) Materials”

M. Grundmann, S. Matysik, M. Bauer and F.-M. Matysik.

Presented at the 2nd EuCheMS Congress 2008 in Torino, Italy.

“Coupling Capillary Electrophoresis to Time-of-Flight Mass Spectrometry – Achieving Fast Separations in Capillaries”

M. Grundmann, M. Rothenhöfer, G. Bernhardt, A. Buschauer and F.-M. Matysik.

Presented at Wissenschaftsforum Chemie 2011, Bremen, Germany.

“Capillary Batch Injection – Improving Injection Efficiency in CE”

M. Grundmann and F.-M. Matysik.

Presented at CE-Forum 2011 in Regensburg, Germany.

“Improving Injection Efficiency in Capillary Electrophoresis: Approaches for Fast CE–MS and (Very) Small Samples”

M. Grundmann and F.-M. Matysik.

Presented at the HPLC 2012, Anaheim, USA.

Declaration of Collaborations

Most theoretical and experimental work presented in this thesis was carried out solely by the author. Some of the results, however, were obtained in collaboration with other researchers and individuals. In accordance with § 8 Abs. 1 Satz 2 Punkt 7 of the *Ordnung zum Erwerb des akademischen Grades eines Doktors der Naturwissenschaften (Dr. rer. nat.) an der Universität Regensburg vom 18. Juni 2009*, this section details the nature of these collaborations. This list is sorted by subject areas and states the sections to which each declaration refers in brackets.

Fast CE–MS of catecholamines (section 4.1). This work was carried out solely by the author.

Fast CE–MS of hyaluronan oligomeres (sections 3.4.1 and 4.2). This work was carried out in collaboration with Martin Rothenhöfer as follows. Experimental work for CE–MS method development and subsequent data evaluation were carried out largely by the author. Sample selection and preparation were carried out by Martin Rothenhöfer. Conceptual experimental design and interpretation of results were carried out in equal parts by Martin Rothenhöfer and the author.

Fast CE–MS of organotin compounds (sections 3.4.1 and 4.3). This work was carried out in collaboration with Ashok Kumar Malik. Initial CE–UV method development was carried out by Ashok Kumar Malik. Sample collection and preparation were carried out by Ashok Kumar Malik. CE–MS method development and CE–MS measurements were carried out by the author. Data evaluation and interpretation of results obtained with CE–MS were carried out by the author.

Fast CE–MS of organoarsenic compounds (section 4.4). This work was carried out in collaboration with Simon Pfeiffer and Claudia Niegel. CE–MS method development was carried out by Simon Pfeiffer within the scope of his Bachelor thesis under the author's guidance, and continued by Claudia Niegel.

Capillary batch injection (sections 3.7, 3.8 and 5). Setting of the specifications for and design of the experiment, selection of suitable components and materials, and mechanical design of new components was carried out by the author. Production of new components was done by the mechanical workshop according to technical drawings created by the author. The glass cell and the glass capillary sleeve were fabricated by the glass workshop. The electronic workshop assisted in design, and performed the production of an auxiliary circuit board. Assembly, test and modification of the experimental setup were carried out by the author. The control software for the setup was designed and written by the author. All experiments as well as subsequent data analysis and evaluation were conducted by the author.

Abbreviations

AsB	Arsenobetaine
AsC	Arsenocholine
BGE	Background electrolyte
BSA	Bovine serum albumin
BTH	Bovine testicular hyaluronidase
CBI	Capillary batch injection
CE	Capillary electrophoresis
DBT	Dibutyltin
DMSO	Dimethyl sulfoxide
DPT	Diphenyltin
EOF	Electroosmotic flow
ESI	Electrospray ionisation
HPLC	High performance liquid chromatography
HT	High throughput
ID	Inner diameter
LC	Liquid chromatography
LOD	Limit of detection
MS	Mass spectrometry
m/z	Mass-to-charge ratio
NH ₄ OAc	Ammonium acetate
RSD	Relative standard deviation
SPE	Solid phase extraction
TBT	Tributyltin
TOF-MS	Time-of-flight mass spectrometry
TPT	Triphenyltin

1 Background

1.1 Capillary Electrophoresis

1.1.1 Principle of Separation

As a separation method in the liquid phase, capillary electrophoresis (CE) is based on a vastly different principle than liquid chromatography (LC). While LC relies on phase equilibria between a liquid mobile and a solid stationary phase, CE separates analytes in an electric field. The necessary requirement for this separation principle is that in order for the analytes to be separated, they must carry a net charge under the separation conditions employed. On the one hand, this limits CE in its applicability to mostly polar analytes. On the other hand, for those analytes for which CE can be used as a separation method, it offers a great deal of freedom in method development, since the net charge of molecules can be tuned very precisely by adjusting the composition of the background electrolyte (BGE).

Analytes migrate relative to their starting position in the capillary. The velocity (u_p) at which they move is proportional to their electrophoretic mobility (μ_p) and the strength of the electric field (E).

$$u_p = \mu_p E$$

The electrophoretic mobility is proportional to the analytes' net charge (z). Its absolute value influences the strength and its sign decides the direction of movement, towards either the cathode or the anode. The electrophoretic mobility is inversely proportional to the viscosity of the BGE (η) and their Stokes radius in the BGE (r).

$$\mu_p = \frac{z}{6\pi\eta r}$$

Temperature (T) and diffusion coefficient (D) of the analytes influence their Stokes radius.

$$r = \frac{k_B T}{6\pi\eta D}$$

In summary, the analytes' electrophoretic mobility is caused by their net charge, and influenced by their size and shape, as well as the BGE in which the separation is conducted.

Separation efficiency in CE is often represented by the number of theoretical plates N . The analogy to phase equilibria in LC is fundamentally flawed, but helpful in representing the parameters that influence separation efficiency. Most importantly, separation efficiency is directly proportional to the electric field strength.

$$N = \frac{\mu_p E}{2D}$$

The second effect that influences analyte migration in CE is the electroosmotic flow (EOF). The acidity of the capillary material, typically fused silica, causes the formation of layers of oppositely charged ions at the very outside of the BGE solution. This creates a locally concentrated sheath of ions around the rest of the BGE solution inside the capillary. When it is subjected to the electric field, it experiences a force towards the oppositely charged electrode and drags the bulk BGE solution with it. This leads to a plug-shaped flow profile in CE, in contrast to the bullet-shaped flow profile in LC. Methods exist to modify the EOF, specifically to increase or decrease it, eliminate it, or reverse its direction, by means of transient or permanent modification of the capillary surface.

When the direction of analyte migration is opposite to the direction of the EOF, the situation is termed counter-electroosmotic. The reverse is termed co-electroosmotic, in which both movements follow the same direction. Typically, the EOF velocity is stronger than the analytes' migration velocity, which even causes counter-electroosmotically migrating analytes to have a net movement in the same direction as the EOF. The EOF can be seen as moving the analytes' starting point. A non-charged substance (EOF marker) can be included in samples in order to mark the passing of this point in electropherograms recorded.

CE has the ability to achieve higher separation efficiencies than LC mainly for two reasons. Firstly, it does not rely on mass transfer between two phases, the main time-limiting factor in LC. Secondly, the flow in a CE capillary is plug-shaped as opposed to the bullet-shaped flow in the pressure-driven LC systems. Both effects are the main contributors to band broadening in LC. With these advantages on the one hand and the limitations of its applicability on the other hand in mind, CE can be seen as a complimentary technique to LC in the analytical lab.

A more detailed discussion of theory, instrumentation, and applications of CE can be found in numerous monographs. [1-7]

1.1.2 Fast CE

Typical CE protocols require analysis times between 10 and 30 min. CE analyses are particularly time-consuming when the analytes of interest are negatively charged under normal (cathodic) (EOF) conditions. In this counter-electroosmotic migration situation, analysis times lie between 30 and 60 min.

When considering those parameters in CE that influence total separation times the most, fast separations can be accomplished by either applying high electric field strengths or shortening the separation pathway. Successful application of very high electric field strengths (up to $2\text{ kV}\cdot\text{cm}^{-1}$) has been shown, [8-11] but is made difficult to implement by the great deal of insulation and shielding required. Use of short separation pathways has found widespread use in the field of microchip electrophoresis, [12] but a number of examples can be found using fused silica capillaries as well. [13-20] Classical capillaries have various advantages over microchips: High quality fused silica capillary material is commercially available at low a cost in a wide range of outer and inner diameters, both its long-term stability and surface chemistry are well-studied, [21,22] and it can be easily cut down to the length needed for a specific separation problem. Microchips on the other hand are costly, fabricated using a variety of techniques resulting in lab-to-lab reproducibility problems, and have a fixed geometry raising the need to redesign and reproduce the chip when an adjustment in the length of the separation path is needed. Injection and interfacing methods are further challenges, especially when a fast succession in determinations is desirable, as is the case for high-throughput (HT) systems.

With a decrease in separation path length, injected sample volumes become smaller as well. This results in a need for detectors which are sensitive, add little or no dead volume and are able to acquire data at a rapid rate. [23]

The usage of small ID capillaries for CE has been pioneered by Ewing's group [24] in conjunction with amperometric detection. Discovering the advantages of working with greatly reduced injection volumes, this was soon applied to single-cell analyses by the research groups of Ewing, [25-28] Jorgenson, [29] and Yeung. [30] Amperometric detection

has thus far proven to be the most sensitive detection method for use with small ID separation capillaries, [24-27, 31] but recent work on single cells also include the use of CE-MS. [32, 33] Shear's group used pulled capillaries to dramatically increase the local field strength and conduct separations within microseconds [18] by generating photoproducts of analytes within a corresponding capillary segment.

1.2 Mass Spectrometry

1.2.1 Principle of Operation

Many current bioanalytical problems require molecular information obtained from mass spectrometry (MS). In a mass spectrometer, three main processes take place. Firstly, the analytes have to be vaporised and ionised. Secondly, the analytes are separated based on their mass-to-charge (m/z) ratio in the mass analyser. Lastly, the analytes are detected.

Ionisation is of greater importance for the research presented here. It is discussed in more detail in the following section.

A number of different approaches for mass analysers have been developed. In the order of their development, the main types are; sector field, time-of-flight, quadrupole, Fourier transform ion cyclotron resonance, ion trap, and orbitrap. From a technical point of view, they can be divided into instruments that filter certain masses and those that natively record full spectra. From a practical point of view, they vary considerably in technical complexity and, hence, cost. Furthermore, combinations of different mass selection and mass analysing techniques into one instrument exist as well.

Two commonly employed instruments are quadrupole- and time-of-flight-based ones. The former is mostly employed for routine analysis that requires less mass precision, and the latter is typically used where a higher mass precision and a lower limit of detection is needed.

Detection in mass spectrometry is mostly based on electron multiplication upon impact of the ions. Those instruments that analyse ions based on maintained trajectories (fourier transform ion cyclotron resonance and orbitrap), employ non-contact induction as detection principle.

The mass spectrometer employed for the research presented here was a time-of-flight mass spectrometer with an electron multiplication-based microchannel plate detector.

1.2.2 Ionisation

Ionisation techniques can be divided based on the energy they transfer to the analytes in soft and hard ionisation techniques, depending on whether they cause the analytes to fragment considerably during ionisation. From a technical point of view, ionisation techniques can also be divided into continuous and non-continuous methods. When a mass spectrometer is used at the detection end of a flow system, a continuous ionisation technique that both vaporises the stream of liquid and ionises the analytes has to be used. Ionisation techniques that fulfil these criteria include; electrospray ionisation, (atmospheric pressure) chemical ionisation and thermospray ionisation. The most commonly employed one is electrospray ionisation (ESI). It is considered a mild ionisation technique and rarely leads to fragmentation.

In ESI, a strong electrical field applied to the surface of a conductive liquid leads to the formation of a Taylor cone, from which charged droplets separate into a plume. This surface of liquid is the end of the flow system's outlet tubing. The charged droplets are drawn towards the mass spectrometer's orifice by the same electric field that caused their formation. A stream of heated gas (typically nitrogen), which flows towards the droplets, causes solvent evaporation. After reaching a certain charge-per-droplet ratio, Coulomb fission starts. Together with further evaporation, this creates smaller droplets until single molecular ions are present. The exact mechanism of the very last step of ion formation is still under debate. ESI produces both singly and multiply charged ions, depending on the size of the ions. While fragmentation is very rare (if not completely unheard of), adduct formation is often encountered and mostly caused by matrix constituents of the liquid. [34]

In contrast to LC, the effluent from a CE capillary is too small to sustain a normal electrospray. There are two main approaches to overcome this problem. [35] One is to miniaturise the spray itself, creating a nanospray, by either using a drawn, tapered, and conductively coated capillary or coupling the separation capillary via a liquid junction to the ESI needle. [36] The other approach includes the use of a make-up liquid, which both establishes electrical contact between the CE BGE and the shared CE and ESI ground electrode and increases the volume flow rate to create a stable electrospray. The main advantage of sheathless interfaces lies in their higher sensitivity. Complex fabrication procedures, the fragility of the tip as well as problems with electrolysis reactions, however, render them more difficult to use than interfaces using a sheath liquid. [37]

In the design of ESI interfaces using make-up liquids two main approaches have been developed, differing in the location where the make-up liquid is added to the CE effluent. The first is to use a liquid junction that creates a combined solution of CE effluent and make-up liquid, which then enters the ESI needle. [38] In the second approach, all solutions are combined coaxially at the spray tip. In this arrangement, the make-up liquid is termed sheath liquid, since it surrounds the separation capillary and concentrically mixes with the CE effluent. [39] Commercial CE-ESI-MS interfaces employ the latter design and add a nebulizer gas at the tip to aid spray formation. Due to the absence of any coupling between separation capillary and ESI needle, user assembly of the interface is simple and capillaries with any inner diameter (ID) can be used. In the research presented here, an interface of that design was employed.

1.3 Capillary Electrophoresis–Mass Spectrometry

Hyphenation of CE with MS is desirable either when samples contain unknown substances that need to be identified, or when a high degree of certainty as to the analytes' identities is required. CE–MS has become a popular tool as indicated by the number of recent reviews on several application-related subjects within CE–MS method development. [40-43]

The usage of MS detection introduces two limitations to CE method development regarding the possible BGEs that can be applied. Firstly, any BGE constituent should be reasonably volatile. This excludes phosphate- and borate-based buffers, which are typically replaced by formate and acetate. Secondly, surfactants cause problems during the ionisation by largely suppressing small molecules. This prevents the use of most dynamic capillary coatings. Micellar electrokinetic chromatography would seem to be similarly difficult to implement, however there are successful approaches of its hyphenation with MS detection. [44]

Even after considering BGE constraints, the interface between CE and MS must not simply be seen as the joining link between two different instruments, but rather as a third one, which requires some attention during CE–MS method development. [45]

Fig. 1 shows the sheath liquid ESI interface and its location within an experimental setup for CE–MS experiments. The separation capillary's outflow and the sheath liquid mix just before spray formation occurs. The ration at which these two solutions mix leads to a dilution of analytes. This dilution increases with increasing sheath liquid flow rate and decreasing capillary outflow (BGE flow), but most significantly with decreasing separation capillary ID. It is a frequently cited assumption that this dilution of the separation capillary outflow directly leads to a signal decrease in the mass spectrometer.

However, mass spectrometers are not directly sensitive to concentration changes in the solution that enters the ESI interface, but rather to the absolute amount of ions that are formed. Over a wide linear range, this absolute ion count is directly proportional to the concentration of the sprayed and ionised solution as long as all other experimental parameters are kept constant. The addition of a sheath liquid, its flow rate, the separation capillary's outflow, and its ID, however, are parameters that can dramatically influence the spray and ion formation processes at the ESI interface. It is therefore reasonable to assume this will produce a less dramatic dilution effect.

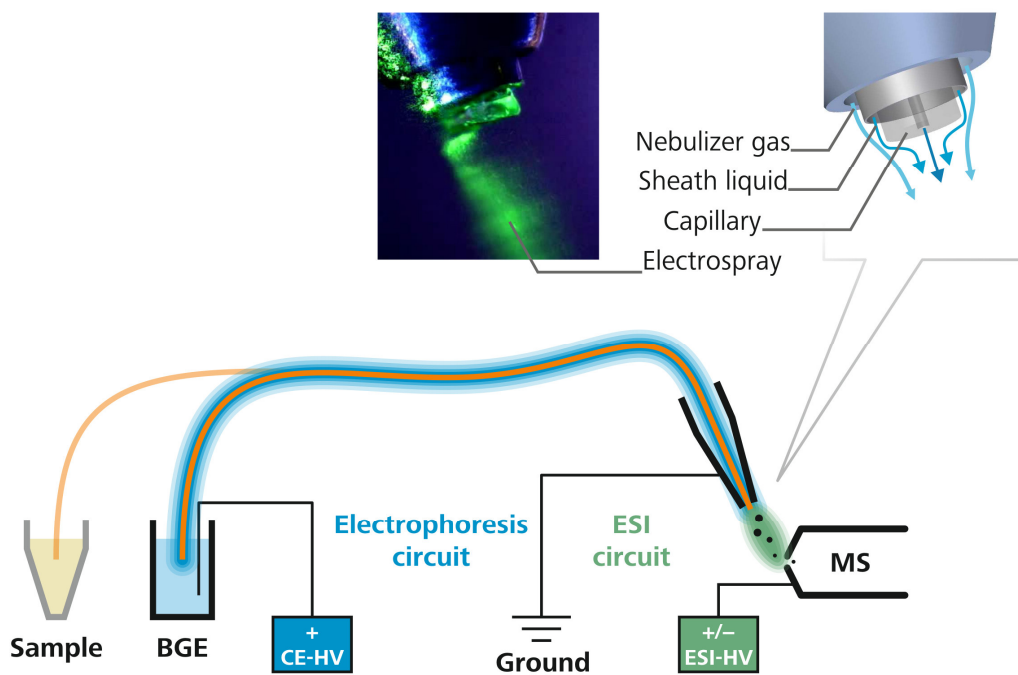


Fig. 1: General setup for a CE-MS experiment. The two different electric circuits (electrophoretic circuit and ESI circuit) are highlighted (blue and green, respectively). The inset details the hydrodynamic situation at the tip of the ESI interface both schematically and through a microphotograph.

The nebulizer gas flow, which mixes with capillary outflow and sheath liquid flow, creates a turbulent hydrodynamic situation at the ESI interface tip. When considering the ESI interface in terms of CE separations, the nebulizer gas flow has a larger influence on the separation performance. Changing the ESI parameters in order to optimise ionisation and MS detection of the target compounds will therefore have an effect on the separation as well, mainly by applying a suction pressure at the capillary end.

Fig. 1 also highlights the combination of the two electric circuits at the ESI interface. Both high voltages circuits of CE and ESI share the tip of the ESI interface. It is therefore of advantage of have the ESI interface as common ground. For positive (negative) ion mode, this requires the mass spectrometer to apply a negative (positive) ESI high voltage to the entrance orifice rather than a positive (negative) high voltage to the ESI interface itself.

1.4 Modern Injection Concepts for CE

Owing to the small capillary dimensions, CE has inherently low injection volumes, typically less than 100 nL.

A number of approaches to reduce the necessary sample volume in CE can be found in the literature. Most of these have been developed originally to use flow injection analysis (FIA) in conjunction with CE, but share the goal to minimise the necessary sample volume. These concepts are: (1) insertion of the separation capillary into the wall of a larger tube carrying sample solution, [46, 47] (2) insertion of the separation capillary into the widened end of a tube carrying sample solution, [48] (3) the so-called H-configuration of a short separation capillary inserted into two tubes, [49] and (4) falling drop interfaces. [50, 51] A detailed discussion and comparison can be found in a review by Opekar et al. [17]

These interfaces differ greatly in design, but share one common disadvantage in relation to very small sample volumes: They were not developed to specifically work with a very small initial sample volume unless this sample is already inside an FIA system. This effectively only moves the actual point of sample introduction from the CE system to the FIA system, where similar limitations regarding injection efficiency hold true as for CE systems. In addition, the introduction of a series of different samples (as opposed to repetitive measurements of the same sample) is difficult with these setups. Compatibility with MS is also a critical issue and only feasible with some of these concepts.

1.5 Capillary Batch Injection

An injection concept for CE separations in short-length capillaries, designed specifically for the direct introduction of very small samples, has been termed capillary batch injection (CBI), [15] and is by design also compatible with MS. Here, the injection end of the separation capillary remains stationary in an injection cell containing the BGE, while a second capillary is positioned facing the separation capillary. The other end of this injection capillary is connected to a microliter syringe, which allows direct movement of sample solutions. The injection takes place in BGE and is accomplished by expelling sample solution onto the separation capillary. Sample solution is then drawn in either by a hydrodynamic flow or electrokinetic injection, after which the CE separation starts.

There are a number of advantages to using a separate capillary for the injection process: Firstly, capillaries of different ID can be used for injection and separation, giving maximum freedom to method development without affecting injection. Secondly, the injection capillary tip shape and geometry can be adjusted to the needs of the injection process, while not having any effect on the separation. Thirdly, any additional equipment needed for precise sampling (e.g., micropositioning devices) can be well separated from the separation capillary, reducing the risk of flashovers. Lastly, keeping the separation capillary immersed in BGE continuously reduces the chance of introducing air bubbles during injection dramatically.

1.6 Model Systems

1.6.1 Catecholamines

The model system consists of the main catecholamines dopamine, epinephrine and norepinephrine, the epinephrine-analogue isoproterenol and histidine. Fig. 2 shows the compounds in the charge state as found in a 0.1 M formic acid solution (pH 2.4) employed as BGE. Histidine would show a deprotonated carboxylic acid group (pK_a 1.82) and both a protonated primary amine group (pK_a 9.17) and protonated imidazole moiety (pK_a 6.04). [52] The pK_a values of the amine groups of dopamine, norepinephrine, and epinephrine are known to be 8.93, 8.55, and 8.58. [53] Isoproterenol has a reported pK_a value of 8.61. [54] All analytes will therefore carry a single positive net charge over a wide pH range, including that of the BGE.

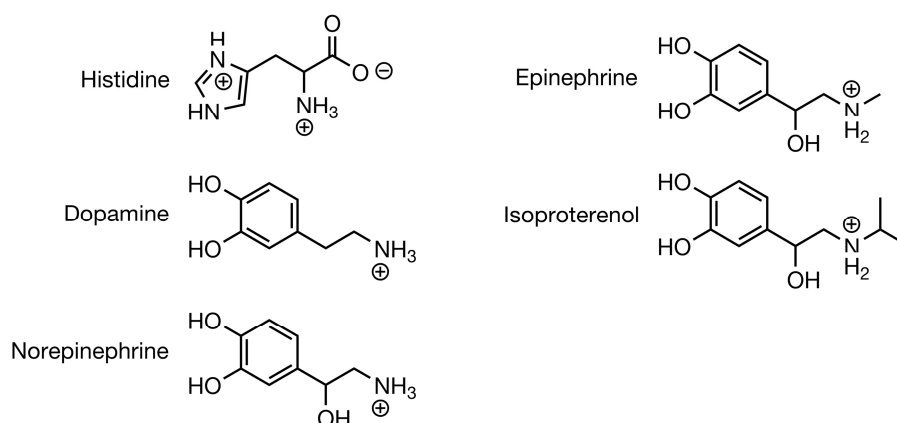


Fig. 2: Structures of the model analytes employed. Charge states given for conditions of the background electrolyte used. The structures are shown in migration order.

1.6.2 Hyaluronan and its Oligomers

Hyaluronan, a major high molecular weight component of the extracellular matrix, is composed of 1→4-linked β -D-glucuronic acid-(1→3)- β -N-acetyl-D-glucosamine disaccharide units. The biopolymer and the corresponding degradation products, oligomers resulting from enzymatic cleavage by hyaluronidases, are supposed to have various size-dependent and, in part, contrary effects on physiological and pathophysiological processes. [55] Effects on tissue regeneration and wound healing, [56, 57] inflammation [58] as well as tumour cell proliferation, invasion, and metastasis [59-61] have been reported. The kinetics

of hyaluronan metabolism is widely unknown due to the lack of fast, selective, and sensitive bioanalytical methods able to monitor the enzymatic degradation of hyaluronan.

Although CE analysis of hyaluronan (high molecular weight polymer) has been reported by Grimshaw et al. in the 1990s, [62, 63] interest in hyaluronan oligosaccharide analysis is more recent. Analytical protocols reported recently employ UV detection and take about 40 min, with an additional 15 min of capillary conditioning. [64, 65] The resulting total analysis time of approximately one hour is prohibitive especially for an enzymological characterisation of hyaluronidases.

Hyaluronan is a biopolymer of glycosaminoglycan structure. The repeating disaccharide unit (hyalobiuronic acid) consists of D-glucuronic acid and D-N-acetylglucosamine. The pK_a of the carboxylic acid groups range between 3 and 4. [66] Fig. 3 shows the monomer unit in its charge state under both physiological and the separation conditions as applied in this study, as well as the three oligosaccharides used for method development. Peak numbering in all electropherograms will refer to the number of monomers, n.

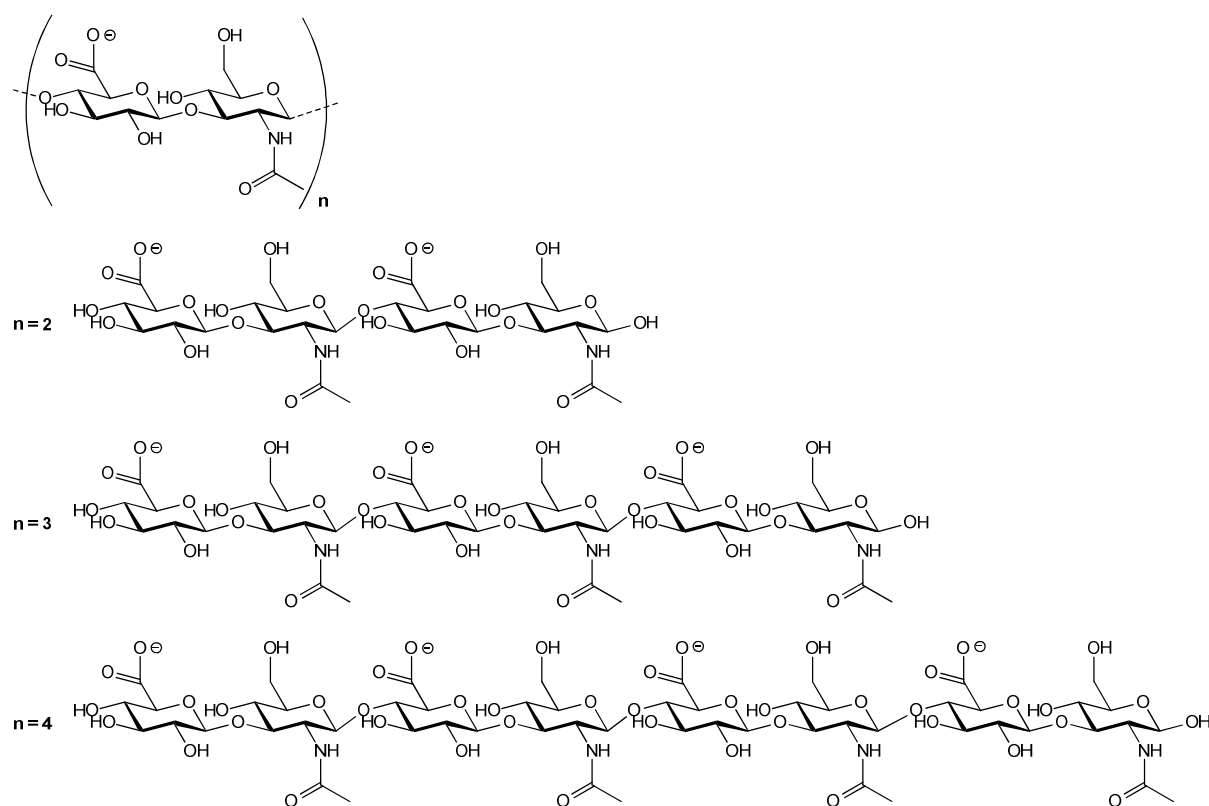


Fig. 3: Structure of hyaluronan oligosaccharides in their charge state under physiological as well as under separation conditions. Peak numbering in all electropherograms will refer to the number of disaccharide units, n.

1.6.3 Organotin Compounds

The presence of organotin compounds in environmental samples is mainly caused by its current or former use in agriculture and industry. Typical areas of usage include antifouling paints, PVC stabilizers, wood preservatives, and pesticides. [67, 68] The total tin content of a given sample is not a useful indicator for its toxicity, since toxicity of organotin compounds strongly varies with the type and degree of substitution. [69, 70] These compounds show a high degree of toxicity especially to marine life, [71] and are prone to bioaccumulation. [68]

The analytes that were included in method development were dibutyltin (DBT), tributyltin (TBT), diphenyltin (DPT), and triphenyltin (TPT).

1.6.4 Organoarsenic Compounds

In contrast to organotin compounds, organoarsenic compounds are mostly of natural origin. Organoarsenic species can be divided into highly toxic, partially non-toxic, and non-toxic species. [72] This simple categorisation is made more complex, however, because e.g. degradation of non-toxic compounds can lead to the formation of compounds that are more toxic. [73]

The analytes that were included in method development (Fig. 4) were arsenobetaine (AsB), arsenocholine (AsC), glycerol oxoarsenosugar (AsS-OH), and sulphate oxoarsenosugar (AsS-SO₄). Arsenobetaine is the two most common organoarsenic species, together with arsenocholine it is found predominately in marine animals; both compounds fall into the category of non-toxic species. Arsenosugars are mostly found in algae and are considered non-toxic as well. All four analytes, however, are known or suspected to produce degradation products or metabolites of higher toxicity. [74]

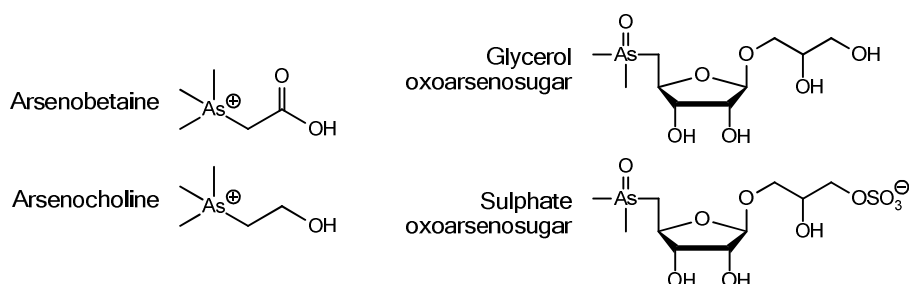


Fig. 4: Structures of the organoarsenic compounds used for method development.

2 Motivation

2.1 Why Fast CE–MS?

When CE instruments first became commercially available about 20 years ago, it was expected that CE would soon become the preferred separation method for many analytical problems. The main advantages over high performance liquid chromatography (HPLC), which was well established at the time, were the simpler instrumentation, use of inexpensive capillary material, very low solvent consumption, and shorter separation times. While HPLC, and recently ultra-performance liquid chromatography, have grown to become by far the most widespread separation method in the liquid phase, CE is less often used for routine analyses. At present, LC separations can be performed in a matter of minutes, while most CE determinations still require between 10 and 30 min with standard instruments. This is an issue, particularly when hyphenation with MS is sought, since the capillary lengths necessary to couple CE and MS instruments lead to long analysis times. Many contemporary analytical problems, however, require much shorter separation times, e.g. to follow reaction kinetics or to achieve a high sample throughput.

A high sample throughput in CE has been achieved using parallel separations in up to 384 capillaries, most famously for genome sequencing. This requires an optical detection method, which is able to detect analytes in multiple capillaries simultaneously. For most analytical problems except a select few, however, this is not practical. MS detection has become an increasingly popular choice owing to its ability to easily identify and verify both known and unknown analytes.

Since CE and LC have very different separation principles, CE can complement LC in the lab. Hyphenation of CE with MS is possible as well, making it attractive for both routine and research use. The one main drawback of CE, when comparing it to LC, is its longer analysis runtime. An improvement towards fast CE–MS would be instrumental in further establishing CE–MS as a helpful tool for various analytical problems. [75]

While electrophoretic separations on microchips (chip electrophoresis) also aim at fast separations, [76, 77] there are a number of disadvantages when comparing this approach to capillary electrophoresis: (1) Design and production of microchips is time-consuming and costly, (2) a large variety of materials used in chip production results in a large variety of

surface chemistries of the separation channel, [78] (3) hyphenation with MS is still at an experimental stage and not trivial to implement. [79] CE in fused silica capillaries, on the other hand, uses cost-effective material with a variety of inner and outer diameters and coatings, can be cut to any desired length, features a well-studied surface chemistry, and is readily hyphenated with MS. Overall, CE in capillaries makes use of a matured separation technique with a large knowledge background in literature.

In order to develop a fast CE–MS methodology that can be easily implemented by other laboratories, an approach using commercial fused silica capillaries and a commercial sheath liquid ESI interface was chosen.

2.2 Why Novel Injection Methods?

The capillaries employed in CE have typical dimensions ranging from 50 to 75 μm ID and 50 to 100 cm in length, although examples with shorter length, [8, 13, 14, 23] smaller ID, [31, 80] and both (as shown in chapter 4, pg. 46) can be found. This results in a small total volume of liquid inside the capillary, and an even smaller injection volume. Typical injection volumes for the capillary dimensions mentioned above are between 10 and 100 nL, but can drop below 1 nL for smaller ID and lengths.

This small injection volume is in stark contrast to the actual sample volume required for CE experiments, both for automated instruments and manual setups. While automated instruments require volumes of at least 50 μL , advanced manual procedures can work with volumes down to 10 μL . To compare injection volume and sample volume in CE experiments, injection efficiency can be defined as actual injected volume divided by sample volume necessary to perform the injection. Here, small values indicate inefficient injections with a large excess of sample, while values approaching 1 indicate an efficient use of sample. Typical injection efficiencies are in the range of 10^{-3} to 10^{-7} , even optimised conditions can only achieve around 10^{-2} .

This situation leaves one inherent feature of capillary electrophoresis, the very small injection volume, unutilized. Analytical problems, where sample volume is strongly limited, would be well suited for analysis by CE, provided high enough injection efficiency can be achieved. Applications that require both a small injection volume and high injection efficiency include the small-scale monitoring of biological systems (microenvironments) up to the study of single-cell metabolomics. One prominent small-sample analytical challenge is microdialysis. [81, 82] There have been reports of microdialysis with subsequent CE analysis, [83-85] but due to the complex setup, hyphenation with MS has not been implemented.

An experimental approach to investigate and optimise all relevant aspects of the injection process, utilizing the previously developed concept of CBI, [15] was chosen. It was further supposed to implement the findings of the fast CE-MS investigations to yield a system that is able to both work efficiently with minimal sample volumes and conduct efficient CE-MS separations with a high throughput.

3 Experimental

3.1 Chemicals and Materials

General. Fused silica capillaries of 360 μm outer diameter and 75, 50, 25, 15 and 5 μm inner diameter were purchased from Polymicro Technologies (Phoenix, AZ, USA). Water purified with an Astacus system (MembraPure, Bodenheim, Germany) and HPLC–MS-grade isopropanol (Carl Roth, Karlsruhe, Germany) were used throughout this study. Formic acid was from Merck (Darmstadt, Germany). A two-part silicone elastomer (Sylgard 182, Dow Corning, www.dowcorning.com) was prepared according to manufacturer's instruction and used for sealing the injection cell as well as to create a seal on top of a fused silica capillary.

Catecholamines. Epinephrine, norepinephrine hydrochloride, dopamine hydrochloride and isoproterenol were from Sigma Aldrich (St. Louis, MO, USA), histidine hydrochloride; dimethyl sulfoxide (DMSO) was from Merck.

Hyaluronan oligomers. Perfluoroheptanoic acid, caesium hydrogen carbonate, and sodium hydroxide solution (50%, w/w) were from Sigma Aldrich. Ammonium acetate (NH_4OAc), ammonia solution (50%, v/v), and formic acid were from Merck. BGE solutions were freshly prepared from an NH_4OAc solution of given concentration, pH-adjusted with ammonia, and filtered through 0.2 μm Millex-GP syringe filter units (Millipore, Cork, Ireland).

Oligosaccharide standards (oligoHA by Hyalose, Oklahoma City, USA) were purchased from amsbio (Abingdon, UK) and used at a concentration of 20 μM for systematic method development. For digestion with bovine testicular hyaluronidase (BTH), Hyalo-Oligo, a hyaluronan preparation with a molecular weight below 10 kDa, kindly provided by Kewpie (Tokyo, Japan), served as substrate. BTH (Neopermease®) was kindly provided by Sanabo (Vienna, Austria). Bovine serum albumin was purchased from Serva (Heidelberg, Germany). Sodium chloride for preparation of the incubation buffer was from VWR (Haasrode, Belgium); citric acid and disodium hydrogen phosphate were from Merck. Phenex-NY 4 mm syringe filters 0.2 μm (Phenomenex, Aschaffenburg, Germany) were used for filtration of hyaluronan digests prior to injection.

Organotin compounds. DBT chloride, TBT benzoate, TPT chloride, DPT chloride and acetic acid (HAc, 99.9%) were purchased from Sigma Aldrich. Ammonium acetate (NH₄Ac), formic acid, methanol (MeOH) and acetonitrile (AN) were obtained from Merck. All reagents were of analytical reagent grade or better. Standard solutions of organotin compounds in the concentration range of 5 – 1,000 µM were prepared in HPLC-grade AN and kept at 4°C in the dark. For CE separations, the standard solutions were freshly prepared by dilution from stock solutions with the running buffer. CE running buffers were prepared by mixing appropriate amounts of HAc, NH₄Ac, MeOH and AN. Before use, the running buffer solutions were filtered through a 0.45 µm syringe filter and degassed by sonication for 4 min. Phenomenex strata C18-E 500 mg solid phase extraction (SPE) cartridges were used for sample extraction.

Organoarsenic compounds. Arsenobetaine and arsenocholine were obtained from Wako Chemicals GmbH (Neuss, Germany). The glycerol oxoarsenosugar and the sulphate oxoarsenosugar were acquired from K. A. Francesconi (Karl-Franzens University, Graz, Austria). Caffeine was an Avocado Research Chemicals Ltd product purchased from ABCR GmbH & Co. KG (Karlsruhe, Germany). The sea plant homogenate reference material IAEA-140/TM was kindly donated by J. R. Oh (International Atomic Energy Association, Monaco). The powdered seagrass was taken from an interlaboratory study. [87] The Wakame algae (Wakame Taipan) were bought at a local Asian store (importer: Arrow Trading Hamburg) and pulverised (particle size > 30 µm).

3.2 Instrumentation

This section lists components used for fast CE–MS experiments. The setup built for CBI–CE–MS experiments is described in section 3.7 (pg. 34).

The setup for fast CE–MS experiments was comprised of a laboratory-built CE assembly, an ESI interface and the mass spectrometer. The CE assembly consisted of a high voltage power supply (model HCN 7E-35000, F.u.G. Elektronik, Rosenheim-Langenpfunzen, Germany), a control unit and a protective plexiglas box. The separation capillary was coupled to a micrOTOF-MS (Bruker Daltonik, Bremen, Germany) using a coaxial sheath-liquid sprayer (Agilent Technologies, Waldbronn, Germany). A mixture of isopropanol/water/formic acid (50:50:0.2, v/v) was used as sheath liquid and delivered by a syringe pump (model 601553, kdScientific, Holliston, MA, USA) from a 2.5 mL glass syringe (ILS, Stützerbach, Germany).

3.3 Software

This section lists free and commercial software used for various purposes in the context of this work. The software specifically developed for control of the CBI setup is described in section 3.8 (pg. 40).

Control of the mass spectrometer and data acquisition was done through micrOTOFcontrol (version 2.3, Bruker Daltonik). Data analysis was performed using DataAnalysis (v. 4.0 SP1, Bruker Daltonik). M/z values for extracted ion traces were calculated using IsotopePattern (Bruker Daltonik), which relies on NIST data for atomic masses. [86] Origin (v. 8, <http://www.originlab.com/>) was used for data visualisation.

Vector-based graphics and schemes were designed using CorelDraw (v. X5, Corel Corporation); bitmap-based graphic manipulation was done using Corel PhotoPaint (v. X5, Corel Corporation) and ImageMagick (v. 6.5.6, <http://www.imagemagick.org/>). Videos were recorded with VirtualDub (v. 1.9.8, <http://virtualdub.org/>) and edited with Avidemux (v. 2.5.4, <http://avidemux.org/>).

The CAD software employed in mechanical design was Solid Edge (v. 12, Electronic Data Systems). Electronic circuit board design work was done in Eagle Layout Editor (v. 5.11, <http://www.cadsoftusa.com/>). For software development, Visual Basic 2010 Express (Microsoft) was used. Serialport communication analysis and debugging was done using RealTerm (v. 2.0, <http://realterm.sourceforge.net/>)

This thesis was set in the free typefaces Linux Biolinum (headings) and Linux Libertine (body) (<http://www.linuxlibertine.org>).

3.4 Methods

3.4.1 Sample Collection and Preparation

Hyaluronan oligomers. The protocol for a hyaluronan digest was essentially performed according to the colorimetric method for determination of hyaluronidase activity [88, 89] and the conditions used by Hofinger et al. for CE analysis. [64, 65] McIlvaine's buffer was prepared by mixing a 0.2 M solution of disodium hydrogen phosphate and a 0.1 M solution of citric acid, each containing 0.1 M of sodium chloride, to reach a pH value of 5.0. The incubation mixture consisted of 400 μ l of buffer, 200 μ l of water, 100 μ l of BSA solution (0.2 mg/ml), 100 μ l of hyaluronan solution (5 mg/ml) and 100 μ l of BTH (400 IU/ml according to supplier's information) dissolved in BSA solution (0.2 mg/ml). After the addition of BTH, the mixture was incubated for 2 h and 24 h, respectively, at 37 °C. The reaction was stopped by boiling for 15 min and denatured protein was removed by centrifugation at 13,000 g for 10 min. Before analysis, samples were filtered through a 0.2 μ m syringe filter. To investigate possible matrix effects, the sample was prepared as described above, except that oligosaccharide standards were used instead of hyaluronan, and BSA solution (0.2 mg/ml) was used instead of enzyme solution.

Organotin compounds. Water samples were collected in PE bottles from the Danube River in Regensburg, Germany. Aliquots of 450 mL were each spiked with 267 μ L of a stock solution containing $3 \cdot 10^{-5}$ M of each analyte, resulting in a spiked concentration of $1.8 \cdot 10^{-8}$ M. Blank samples and spiked samples were then subjected to the following procedure. The sample solution was acidified to pH 2 with diluted HCl and filtered through a 0.45 μ m membrane filter. SPE cartridges were conditioned with 5 mL of methanol followed by 10 mL of water (pH 2). The sample solution was then passed through the cartridge at a rate of 5 mL/min. The cartridge was rinsed with 10 mL water and dried by pumping air through it for 2 min. Elution of the analytes was performed with 4 mL of CE buffer and the volume of the extract was then adjusted to exactly 4.00 mL.

Organoarsenic compounds. A simple extraction protocol was used for the extraction of a dried Wakame and seagrass powder as well as a brown algae homogenate reference material (IAEA-140/TM, Fucus sp., Sea Plant Homogenate). 100 mg of algae sample were weighed into 15 mL PP centrifuge tubes. 5 mL of deionised water were added and the sample was thoroughly mixed by vortexing for a few minutes. Afterwards the samples were extracted by ultrasonication at 30 °C for 3 h. After centrifugation for 30 min at 10,000 rpm,

the supernatant was filtered through a membrane syringe filter (regenerated cellulose, 0.45 µm, phenomenex, Aschaffenburg, Germany) and the filtrate was transferred to 1.5 mL Eppendorf tubes. 300 µL of the filtrate were transferred to 0.5 mL Eppendorf tubes and evaporated to dryness in a slight nitrogen stream. The residue was re-dissolved in 29.2 mL deionised water. 0.8 mL of a 10^{-2} M caffeine standard was added to the extracts before analysis. Unless samples were analysed the same day, they were stored frozen.

3.4.2 Manual Sample Injection Technique

A manual hydrodynamic sample injection protocol was used throughout this study. The laminar flow through the capillary, which is necessary to accomplish injections, is present due to the design of the coaxial sheath liquid interface. This interface uses a flow of nitrogen to aid nebulization of the combined sheath liquid and capillary effluent. The high velocity of the nebulizer gas at the tip of the interface creates a turbulent aerodynamic situation, which in turn leads to a suction pressure applied to the outlet of the separation capillary, the extent of which depends on the nebulizer gas pressure. [90] This suction pressure creates a constant laminar flow through the capillary, the extent of which depends on capillary length and ID.

This laminar flow can be utilized to accomplish hydrodynamic injections, with no need for any additional pressure applied to the sample vial, for larger capillary IDs (75 to 25 µm). Injection was accomplished by manually transferring the capillary from the buffer vial to the sample vial for a given time interval, and back. While the trapping of air bubbles is a potential problem with this procedure, the use of aqueous BGEs and a fast transfer of the capillary between the vials was found to be sufficient for successful injections. For smaller ID capillaries (15 and 5 µm), where the laminar flow through the capillary becomes very small and the necessary injection times would become impractical, additional pressure was applied. The sample vial was closed with a cap and septum, through which the capillary was led into the sample solution, and pressure was applied using a syringe. In these cases, the injection time refers to the time during which pressure was applied to the sample vial.

For both injection protocols, the laminar flow through the capillary under injection conditions had to be determined in order to adjust injection times. In case of the simple injection procedure for larger ID capillaries, the injection was carried out as outlined above, but after returning the capillary to the buffer vial, no CE high voltage was applied to the

capillary, effectively conducting a capillary flow-injection experiment. [91] In case of the pressure-assisted injection for smaller ID capillaries, the same pressure was applied to the buffer vial after injection. Flow rates were found to be reproducible for both injection protocols (relative standard deviation of $n = 5$ consecutive experiments was between 0.3% and 2.8% for the different ID).

Different injection volumes were investigated as to their influence on peak height, area, and width (width at half maximum). Fig. 5 shows the results of these investigations.

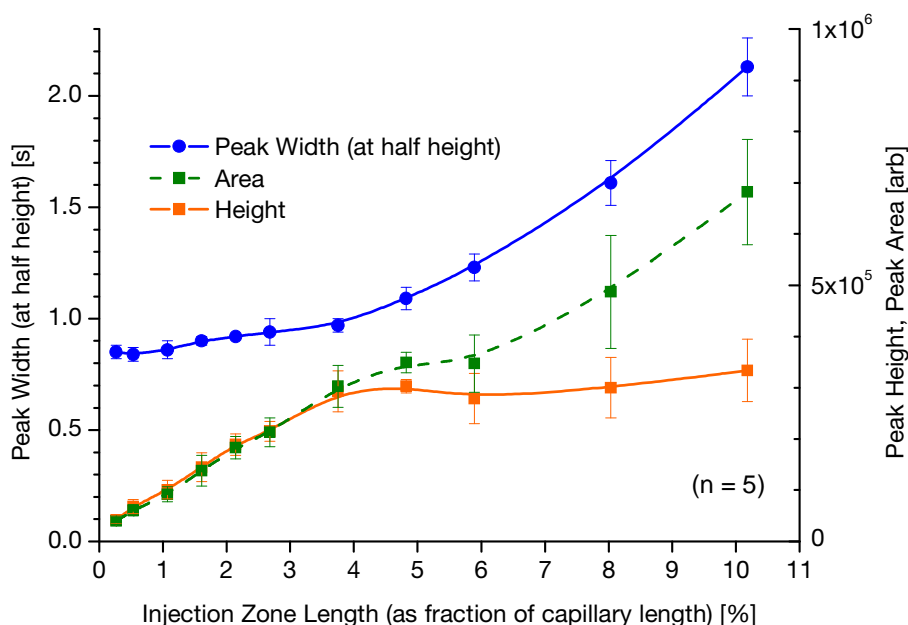


Fig. 5: Dependence of signal height, signal area, and signal width on the injection volume. Injection volume is given as injection zone length as fraction of the capillary length (or injection zone volume as fraction of the total capillary volume). The x-axis for the peak widths is on the left, the one for peak height and area on the right.

It was found that while peak areas increased linearly with the amount injected, peak heights reached a plateau at injections equalling 4% of the capillary length. Peak widths only increased marginally up to this point, while rising strongly afterwards. As a compromise between peak width and peak height, an injection volume corresponding to 2% of the capillary length was chosen for all further experiments. Table 1 summarizes the injection conditions that were employed for different capillary IDs.

Table 1: Injection conditions for capillaries of different ID for injections corresponding to 2% of the capillary length.

Capillary ID [μm]	Applied pressure [bar]	Flow rate [cm/s] ^a	Injection time [s]	Injected Volume [nL] ^b
75	(none)	11.2 \pm 0.3	3	25
50	(none)	7.4 \pm 0.2	5	11
25	(none)	1.11 \pm 0.03	30	2.8
15	0.2	8.77 \pm 0.03	8	0.99
5	1.0	3.94 \pm 0.06	9	0.11

a Values determined experimentally; absolute standard deviation of $n=3$ consecutive determinations given as uncertainty.

b Values calculated from the flow rate in the capillary under injection conditions.

3.4.3 Cooling of Separation Capillary

With the BGEs and capillary dimensions employed, excessive Joule heating in the separation capillary was mostly not an issue. For this reason, and in order to aid a simple experimental setup, separation capillaries were not cooled. In some cases, however, Joule heating affected separations considerably, which resulted in strong peak broadening or a breakdown of the electrophoretic circuit. The latter occurred while conducting separations in 75 μm ID capillaries with 0.1 M formic acid as BGE (section 4.1.3, pg. 51), where the BGE heated up so quickly, when applying high field strengths that the CE circuit collapsed almost immediately after having applied the high voltage.

About 12 cm of the capillary is inside the ESI interface, where it cannot be accessed and is mostly surrounded by the sheath liquid. The cooling for the remaining part had to be simple in design so as to allow handling of the short capillaries during injections. A gas-based cooling system was preferred over one employing a liquid coolant, since the latter would have dramatically increased the risk of flashovers between the high voltage electrode in the buffer vial and the grounded mass spectrometer.

The accessible part of the separation capillary was inserted into a silicone tube of 4 mm ID. A laboratory-made adapter piece (Fig. 6) was used at the interface end of the capillary to

connect the silicone tubing to the gas source while maintaining a straight path for the separation capillary. Nitrogen gas, cooled to approx. 10 °C using ice, was blown through the tubing at high speed, and exited towards the injection end of the capillary, maximizing the portion of the capillary that was cooled.

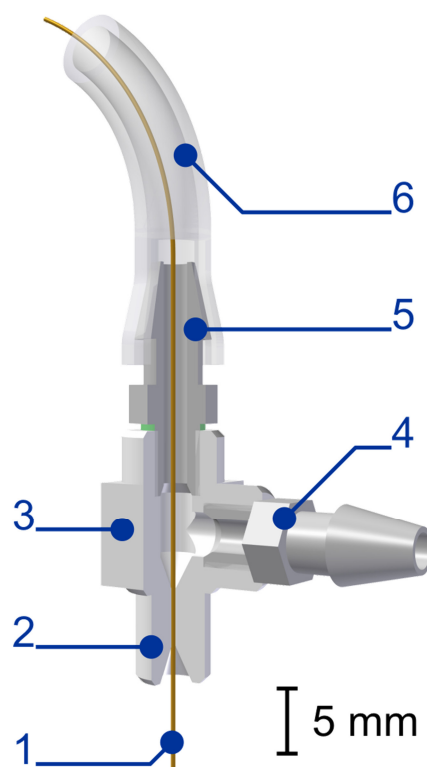


Fig. 6: Adapter piece for cooling of short separation capillaries. The assembly consists of (1) separation capillary, (2) cylinder that fits onto ESI interface (3) body with conical capillary guides, (4) tubing barb for gas supply, (5) tubing barb for (6) silicon tubing around separation capillary. The stream of cooled nitrogen gas enters through (4) and exits through (5), with a small part being diverted downwards, exiting through (2). Detailed schematics for this adapter piece are included in the appendix (section 9.1.1, pg. 102).

3.4.4 Microscopic Investigation of Electrospray

The ESI interface is of particular relevance in fast CE–MS method development. Specifically, the electrospray was found to have a crucial impact on peak shapes and sensitivity. After preliminary experiments showed a correlation between visual appearance of the electrospray and parameters such as TIC stability and peak width, a permanent solution for microscopic electrospray investigation was developed and implemented.

Visual investigation itself was done by modifying a microscopic video camera (model DigiMicro 1.3, dnt, Dietzenbach, Germany) to fit into the spray chamber. A holder for the camera was built to keep it in place and adjust its position. Five different fixed focal length-

cylinders were built to yield different fields of view (width of picture) in focus (Table 2). The spray was typically viewed with a field of view of 2 mm.

Table 2: Fields of view achievable with the modified microscopic camera.

Focus Cylinder	Length [mm]	Field of view (in focus), adjustable range [mm]
1	16	$\infty - 9$
2	22.5	10.5 - 4.7
3	28	5.1 - 3.2
4	36	3.0 - 2.2
5	46	2.0 - 1.6
5+3	74	1.0
6	95	0.7
6+7	135	0.5

The electro spray is very thin and practically invisible with normal illumination. It was found that a laser beam, which is directed at the spray from opposite the viewpoint, yields good results. Using an adjustable mirror holder and a green (532 nm) laser diode (model CW532 050, Roithner, Vienna, Austria), a fixture was designed to attach this light source to the spray chamber. Fine-tuning of the laser beam was possible using the adjustable mirror. The intensity of the laser beam could be regulated.

Since using only the laser beam as light source did not yield sufficient background illumination for the camera to record images at a reasonable frame rate, a second fixture was designed, such that four different high-luminescence LEDs shed light on background objects in the spray chamber. Two white LEDs were directed at a background area of the field of view and at the spray itself, respectively. One blue and one red LED were directed at the background as well. Since their emission wavelength is outside the camera sensor's green pixels, it was possible to yield high-frame rate videos of the electro spray with only the spray visible in front of a black background. All LEDs could be switched on independently of each other and the laser diode.

3.4.5 Preparation of Capillary Seal

In order to coat the end of a fused silica capillary with a silicone elastomer, to act as a seal between two capillaries, the following manual procedure was developed. The capillary end was cut as clean as possible and the polyimide removed at a length of about 5 mm using a microburner. The capillary end was then polished with a coarse polishing paper (grit size 400, 35 μm particles) at a 90° angle. The resulting rough surface improved adhesion of the elastomer as opposed to surfaces polished with finer polishing paper or purely cut capillary ends.

A small amount of silicone monomer was prepared according to manufacturer's instructions and degassed. The far end of the capillary was inserted into a pressurized vial to yield an air flow through the capillary. This air flow should be as high as possible to avoid the partial obstruction of the capillary inner diameter by the seal. The end to be coated was then brought in contact with the silicone monomer solution just enough to cover the surface. Excess silicone monomer was removed from the side of the capillary by carefully wiping it with a lint-free tissue, leaving only the top of the capillary covered in silicone monomer. The result was inspected under a microscope and found to give a good idea of the final elastomer seal after curing. If unsatisfactory, the monomer can be simply wiped off and the above steps repeated until the desired seal shape is achieved.

While ordinary curing times for this silicone elastomer are about one hour, a much quicker procedure for the small amounts applied here was used. The capillary tip with silicone monomer was slowly brought in close vicinity (but not contact) with a heat source of approx. 300–400 °C. This reduced the curing time to a few seconds. If there are bubbles present in the cured elastomer under microscopic inspection, the temperature applied during curing was most likely too high and the seal will be of inferior quality (less flexible, more likely to rupture). In this case, the seal can be removed mechanically by scraping and a new seal can be applied starting with the coating step.

3.5 CE Method Development

Development of methods for fast CE–MS consisted of finding an appropriate BGE composition, a capillary of certain length and ID, as well as an EOF marker.

BGE composition for the main part focussing on method development for fast CE–MS using a catecholamine model system was deliberately kept simple. Mostly, a 0.1 M aqueous formic acid solution was employed as BGE, with exceptions discussed in more detail in the appropriate sections. The usage of this simple BGE allowed focussing on instrumental aspects and effects. BGEs of more complex composition were required for other sets of analytes. Their optimisation is detailed in sections 4.2.3 (hyaluronan oligomeres, pg. 59), 4.3.1 (organotin compounds, pg. 66), and 4.4.3 (organoarsenic compounds, pg. 74).

Optimisation of capillary length and ID are central to the findings presented in this thesis and are discussed in detail in sections 4.1.2 (pg. 50), 4.1.3 (pg. 51), 4.2.1 (pg. 56) and 4.2.2 (pg. 57).

3.5.1 EOF Marker

While an EOF marker is not necessarily required for a CE method, it can be used to compensate for runtime migration time fluctuations, since the migration time relative to the EOF is often more constant than the absolute migration time. Furthermore, during method development it is instrumental in measuring and adjusting the migration time difference between neutral components (often matrix components) and the analytes.

Typical aqueous CE–UV methods employ small amounts of organic solvents (e.g. acetone) as EOF marker. For CE–MS, however, potential EOF markers have to be within the mass range of interest in order to be detected.

Catecholamines. Even with a focus on a low mass range (as in the case with these analytes), molecules below approx. 75 m/z cannot be detected at all by the mass spectrometer. DMSO was used as EOF marker. Experiments showed that addition of DMSO up to concentrations of 140 mM (= 1%) had no influence on migration behaviour and signal intensity. A concentration of 14 mM (= 0.1%) was used for all further experiments.

Hyaluronan oligomers. Since the analytes of interest were in the mass range of 250 m/z and above, a substance had to be found that is of corresponding mass, soluble and of zero net-charge in the aqueous BGE employed, and ionizable in the ESI interface. Pittman et al. could show that rhodamine B (Fig. 7) has zero net charge in the pH range of 8.3–9.0 and can be used as EOF marker. [92] However, rhodamine B is only ionized in positive ion mode, while the analytes require the use of negative ion mode. Therefore, it was necessary to switch between positive and negative ion mode while recording analyses. Since this polarity change takes approximately 20 s, it was impossible to record both EOF marker and analytes during final fast CE–MS experiments. Rhodamine B was added to analyte solutions yielding a concentration of 1 μM .

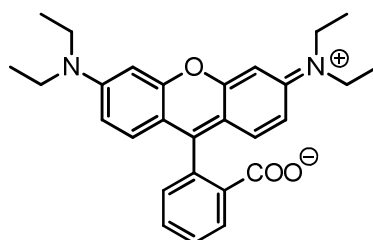


Fig. 7: Rhodamine B in the charge state under background electrolyte conditions.

3.6 MS Method Development

Prior to the systematic development of the CE methods, an MS method had to be optimised for each set of analytes. This focussed on instrumental parameters of the ESI interface and TOF-MS ion transfer optics. Optimisation was always aimed at highest sensitivity, as opposed to highest mass resolution. This section details the general approach in MS method development as well as optimised parameters for each set of analytes.

3.6.1 General Approach

Generally, an MS method was optimised along the path analytes take from the point where they exit the separation capillary up to the detector unit inside the mass spectrometer. Instead of using the analytes themselves during this procedure, employing cluster-forming mixtures (e.g. sodium formate clusters) was found to yield a more robust MS method. In contrast to mixtures of a small number of analytes, cluster distributions show MS sensitivity in a larger m/z region. The distribution of cluster species itself can be used as a marker to judge sensitivity *distribution* over the mass range investigated. This is due to differently sized clusters of the same substance showing a very similar MS sensitivity, an assumption that cannot be made for a set of (chemically different) analytes.

3.6.2 ESI Interface

The first step of the optimisation procedure is the ESI interface. Here, the best combination of sheath liquid (type of organic solvent, its content, acidic/basic additive) and ionisation mode (positive/negative ion mode) has to be found. Sheath liquid flow rate and nebulizer gas pressure will have to be adjusted to give a stable electrospray. Fine-tuning of these two parameters, however, is done during CE method development.

One commonly applied sheath liquid was found to be ideal for all sets of analytes. The composition was a mixture of water, isopropanol, and formic acid in the ratio of 50:50:0.2 (v/v/v). Even substances that were analysed in negative ion mode (hyaluronan oligomeres) were best ionized with this acidic sheath liquid.

3.6.3 Ion Optics

During the second step, ion optics in the mass spectrometer are adjusted. The lens 1 timings limit the usable mass range by cutting off ion transmission, but otherwise have no influence on sensitivity. The hexapole RF is instrumental in adjusting sensitivity to and within the

desired mass range. The width of the usable mass range (i.e. the range with reasonable sensitivity) varies: it is wide for high m/z values, but gets very narrow for small m/z . It is important to note that it is not possible to have an even sensitivity distribution over a wide mass range which includes small masses. Further parameters that can be adjusted are the voltages of transfer capillary, transfer capillary exit, and skimmer 1. Table 3 gives an overview of parameter values used for the different sets of analytes.

3.6.4 Mass Trace Selection

The third step of MS method development dealt with the selection of extracted ion traces. While it is necessary to have mass traces for the previous optimisation process already, final adjustments have to be made after settling on ionisation and ion guide parameters, since these can have an influence on adduct formation and the distribution between different ion species arising from a single compound in solution. Mass traces for inclusion in the final method were selected after experimentally observed signals could be verified as originating from the target compound, either as simple ions (e.g. $[M +/ - zH]^{z+/-}$) or as adducts (e.g. $[M + \text{HCOOH} + \text{H}]^+$ or $[M + y\text{Na} - (z+y)\text{H}]^{z-}$). With regard to isotope signals, only m/z values that had an abundance of at least 20% of the species' base peak were used. The same threshold was applied when inclusion of species arising from adduct formation was decided. M/z values for mass traces were always exact (calculated) ones, as opposed to experimentally determined ones.

3.6.5 Mass Calibration

Mass calibration was routinely done by using sodium formate clusters as reference masses. When using capillaries with a larger ID (50 μm and above), a sodium formate solution was infused. For small ID capillaries (25 μm and below), this procedure did not yield high enough signal intensities for the resulting formate clusters. Instead, a 1 M sodium hydroxide solution was forced through the capillary, which created sodium formate upon mixing with the sheath liquid.

Experiments with a focus on the mass range above 1300 m/z required a different calibration, since the sodium formate cluster intensity sharply declines after about 1000 m/z . Here, caesium perfluoroheptanoic acid clusters were used. [93]

Table 3: Parameter values for different TOF-MS methods. The order of parameters follows the path of ions through the instrument. Parameter names in bold indicate parameters with a high impact on mass range selection and sensitivity.

Parameter	Catechol-	Organotin	Hyaluronan Oligomer	
	amines	Comp.	full range	small m/z
Polarity	positive	positive	negative	negative
Mass range upper limit [m/z]	50	50	300	300
Mass range lower limit [m/z]	300	1000	3000	1200
Spectra rate [Hz]	25	5	10	10
End Plate Offset [V]	-500	-500	-500	-500
Capillary [V]	-4000	-5000	4500	5000
Nebulizer [bar]	1.2	1.5	1	1.2
Dry Gas [L/min]	4	4	4	4
Dry Temp [°C]	190	190	190	190
Capillary Exit [V]	75	100	-100	-100
Skimmer1 [V]	25.3	33.7	-33	-33
Hexapole1 [V]	23	23	-22.5	-22.5
Hexapole RF [V_{pp}]	65	200	800	300
Skimmer2 [V]	23	23	-22	-22
Lens1 Transfer [μ s]	49	49	49	40
Lens1 Pre Puls Storage [μ s]	5	15	10	10
P1S [V]	30	30	-30	-30
P1E [V]	20.8	20.8	-20.8	-20.8
Lens2 [V]	-45	14	-8	-8
Lens3 [V]	15	-20	20	20
Lens4 [V]	2	3	0	0
Lens5 [V]	0	-20	28.5	28.5

3.7 Experimental Setup for Capillary Batch Injection

3.7.1 Initial Tests

A setup comprised of simple components was used to evaluate some key parameters governing the injection process of CBI in conjunction with the ESI interface, prior to developing the final CBI setup. Fig. 8 shows a schematic of this setup.

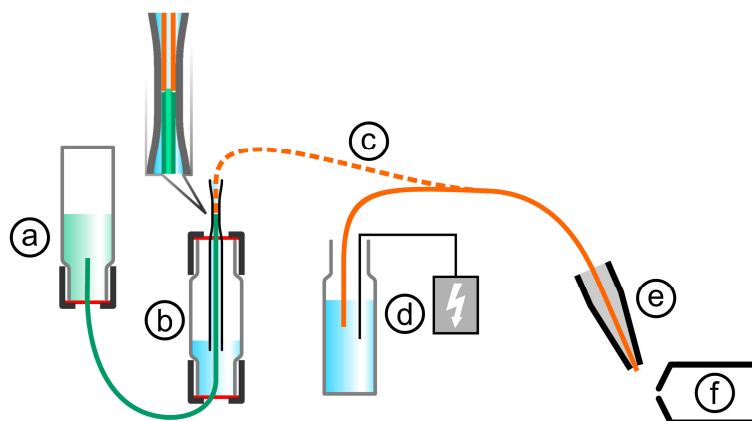


Fig. 8: Experimental setup used for initial CBI tests, consisting of (a) vial with sample solution and sample transfer capillary, (b) modified vial with injection sleeve and flush solution, (c) separation capillary during separation (solid line) and during injection (dashed line), (d) buffer vial with CE high voltage source, (e) electrospray interface, (f) time-of-flight mass spectrometer.

This setup is similar to CBI in that the separation capillary is brought in close contact with a capillary carrying sample solution (injection capillary in CBI). Alignment of both capillaries at the point of injection was achieved by using a glass tube, which has been drawn out to have an inner diameter only slightly larger than the capillaries' outer diameter. Fabrication of this glass tube was done manually; the optimal specimen restricted the capillaries to lateral movements of less than 20 μm .

Fig. 9 shows both separation capillary and sample delivery capillary at the point of injection, aligned by the glass sleeve.

The sample vial could be either pressurized, which led to a forced flow of sample solution through the sample delivery capillary or alternatively, a pressure-free situation could be created by inserting a needle through the septum into the headspace of the vial.

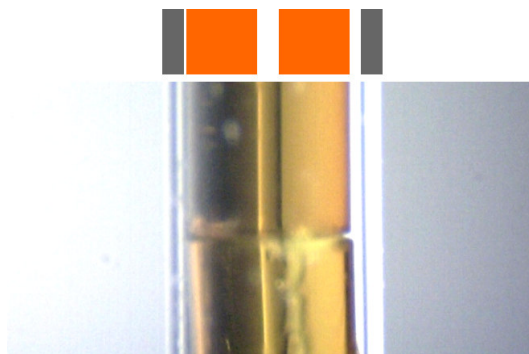


Fig. 9: Microphotograph of the injection region of the setup detailed in Fig. 8. Horizontal dimensions of capillary (orange) and glass sleeve (gray) are shown above for clarification. For scale comparison, the capillary ID is 50 μm .

It was found difficult to lead both the glass sleeve and the sample delivery capillary through the septum of a normal vial, since the sample delivery capillary would be sharply bent inside the vial. A vial with two screw cap ends was fabricated by the glass workshop, allowing a straight path for the sample delivery capillary. A small pressure applied to the injection vial led to a small but constant flow of flush solution through the glass sleeve, keeping the injection area free of air and removing excess sample solution. The solution that was used as BGE was employed as flush solution as well.

Injections were carried out by moving the separation capillary from the buffer vial into the glass sleeve on top of the sample delivery capillary for a certain period of time, and back.

3.7.2 Main Setup

The experimental setup was comprised of a purpose-built injection device, a lab-built high voltage source, a coaxial sheath-liquid electrospray interface (Agilent Technologies, www.agilent.com) and a micrOTOF-MS (Bruker Daltonik, www.bdal.com). Fig. 10 gives an overview of the overall experimental setup.

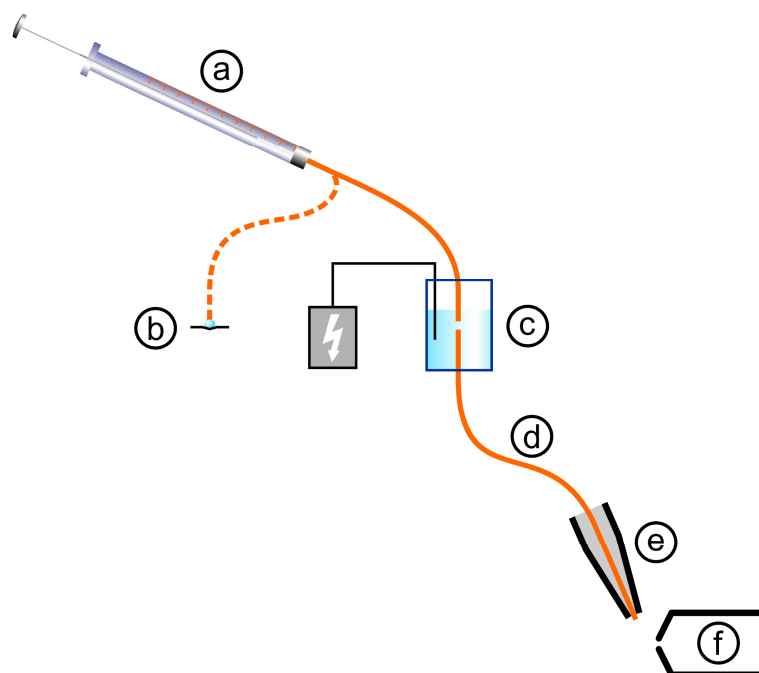


Fig. 10: Schematic overview of the overall experimental setup employed in this study, consisting of (a) microliter syringe with injection capillary during sample take-up (dashed line) and during injection (solid line), (b) sample, (c) injection cell with CE high voltage source, (d) separation capillary, (e) electrospray interface, (f) time-of-flight mass spectrometer.

The injection device consists of an injection cell, an injection capillary positioning unit (both shown in detail in Fig. 11) and a base unit (complete setup shown in Fig. 12). The injection process takes place in the injection cell (4; numbers refer to Fig. 11 and Fig. 12). The separation capillary (9) is fixed vertically in the cell base (8) using a fitting (7). The injection capillary (1) is led into the injection cell from the top through a 0.38 mm ID glass guide (3) (Hilgenberg, www.hilgenberg-gmbh.de/), which is fixed in a manual x,y-positioner (2). This allows the injection capillary to be repositioned in a precisely defined location. The injection cell base was sealed using a silicone elastomer. A high voltage electrode enters the cell from above (not shown). Care was taken to ensure chemical compatibility of the injection cell. Any solution inside the injection cell is exposed to borosilicate glass, PTFE, PEEK and silicone. Hence, both aqueous and non-aqueous solutions can be used as background electrolyte.

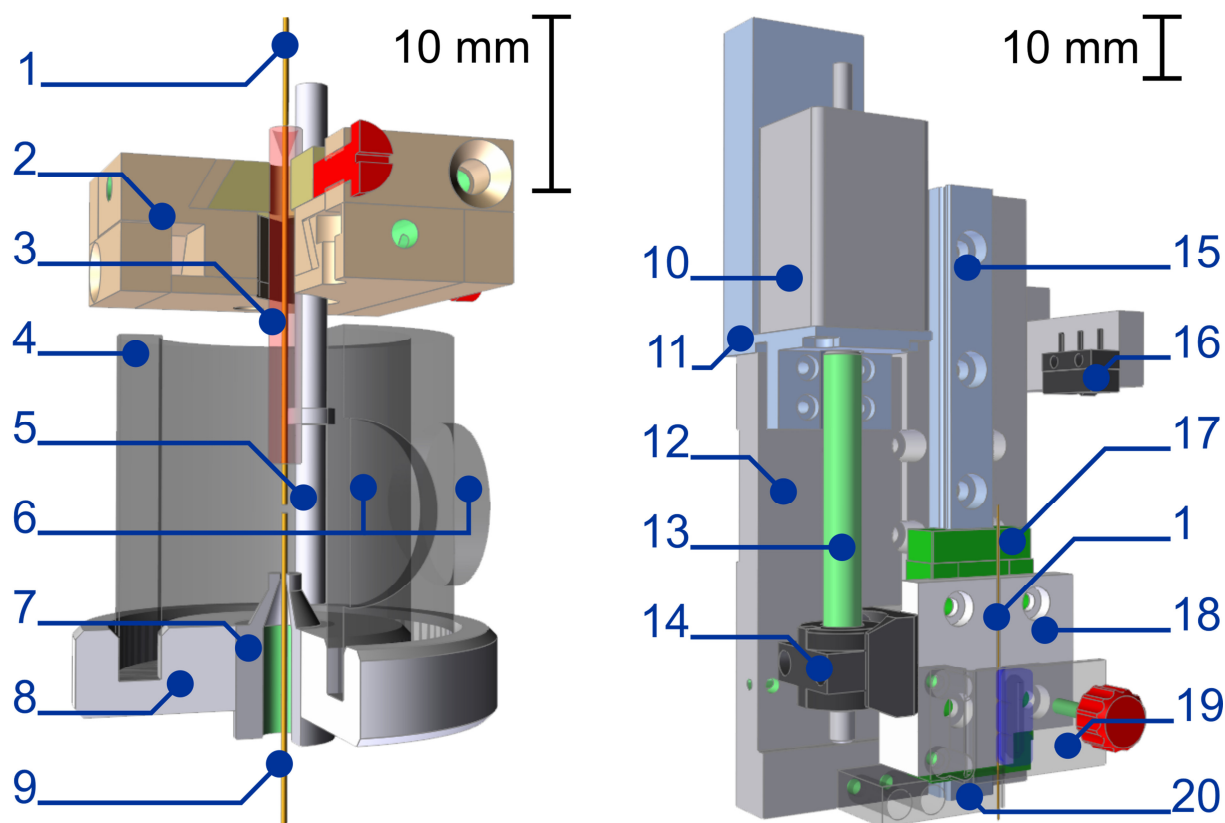


Fig. 11: Injection cell (left) and injection capillary positioning unit (right). 1 Injection capillary, 2 x,y-positioner, 3 capillary guide, 4 glass cell, 5 stirrer, 6 planar windows, 7 separation capillary fitting, 8 cell base, 9 separation capillary, 10 stepper motor, 11 stepper motor mount and heat sink, 12 vertical positioning base, 13 precision leadscrew, 14 precision nut and holder, 15 linear guideway rail, 16 end switch, 17 linear guideway block, 18 holder for injection capillary, 19 retainer for injection capillary, 20 injection capillary guide. Detailed schematics for the x,y-positioner are included in the appendix (section 9.1.2, pg. 103).

The injection capillary positioning unit performs the injection capillary's vertical positioning. The injection capillary is fixed between a retainer (19) and a holder (18), which in turn is mounted on a linear guideway block (17) (model MGN9HZ1HM and MGNR90100HM, Hiwin, www.hiwin.de/). Vertical movement is accomplished using a 1.8° stepper motor (10) with a precision leadscrew (13) (Nanotec, www.nanotec.de), which translates to a positioning precision of 1 µm/step. At the lower end, the injection capillary is guided in a PMMA block (20).

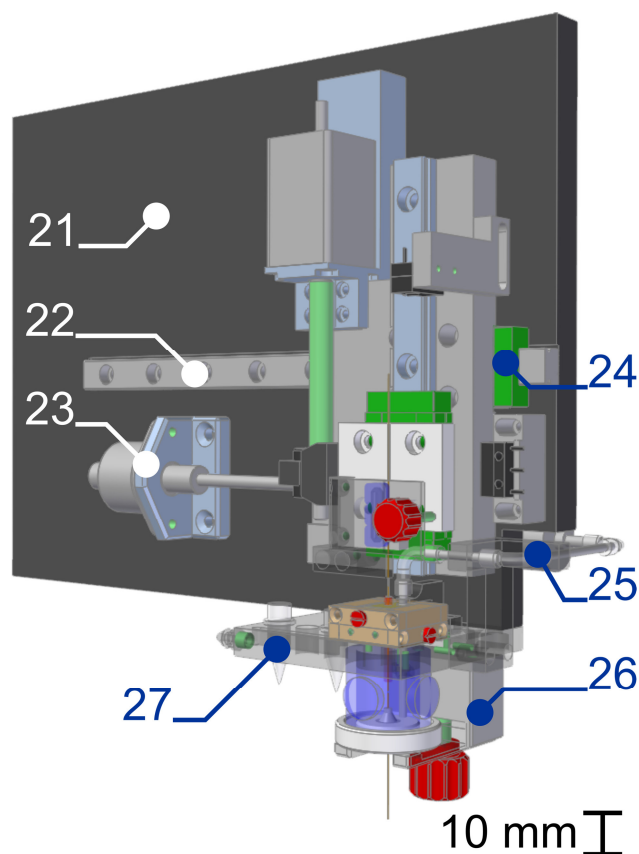


Fig. 12: Injection device with injection cell and injection capillary positioning unit. Further items are: 21 support, 22 linear guideway rail, 23 stepper motor with leadscrew, 24 linear guideway block, 25 stirrer motor, 26 retainer for injection cell, 27 injection cell holder with sample vials.

In the complete assembly, the injection capillary positioning unit is mounted on a linear guideway (22, 24) (model MGN9HZ1HM and MGNR90160HM, Hiwin) and is located above the injection cell such that both capillary guides (3 and 20) line up. Horizontal movement is accomplished using a stepper motor with leadscrew (23) (model 20DAM40D1B-L, Portescap, www.portescap.com). The injection cell is mounted below the cell holder (27) which also holds sample vials and the high voltage electrode and connector.

In addition, the setup required electronics (mainly two stepper motor controllers SMCI12, Nanotec), a microliter syringe (10 μ L Nanofil syringe, WPI, www.wpiinc.com), a syringe pump (UMP3, WPI), as well as a stirrer motor (model IG-16GM04, Shayang Ye, Taiwan, www.shayye.com.tw)

Capillary positioning and injection optimisation was visually controlled using a laboratory-modified microscopic video camera (model DigiMicro 1.3, dnt, www.dnt.de).

Liquid movement inside the injection capillary is handled by a microliter syringe connected at the capillary's other end. In order to transmit syringe piston movements to liquid inside the capillary, both syringe and capillary need to be filled with liquid. A perfectly air-free coupling of syringe and capillary is required for reliable and reproducible operation. In addition, this backfilling liquid can also be used to flush the capillary, since its volume is large compared to the sample volume (10 μ L vs. 10 nL). Driven by a syringe pump, this setup can draw up and expel sample solution in the nanoliter range precisely.

Even though high voltage issues were taken into account at design time, the setup as shown in Fig. 12 required some additional modification to prevent flashovers under demanding experimental conditions. Specifically, these were experiments with high voltages approaching the upper limit of the high voltage source, which were conducted during high temperature and high humidity weather situations. The modifications consisted of non-conductive shielding for some components and grounding for other components. While the latter cannot prevent flashovers, the potentially disastrous impact of a flashover or stray current on the subsequent electronics is minimised. Shielding using PTFE films of 0.25 and 0.5 mm was attached to the vertical linear guide rail and block, to both end switches, and to the vertical stepper motor and lead screw. Grounding connections were applied to both stepper motors, both lead screws, and the microliter syringe plunger.

3.8 Control Software for Capillary Batch Injection

The CBI assembly is controlled by a computer from a single graphical user interface, specifically designed for complete and fine-tuned control over all parameters relating to the injection process. Microsoft Visual Basic 2010 Express was chosen to develop this control software, termed “CBI-Control”, fast and efficiently. General features, its user interface and its structure will be described in the following.

3.8.1 General

The main software design objective was functionality for the user, with an emphasis on simple access to all variables of the injection process.

The primary software features are parameterisation and control of the external devices (motors, syringe pump, high voltage source), user input for these parameters, and injection process event control.

Secondary software features are designed to increase productivity and improve the user experience. They include an automatic software update, automatic searching for and connecting to all devices on program startup, import and export of the run table, as well as window arrangement to use the available desktop space optimally.

3.8.2 User Interface

The graphical user interface was divided into four separate forms (“windows”), both to group separate content visually and to allow for the deactivation of unneeded forms to maximise working space.

Main form. Most user interaction takes place with the main form shown in Fig. 13. Its central element is the “run table”. Each cell in the run table represents one single element of an injection procedure, e.g. “z-motor move to injection position”, “syringe withdraw 20 nL” or “stirr for 1500 ms”. During execution, the run table is worked from left to right, top to bottom. Each column has a specific function, with its tooltips (not shown) explaining the expected format for data entry. Table 4 describes these functions. Since an injection process would often consist of a certain sequence of steps, the columns were arranged in this expected order and some columns were duplicated. This minimizes the number of rows necessary to define an injection process, aiding in a better overview. To the right of the run

table, there are controls to open and close the other three windows, execute an injection procedure, and stop execution.



Fig. 13: CBI-Control’s main window shown during a run through an injection procedure. Completed tasks are marked green, the current task is marked orange, scheduled tasks are marked blue.

Table 4: Function of the run table’s columns

Column	Function
Order	Reordering of the rows
Move to Z	Z-motor movement to specified position (selection via drop-down menu)
Move to X	X-motor movement to specified position (selection via drop-down menu)
Wait	Halt execution for specified time [ms]
Syringe	Withdraw (negative values) or expel defined volume [nL] at defined speed [nL/s]
HV Inj	Inject electrokinetically with a defined voltage [kV] for the defined time [s]
Stir	Activate stirrer for defined time [ms]
HV Sep	Start separation with defined voltage [kV], with or without TOF-MS data acquisition
Prompt	Halt execution and prompt for continuation

Settings form. All settings that usually need no changing during injection procedure optimisation are located in the “Settings” form, where controls are grouped in five tabs (Fig. 14). In “Motor Positions”, the target positions, speeds and ramps for z- and x-motor movements, along with descriptive identifiers for all datasets are held. “Motors” has an automated motor initialisation routine for fixing the injection capillary. “Syringe Pump”

and “HV Source” hold additional parameters for those instruments. “System” has controls for serial port connections and window manipulation.

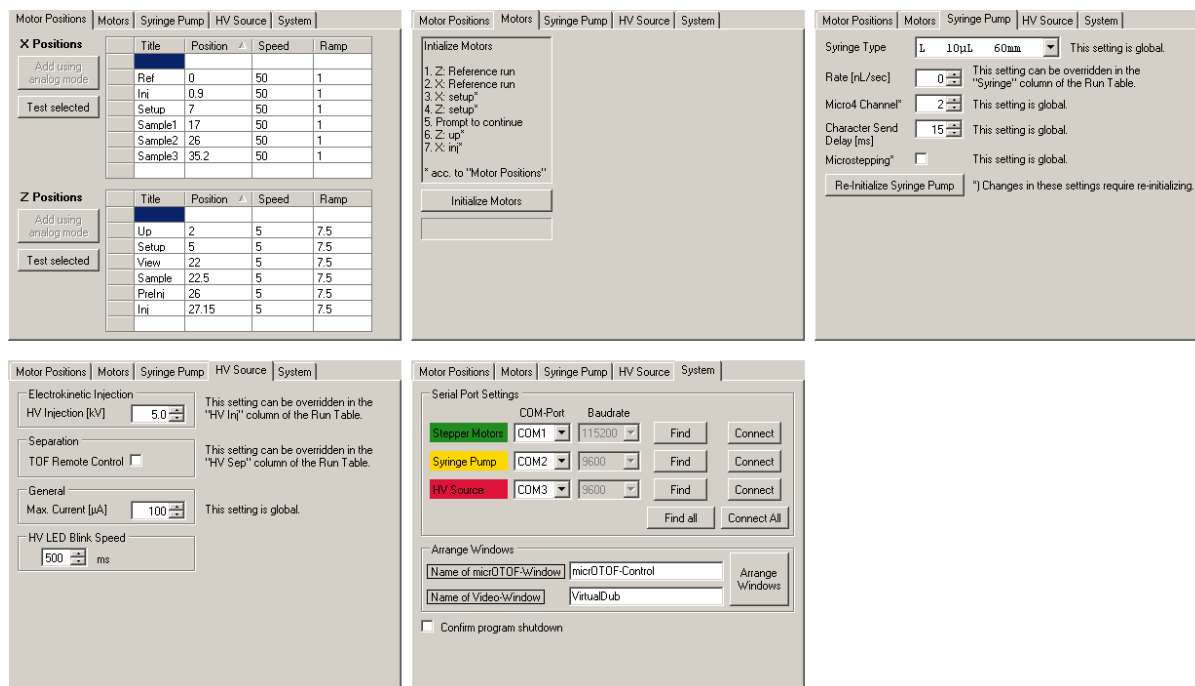


Fig. 14: All five tabs of the “Settings” form.

Manual form. The “Manual” (Fig. 15) form allows quick access to most instrument features outside the run table.

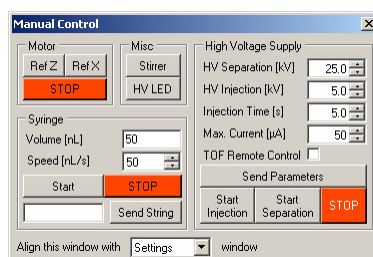


Fig. 15: The “Manual” form.

Log form. CBI-Control logs all important events to a table on the “Log” form (Fig. 16). All communication sent to and received from the external devices is shown here, with additional notes entered at relevant points during program execution. It mostly aids debugging of the experimental setup, serial connections, and the software itself. The log is exported to a text file at program shutdown or upon user request.

Time	Device	Serial Com	Action/Message
13:10:42.100	WARNING	HV Src	HV Source not found.
13:10:42.116	Motor <		Searching for Motor...
13:10:42.491	WARNING	Motor	Motor not found.
13:10:42.507	Syringe <		Searching for Syringe Pump...
13:10:42.913	WARNING	Syringe	Syringe Pump not found.
13:10:42.929	HV <		Searching for HV Source...
13:10:43.335	WARNING	HV Src	HV Source not found.
13:10:43.355	WARNING		Some or all devices could not be connected successfully. See above for details.
13:10:43.362	Motor <	#2W=1	Repetitions = none
13:10:43.413	ERROR	Motor	The port is closed.

Fig. 16: The “Log” form.

User desktop. CBI-Control was designed with minimal space requirement on the user desktop in mind, since other programs would have to be visible at the same time. Fig. 17 shows the user desktop during a CE-MS separation following an injection procedure. The TOF-MS data acquisition software, CBI-Control (with the “Log” form deactivated) and software displaying a life microscopic image of the injection area inside the injection cell, are all visible and use the space as efficient as possible.

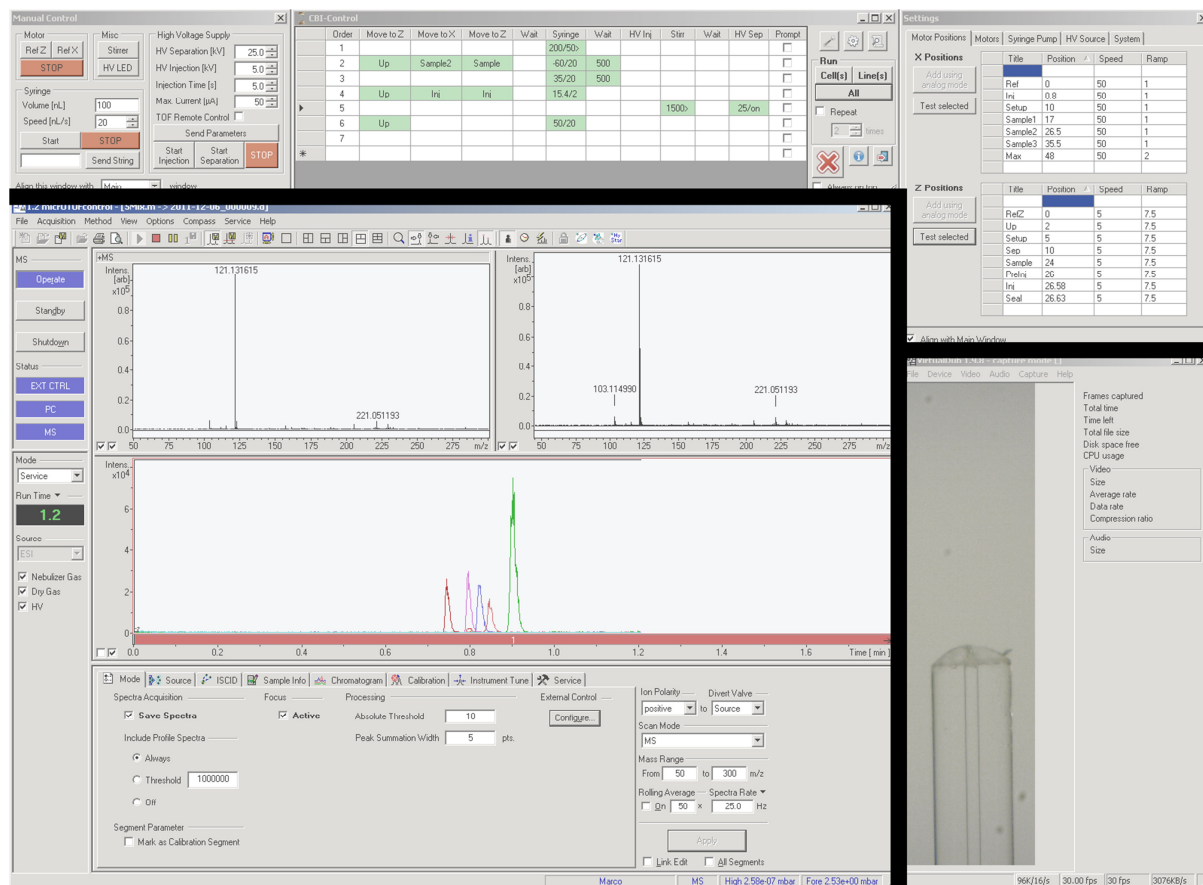


Fig. 17: User desktop during CBI-CE-MS experiments. The TOF-MS data acquisition software occupies the largest single space (center), CBI-Control is located at the top, and a video display and recording software is located at the bottom right.

3.8.3 Program Structure

Following the object-oriented nature of the Visual Basic programming language, important routines were grouped into modules and class definitions were created for the external devices. Data relating to the program and user interface was stored in a settings file. Data relating to the injection process, specifically motor positions and the run table, was stored in a Microsoft Access database file. This allowed simple access and manipulation with an external program, and had the additional advantage of automated immediate data synchronisation upon user input, preventing data loss in cases of unexpected program failure.

The “Com” module handles all serial communication with external devices. This includes operation of the serial ports, finding of and connecting to devices, as well as sending commands and receiving responses. These routines represent the lowest-level device communication and are used by the device classes.

The classes “SyringePump”, “StepperMotor” and “HighVoltageSource” expose all relevant parameters, and include routines to initialise, parameterise, command, and analyse the status of the corresponding devices. These routines represent the higher-level device communication used throughout the program.

The module “Action” handles the execution of all user-selected actions for an injection process, by retrieving and checking the parameters entered in the run table and executing the corresponding device-specific commands.

The module “Dbg” provides logging functionality to all other routines, feeds the log window, and exports log files at program shutdown and user request.

The module “WindowManipulation” contains routines to find windows of other programs and manipulate their position and size. This is used to optimise the user desktop for space usage efficiency as described in the preceding section.

The classes belonging to the forms (“Form1”, “Form_Settings”, “Form_Manual”, “Form_Log”) mainly take care of user interaction. In addition, the class “Form1” (belonging to the main form) handles the application’s startup and shutdown, and manages data exchange between the run table and the database, including input validation. The class

“Form_Settings” manages data exchange between the motor positions tables and the database, including input validation.

4 Fast Capillary Electrophoresis–Mass Spectrometry

Development of methods for and study of fast CE–MS was initially conducted by using a model system. Section 4.1 focusses on fundamental aspects regarding parameter influence and optimisation procedures.

An application of this procedure to a bioanalytical problem is detailed in section 4.2. At the same time, emphasis is put on the effect of a counter-electroosmotic migration situation on the fast CE–MS methodology.

With the previous sets of analytes being investigated in aqueous BGEs, sections 4.3 and 4.4 focus on fast CE–MS separations under non-aqueous conditions and discuss the differences arising from this change in BGE chemistry.

4.1 Method Development

In this section, the development of a fast CE–MS method is discussed based on a model system (see section 1.6.1, pg. 12, for a detailed discussion) consisting of the main catecholamines dopamine, epinephrine, norepinephrine, as well as histidine and the epinephrine-analogue isoproterenol.

First, parameters relating to the CE–ESI–MS coupling that influence separation and detection efficiencies are investigated with a focus on effects that become more important with faster separations. Then, the influence of high electric field strengths and capillary dimensions on separation efficiency is discussed.

4.1.1 Optimisation of ESI Parameters

Transfer of the analytes from the separation capillary to the mass spectrometer was achieved using a coaxial sheath-liquid ESI interface. In order to successfully achieve a stable Taylor cone for ESI-MS experiments, a number of correlated parameters need to be adjusted, including geometry of the sprayer tip, composition of the solvent (pH, conductivity, surface tension, viscosity, evaporation), its flow rate, as well as the potential difference between spray and MS inlet (electrospray high voltage). [94] The use of a coaxial sheath-liquid sprayer employed in this work simplifies optimisation by utilizing a sheath liquid, which greatly diminishes the influence of CE buffer composition due to dilution of the solvent, and nebulizer gas, which aids spray formation. Sheath liquid flow rate and nebulizer gas

pressure were found to be of particular importance. While conducting CE experiments, a second high voltage circuit terminates at the ESI tip, which acts as shared electrode. It has been shown that the two resulting electrolysis processes do not cancel each other out, but instead take place side-by-side, [95] which can impair the stability of the spray. It was observed that combinations of sheath flow and nebulizer gas that create a stable spray under non-CE conditions might prove to result in an unstable spray during CE experiments, so that parameters needed to be confirmed under both conditions.

An unstable electrospray leads to varying ionisation conditions, making separations and especially signal intensities irreproducible. The noise of the total ion current (TIC) is a good indicator for spray stability as a high noise level can be attributed to unstable spray conditions in many cases. [96] In addition, microscopic images of the sprayer tip and the electrospray (see section 3.4.4, pg. 26, for experimental details) were found to give insights into the effects of different parameters.

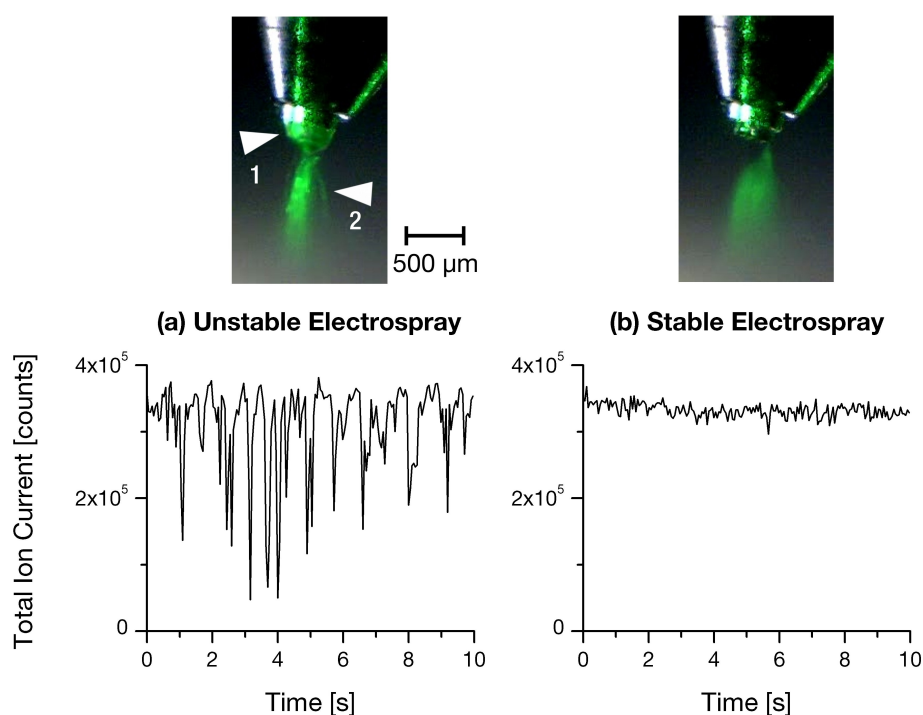


Fig. 18: Recordings of the total ion current (TIC) and microscopic pictures of the electrospray under unstable (a) and stable spray conditions (b). The ESI interface was operated at a sheath liquid flow rate of $8\mu\text{L}\cdot\text{min}^{-1}$ and nebulizer gas pressures of 0.4 (a) and 1.0 bar (b). The capillary was filled with electrolyte and a potential of 35kV was applied. The spray was illuminated by directing a green laser pointer at the spray just below the end of the interface. The arrows indicate a large volume of sheath liquid (1) and visible droplets (2).

Fig. 18 shows TIC recordings under unstable and stable spray conditions as well as microscopic pictures of the electrospray with a CE high voltage of 35 kV applied to the separation capillary. Comparing the microscopic pictures, the presence of a large volume of sheath liquid (arrow 1) is visible during operation with a low nebulizer gas pressure. This situation leads to considerable peak broadening under CE conditions as discussed below. The main difference between unstable and stable spray conditions is the size of the droplets that leave the interface (arrow 2). While there are visible large droplets under low nebulizer gas pressure conditions, a uniform spray is formed using a higher pressure. A further increase in nebulizer gas pressure can lead to a situation where sheath liquid is drawn out at a higher rate from the ESI capillary, which carries the sheath liquid, than the actual sheath liquid flow rate. This leads to intermittent absence of sheath liquid at the sprayer tip, causing a TIC recording similar to that shown in Fig. 18 (a). It could be argued that under the high nebulizer gas pressure conditions used in Fig. 18 (b) and throughout this study, spray formation is influenced highly by pneumatic nebulization and less by the electrospray process.

Looking at the influence of the sheath flow rate on spray stability and dilution, the result of a series of experiments is shown in Fig. 19.

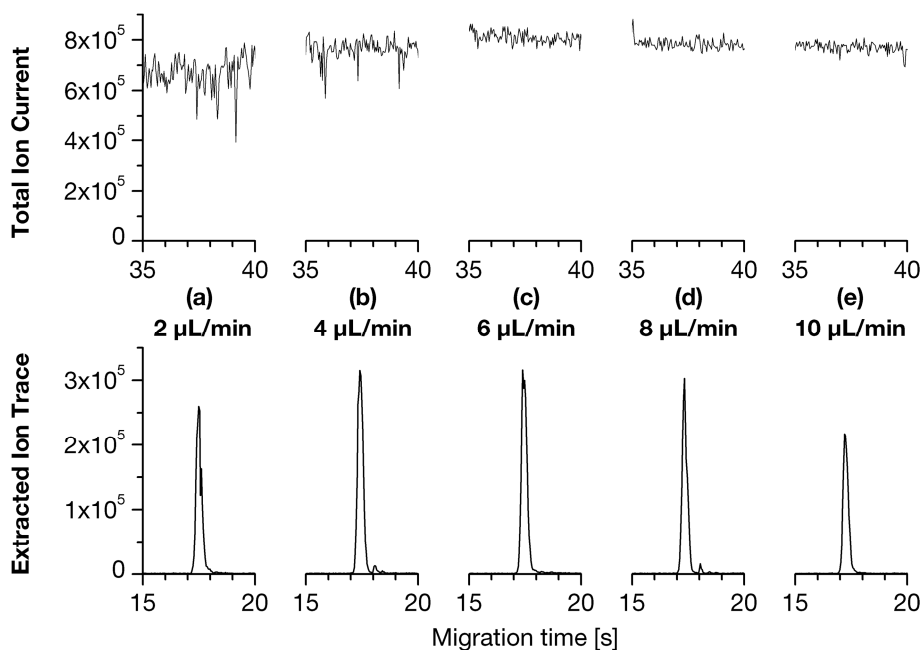


Fig. 19: Influence of the sheath liquid flow rate on sensitivity and spray stability for dopamine determinations. Total ion current (TIC) recordings (upper), as well as extracted ion traces (lower), are given for sheath liquid flow rates from 2 to 10 $\mu\text{L}\cdot\text{min}^{-1}$ (a – e). Injected amounts were adjusted to correspond to 2% of the capillary length. Nebulizer gas pressure was 1.0 bar.

In contrast to the frequently cited disadvantage of sheath liquid interfaces, [97] no significant dilution (as should be visible by decreased peak height) could be observed over a wide range of sheath flow rates. It should be noted that injection times were adjusted for each experiment to achieve a sample plug corresponding to 2% of the capillary length. This way, possible variations in suction pressure can be ruled out as an explanation for almost identical peak heights. However, these results clearly show the negative influence of *too low* a sheath flow rate on spray stability, as shown by a high TIC noise level (Fig. 19 a and b).

Unfavourable sheath flow rate and nebulizer gas pressure settings can lead to situations where analyte zones are retained at the interface tip. Particularly in fast CE experiments, this leads to considerable peak broadening. This effect has been observed when the conditions at the ESI tip allow for a partial backflow of CE effluent to the sheath liquid bulk phase around the separation capillary. A situation where a larger amount of sheath liquid accumulated at the interface tip can be seen in Fig. 18 (a), indicated by arrow (1). Fig. 20 compares two separations where different nebulizer gas pressure settings strongly affected peak tailing. A lower nebulizer gas pressure setting (a) allows for the formation of a sheath liquid dead volume, while a higher nebulizer gas pressure (b) leads to a direct transfer of the CE effluent to the spray.

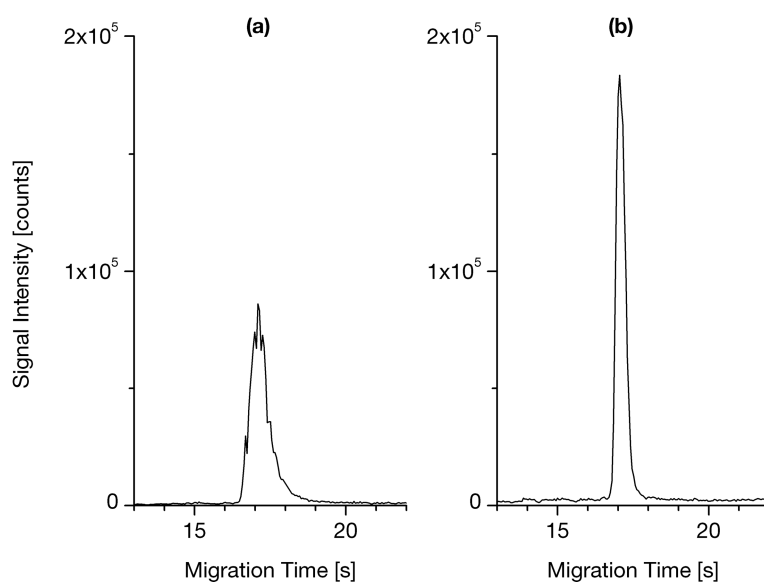


Fig. 20: Influence of nebulizer gas pressure on peak broadening at the ESI interface tip for dopamine determinations. Extracted ion traces for CE separations with a nebulizer gas pressure of 0.6 bar (a) or 1.0 bar (b) are shown. Sheath liquid flow rate was 8 $\mu\text{L}/\text{min}$.

Generally, higher sheath flow rates and nebulizer gas pressure settings have been found to aid both stable spray formation and reduced peak broadening at the interface under the present conditions. A sheath flow rate of $8\ \mu\text{L}\cdot\text{min}^{-1}$ and a nebulizer gas pressure of 1.0 bar were chosen for all further experiments.

4.1.2 Fast CE–MS Separations

Due to the usage of an acidic BGE, the electroosmotic flow is largely suppressed, [98] so that the residence time of the analytes in the separation capillary mainly depends on their individual electrophoretic velocity and the laminar flow caused by the suction pressure. Typical CE–MS protocols found in the literature for the separation of these compounds result in migration times between 15 and 25 mins. [99, 100]

Based on the optimised conditions above and using a combination of short capillaries and high electric field strengths, very fast CE–MS measurements could be realized. Fig. 21 shows a separation of all model analytes under optimised conditions in 20 s (35 s with EOF). With peak at half maximum between 0.2 and 0.3 s, the TOF-MS was operated at a sampling rate of 25 Hz (full spectra per second).

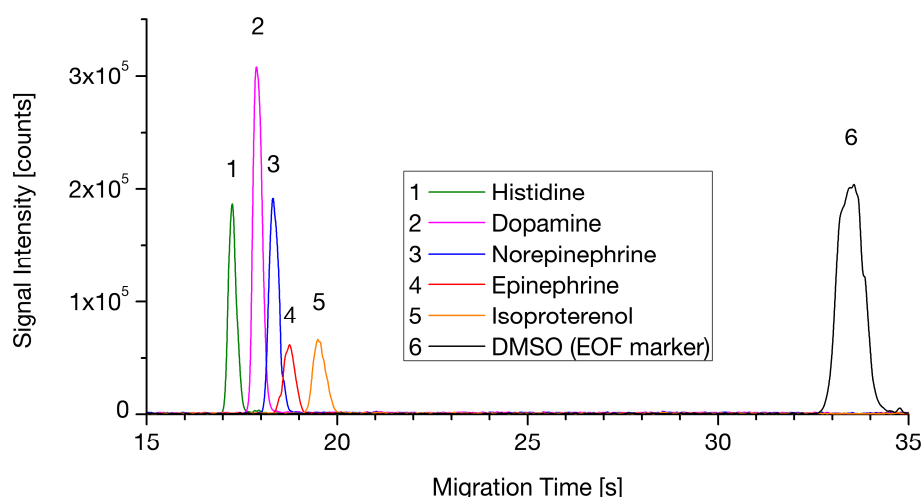


Fig. 21: Fast CE–ESI–TOF–MS separation under optimised conditions. Extracted ion traces for the analytes and DMSO (EOF marker) are shown. The separation was carried out at 35 kV in a $28\ \text{cm} \times 50\ \mu\text{m}$ capillary (equaling $1.25\ \text{kV}\cdot\text{cm}^{-1}$). The BGE was 0.1 M formic acid, the sheath flow rate was $8\ \mu\text{L}\cdot\text{min}^{-1}$ and the nebulizer gas pressure 1.0 bar; these parameters were kept constant for all following measurements, unless otherwise noted.

A comparison of separations at different electric field strengths up to $1.25\ \text{kV}\cdot\text{cm}^{-1}$ is shown in Fig. 22. Higher field strengths have two main effects: Comparing the two extremes of this series (0.50 and $1.25\ \text{kV}\cdot\text{cm}^{-1}$), migration times are drastically reduced from 70 to 20 s, and

signal intensities increase three-fold. In addition, closer inspection of these separations reveals that the latter effect is slightly more pronounced than the former, leading to an increase in resolution. As can be seen in the graph, compounds 2, 3 and 4 are not baseline-separated, however, a slight peak overlap in ESI-TOF-MS is considered to have no substantial influence on the ionisation efficiency, of either compound, [101, 102] and hence quantification. A separation high voltage of 35 kV (equalling a field strength of $1.25 \text{ kV}\cdot\text{cm}^{-1}$ in the 28 cm long capillaries used) was chosen for further experiments. Repeatability was found to be 0.92% for migrations times and 10% for peak heights (expressed as relative standard deviation of $n = 9$ consecutive measurements).

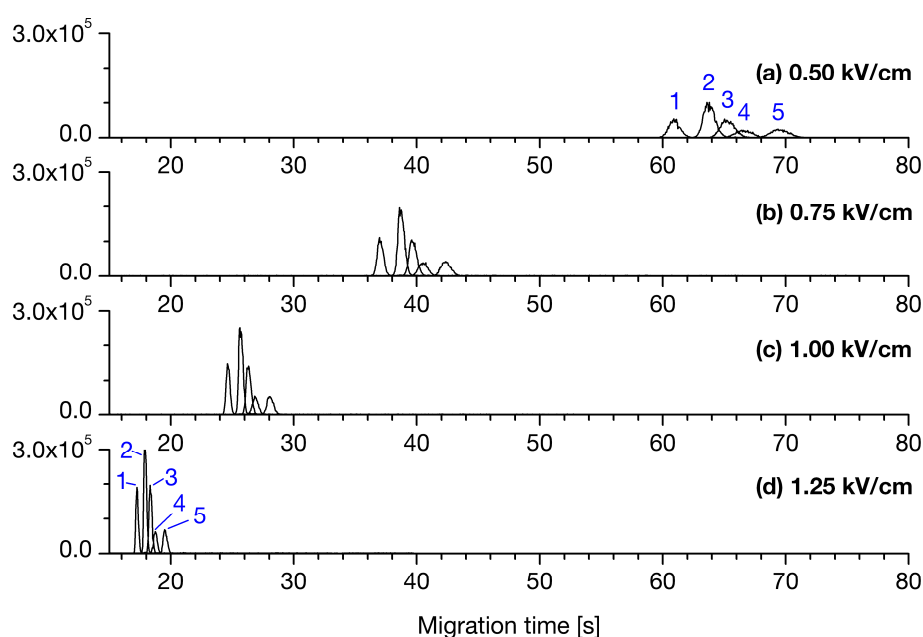


Fig. 22: Separations of the model analytes at field strengths of 0.50 (a), 0.75 (b), 1.00 (c) and $1.25 \text{ kV}\cdot\text{cm}^{-1}$ (d) (14, 21, 28 and 35 kV, respectively). Other conditions and peak numbering as in Fig. 21.

4.1.3 Advantages and Disadvantages of Small ID Capillaries

When detailed analytical information about microenvironments is required, the spatial resolution that can be obtained largely depends on the necessary sample volume for the analytical method. When cell structures or single cells comprise the sample of interest, only very small volumes of surrounding medium can be used for analysis. The simplest approach for reducing the injected sample volume in CE is to decrease the injection time. With an injection time of only 5 s though, not more than a five-fold decrease can be achieved without problems in the injection protocol. The use of smaller ID capillaries on the other hand offers more advantages. With decreasing ID, the suction pressure-induced laminar

flow in the capillary is greatly reduced, leading to reduced band broadening. Additionally, the electrophoretic current in the capillary is reduced, which largely eliminates band broadening caused by Joule heating. Both laminar flow and electrophoretic current in the capillary depend on the square of the ID. This allows for the use of BGE with a higher conductivity, e.g. higher BGE concentrations or a wider range of BGE compositions.

Fig. 23 shows electropherograms for separations in 28 cm long capillaries ranging from 75 to 5 μm ID. Injection conditions were adjusted in such a way that the injection plug length is kept constant at 2% of the capillary length.

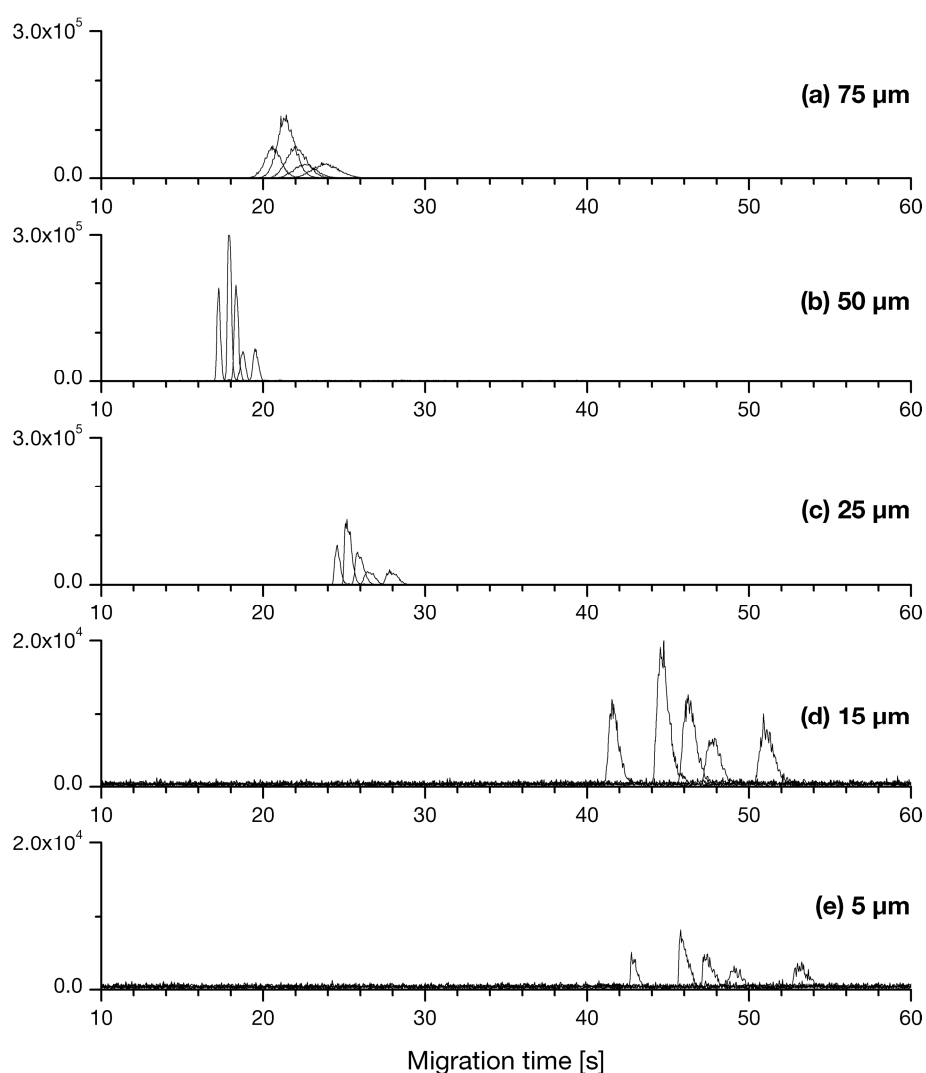


Fig. 23: Influence of the capillary ID on migration times and sensitivity for capillaries with 75 (a), 50 (b), 25 (c), 15 (d) and 5 μm ID (e). Injection conditions were adjusted to correspond to 2% of the capillary length. BGE was 50 mM (a) or 100 mM (b–e) formic acid. Other conditions as in Fig. 21.

A number of effects can be seen here. Firstly, a large ID leads to excessive Joule heating. In the case of the 75 μm ID capillary, the buffer concentration had to be lowered to 50 mM and the capillary was cooled with a strong stream of cooled nitrogen gas (see section 3.4.3, pg. 25, for experimental details), in order to successfully apply the separation voltage. Nevertheless, the electropherogram still shows strong peak broadening. Secondly, the laminar flow through the capillary decreases with decreasing ID, so that separation times increase from 20 up to 55 s. Lastly, the main drawback of decreased sample volume shows in a reduction of signal intensity. When comparing results for the 50 and 5 μm ID capillaries, peak height decreases by a factor of 25. However, the amount of injected sample decreased by a factor of 100, from 11 nL to 110 pL. This apparent four-fold *increase* in MS sensitivity is attributed to a more efficient ionisation and transfer of analytes into the MS.

The reduced electrophoretic current in capillaries with smaller IDs leads to more freedom in the choice of BGEs. Buffer compositions, which are less MS-compatible are not as likely to be the cause of concern, since the overall (volumetric) flow into the MS is very small. It is possible to work with buffer concentrations far beyond the limit of traditionally employed capillaries. Fig. 24 shows separations in a 28 cm \times 5 μm capillary using formic acid as BGE in concentrations ranging from 50 mM up to 20 M (pure formic acid being 26 M). While separation times increase due to a more strongly suppressed EOF, analyte zones are compressed, leading to narrower and higher signals up to optimum values reached at a formic acid concentration of 5 M (pH 1.5). No sign of capillary deterioration resulting from the use of this BGE was observed, however the initial run-in period was longer when compared to BGE concentrations in the mM range. The increased resolution of this separation could be used to either separate mixtures that are more complex, or employ shorter capillaries, leading to separation times shorter than the optimum values reported here. The latter, however, is impractical for use with the experimental setup used here, because the sheath liquid sprayer occupies about 12 cm of the capillary and the manual injection protocol requires a certain length of capillary. An application of the combination of shorter capillaries and BGEs with a higher concentration is shown in section 5.7 (pg. 89) using the CBI setup.

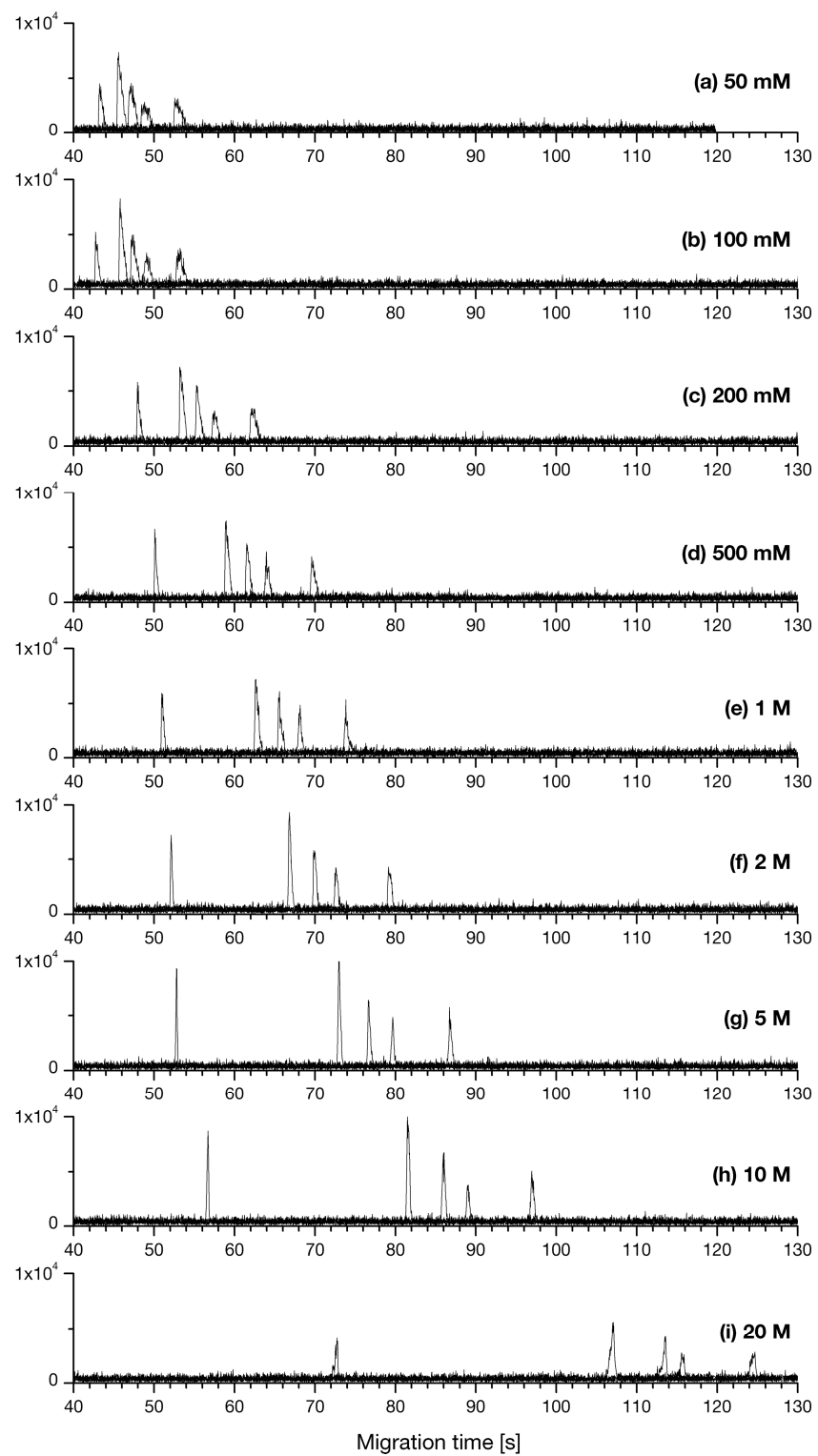


Fig. 24: Effect of BGE concentration on migration times and separation efficiency. BGE was aqueous formic acid with concentrations of 50 mM (a), 100 mM (b), 200 mM (c), 500 mM (d), 1 M (e), 2 M (f), 5 M (g), 10 M (h) and 20 M (i). Separations were carried out in a 28 cm \times 5 μ m capillary at 1.25 kV \cdot cm $^{-1}$. Other conditions as in Fig. 21.

4.1.4 Conclusions

Based on a model system consisting mainly of catecholamines, efficient CE–MS separations can be completed in 20 s. The usage of short-length capillaries in conjunction with high electric field strengths was most important in achieving these fast separations. The main drawback using current commercial CE instrumentation in conjunction with MS lies in the usage of long capillaries, which leads to long migration times. Using the approach shown in this section, CE separations on the timescale of seconds can be done while maintaining compatibility with MS. This is particularly advantageous when compared to microchip-based CE, which requires rather long times for sample change, features large sample dead volumes to fill on-chip reservoirs, and is more difficult to hyphenate with MS.

Whilst current HT-CE systems are based on separations in (long) parallel capillaries, which is incompatible with MS, this approach based on short capillaries could be used to devise HT-CE systems with MS detection. This would greatly increase their usefulness in areas concerned with metabolomics, where mass spectrometric information is required.

Separations in capillaries with IDs smaller than 50 μm offer two major advantages: Firstly, it is possible to study sub-nL sample volumes. Secondly, the greatly reduced Joule heating allows for the use of higher BGE concentrations (up to the mol/L range in case of formic acid), which leads to sharper signals. At the same time they pose a challenge for both detection and injection systems.

4.2 Application to Hyaluronan Oligomers

This section details the development of a fast CE–MS method for the analysis of hyaluronan oligomers (see section 1.6.2, pg. 12, for a discussion of the analytes). This method development relies on results obtained from the investigations laid out in the preceding section, and applies them to the counter-electroosmotic separation situation, which is encountered with these analytes. Later, the method is applied to enzymatic digests.

Starting from a typical set of CE method parameters for hyaluronan oligosaccharide analysis, capillary length, capillary ID, buffer concentration, and buffer pH were optimised. It should be noted that different combinations of the parameters investigated were explored, but only the relevant ones are presented in a logical order. Peak height and peak width at half-maximum are used to compare separations.

4.2.1 Capillary Length

The strong influence of the electric field strength on separation speed and efficiency was already demonstrated in section 4.1.2 (pg. 50). There, increasing separation high voltages were applied to the same capillary, increasing the field strength. Most CE instruments, whether commercial or laboratory-built, however, have an upper limit of the high voltage they can deliver in the 30 kV range. Here, the focus is put on the effects of reducing the capillary length while keeping the separation high voltage constant, again increasing the field strength.

Fig. 25 compares separations obtained at 35 kV in capillaries of different length. The reduction in capillary length and increase in field strength lead to three effects. 1) The separation time decreases from over 7 to 1.3 min; 2) the separation efficiency is almost not adversely affected; 3) signal intensities increase initially and then stay constant. The latter result is of particular interest, since the relative injection amount is kept constant at 2% of the capillary length, but the absolute injection amount decreased with capillary length. A capillary length of 28 cm and a high voltage of 35 kV (corresponding to $1.25 \text{ kV}\cdot\text{cm}^{-1}$) were chosen for all further experiments.

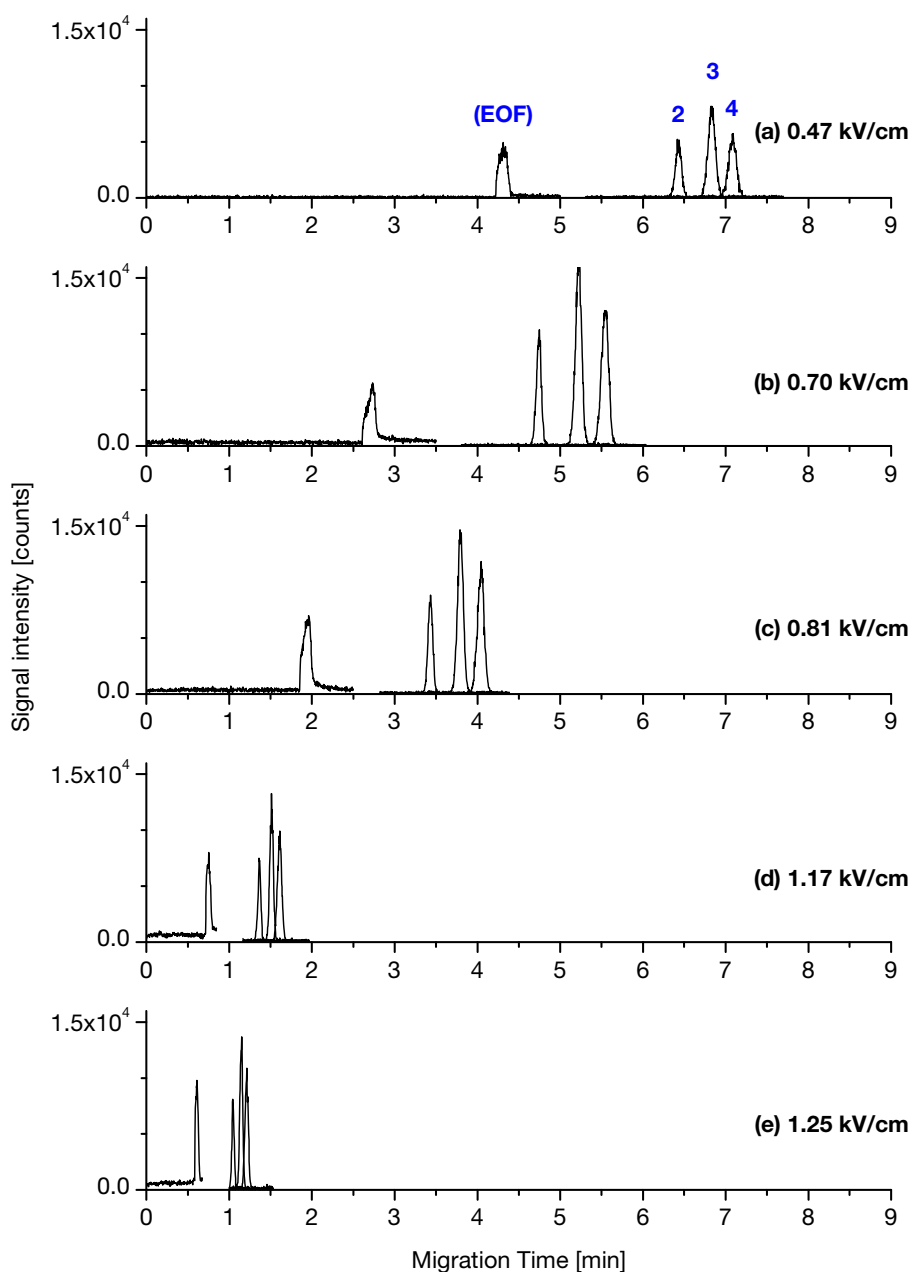


Fig. 25: CE-MS determinations of the three hyaluronan oligosaccharides at different electric field strength, but constant separation high voltage of 35 kV. Mass traces shown are extracted ion traces. Ion selection for all traces is discussed in section 3.6.4, pg. 32. Analytes were 20 μ M and signals numbered as in Fig. 3 (pg. 13). Separation capillaries were of 50 μ m ID and 75 cm (a), 50 cm (b), 43 cm (c), 30 cm (d), and 28 cm (e) in length. BGE was 25 mM NH_4OAc of pH 8.5.

4.2.2 Capillary ID

Method development for the separation of catecholamines showed that the usage of capillaries with smaller ID can result in an increased separation efficiency (see section 4.1.3, pg. 51). Separation efficiency was further increased by using a BGE with a higher concentration. At the same time, peak heights decreased for capillaries with ID smaller than 50 μ m.

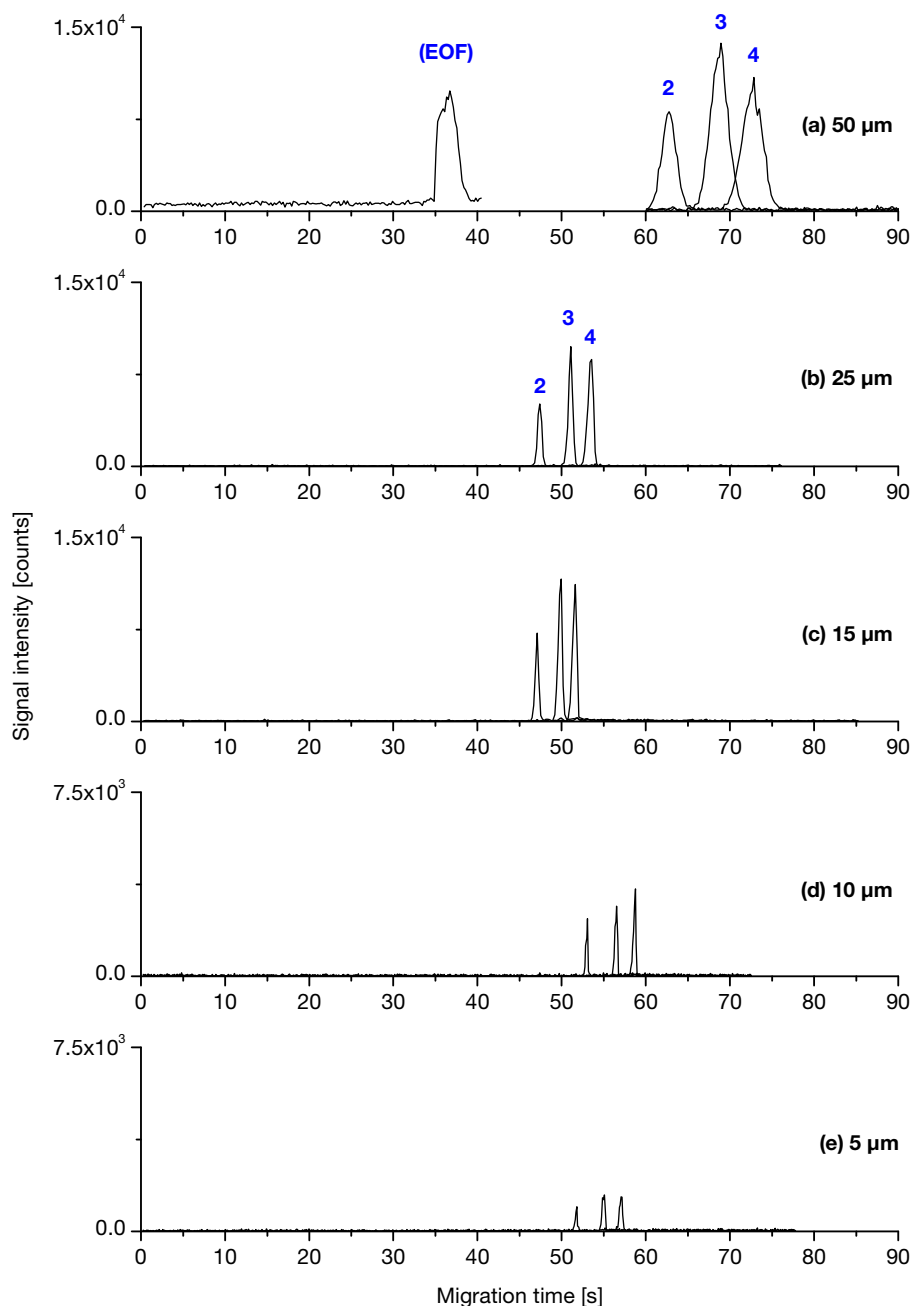


Fig. 26: Influence of capillary ID on separation. Separations at 35 kV were done in capillaries of 28 cm length (corresponding to $1.25 \text{ kV} \cdot \text{cm}^{-1}$) and 50 μm (a), 25 μm (b), 15 μm (c), 10 μm (d), and 5 μm (e) ID. BGE composition, analyte concentration and signal numbering as in Fig. 25. Data acquisition rate was 5 Hz (a–c) and 10 Hz (d, e).

Here, the latter effect is much less pronounced. As can be seen in Fig. 26, peak heights remain constant from 50 to 15 μm ID, even though the injection volume decreases by a factor of 11. For ID 10 and 5 μm , peak heights decrease noticeably. Separation efficiency improves with decreasing capillary ID. The resulting narrower peaks required an increase in the data acquisition rate from 5 to 10 Hz. While this change had no influence on signal-

to-noise ratios, absolute signal intensity decreased by a factor of two. Y-axis scaling in Fig. 26 was adjusted accordingly.

A capillary ID of 15 μm was chosen for further experiments. Out of the ID investigated, it was the smallest without noticeable peak height decrease while allowing a wider choice in BGE conductivity.

4.2.3 BGE Composition

BGE optimisation started with conditions reported for CE-UV methods, [64, 65] which were adjusted to be compatible with ESI-MS by replacing the phosphate/borate buffer system with an ammonium acetate buffer.

The BGE used here was aqueous NH_4OAc , adjusted to the desired pH. The concentration of this buffer had an unexpected effect on separations as is shown in Fig. 27.

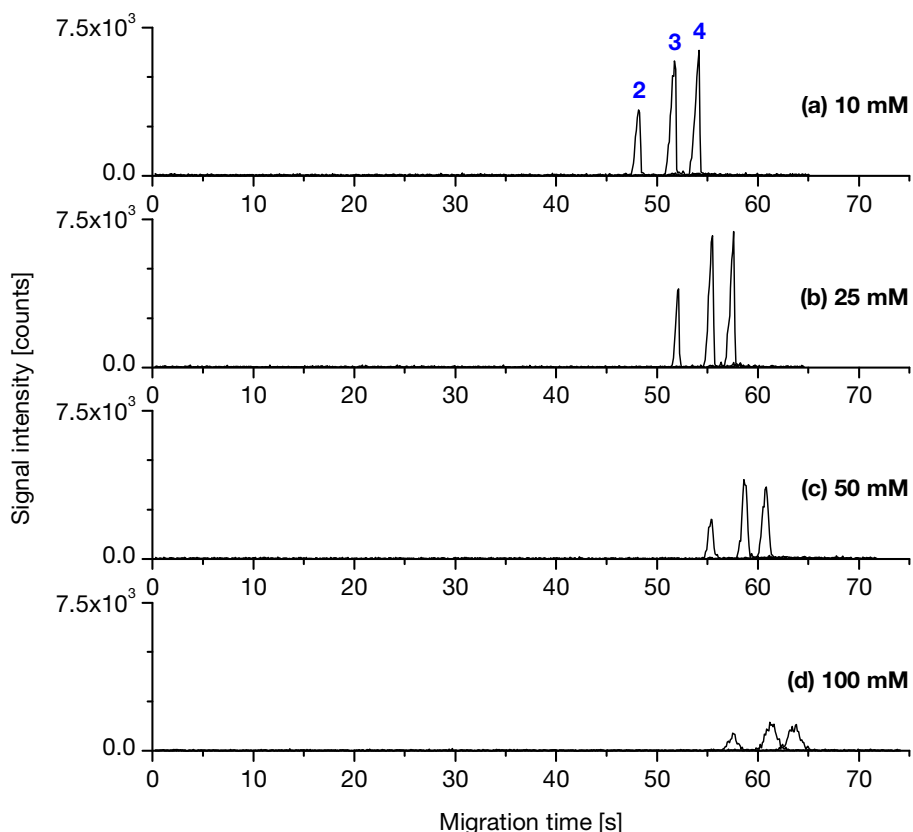


Fig. 27: Influence of BGE concentration on separation. BGE was 10 mM (a), 25 mM (b), 50 mM (c), and 100 mM (d) NH_4OAc , adjusted with ammonia to pH8.5. Separation capillary was of 28 cm length and 15 μm ID. Separations were done at 35 kV (corresponding to $1.25 \text{ kV} \cdot \text{cm}^{-1}$). Analyte concentration and signal numbering as in Fig. 25.

An increase in buffer concentration led to a decrease in signal intensity. Since peak areas remain constant between separations with different BGE concentrations, ion suppression can be ruled out as explanation. Peak broadening due to Joule heating is more likely; for the highest concentration, 100 mM, this can be clearly seen. For further experiments, a BGE concentration of 25 mM was chosen, since it resulted in the same peak height as a 10 mM BGE, while providing a higher buffer capacity.

The influence of BGE pH is shown in Fig. 28. An increasing pH led to sharpened signals and shorter migration times, but also decreased separation efficiency. As a compromise between these parameters, a BGE pH of 8.5 was selected for further experiments.

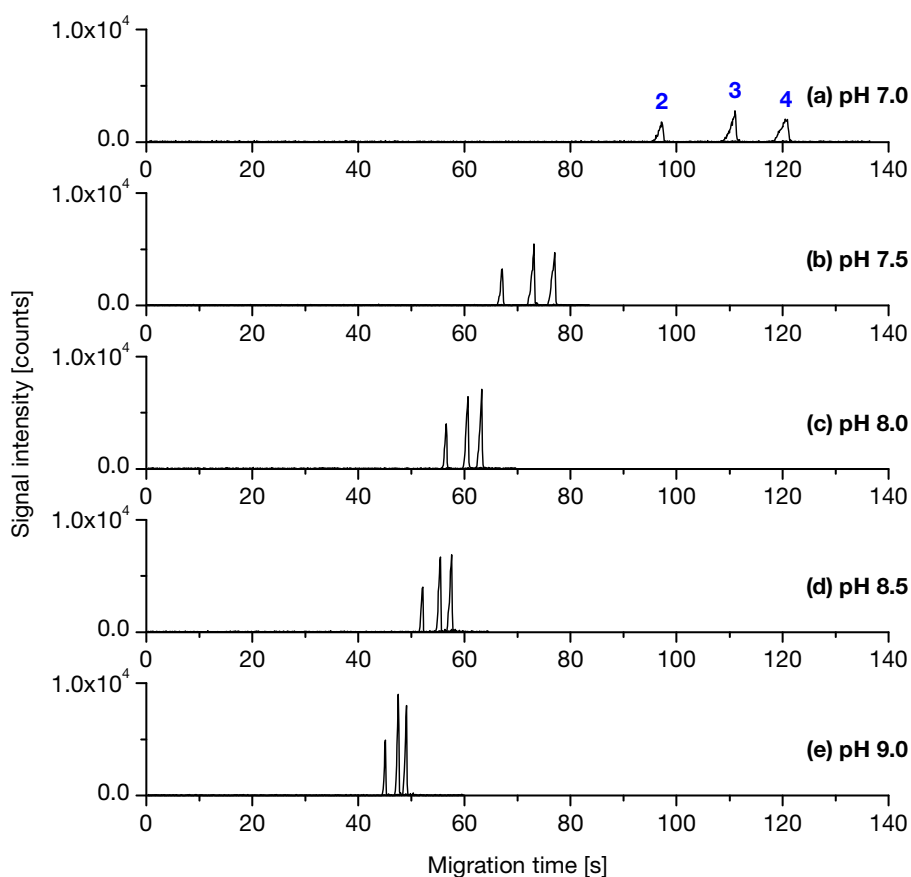


Fig. 28: Influence of BGE pH on separation. BGE was 25 mM NH_4OAc , adjusted with ammonia to pH 7.0 (a), 7.5 (b), 8.0 (c), 8.5 (d), and 9.0 (e). Other conditions as in Fig. 27.

4.2.4 Optimised Method Parameters

Capillaries of 28 cm length and 15 μm ID were found to give best results. The BGE consisted of 25 mM aqueous NH_4OAc adjusted with ammonia to pH 8.5. The limits of detection for the analytes investigated were in the range of $4\text{--}7 \cdot 10^{-7}$ M. Further figures of merit for the optimised method are summarized in Table 5. Determinations could be completed within

about 70 s after injection. When including the injection protocol and manual handling, determinations could be run at 100 s intervals under optimal conditions.

Table 5: Figures of merit for the final CE-MS method. Determinations were conducted five-fold.

Compound	2	3	4
Linear range investigated	$1 \cdot 10^{-6} \text{ M} - 4 \cdot 10^{-5} \text{ M}$		
Coefficient of determination R^2	0.997	0.997	0.993
Limit of detection (S/N = 3)	$7.6 \cdot 10^{-7} \text{ M}$	$5.2 \cdot 10^{-7} \text{ M}$	$4.6 \cdot 10^{-7} \text{ M}$
RSD of migration times (n = 5)	0.38%		
RSD of peak heights ($1 \cdot 10^{-5} \text{ M}$; n = 5)	8.1%		

No adverse effect of injecting BSA-containing samples was observed, even after repeated runs without capillary conditioning in between. Most matrix components showed very low or no electrophoretic mobility, so that the analytes were separated by about 30 s from the matrix components. Fig. 29 shows the large migration time gap between neutral components (band at 18 s) and the analytes (50–65 s). No influence on quantification could be observed when comparing samples containing only the analytes of interest and samples that contained BSA in addition.

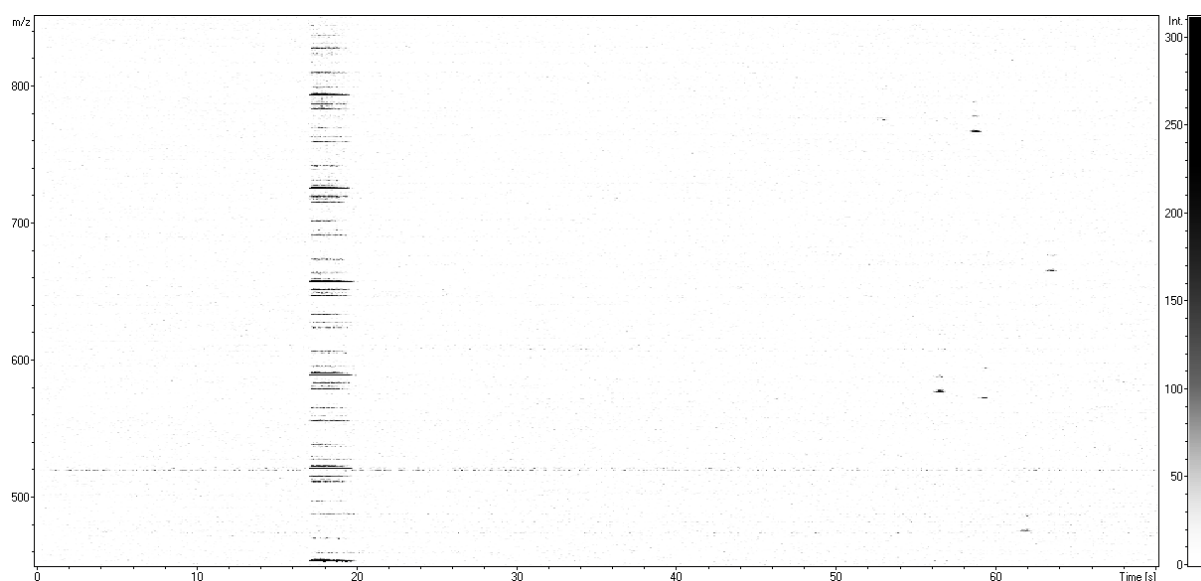


Fig. 29: Density plot of a separation of a sample containing six different analytes, as well as bovine serum albumin. Matrix components can be observed at 18 s, while the analytes of interest show migration times between 50 and 65 s.

4.2.5 Application to Hyaluronan Digest Analysis

A sample of hyaluronan was subjected to hydrolysis by bovine testicular hyaluronidase (BTH) as detailed in section 3.4.1 (pg. 22). Direct injection of digest samples led to strong peak broadening. Dilution of 1:10 with water was found to yield best signal intensity and separation efficiency. Higher dilutions resulted in a loss of sensitivity, while lower dilutions still showed peak broadening. Fig. 30 shows separations of a 2 h and a 24 h digest. In addition to the three known analytes (2, 3, and 4), a further three hyaluronan oligosaccharides could be identified, which were not previously included in the method development. The 2 h digest shows two larger oligosaccharides (5 and 6), while the 24 h digest shows formation of the monomer (1). Fig. 31 shows experimental and calculated mass spectra for compound 5, which were used for identification. The sums of peak heights within each digest show good agreement between the two samples, indicating that all products of the enzymatic digest were accounted for.

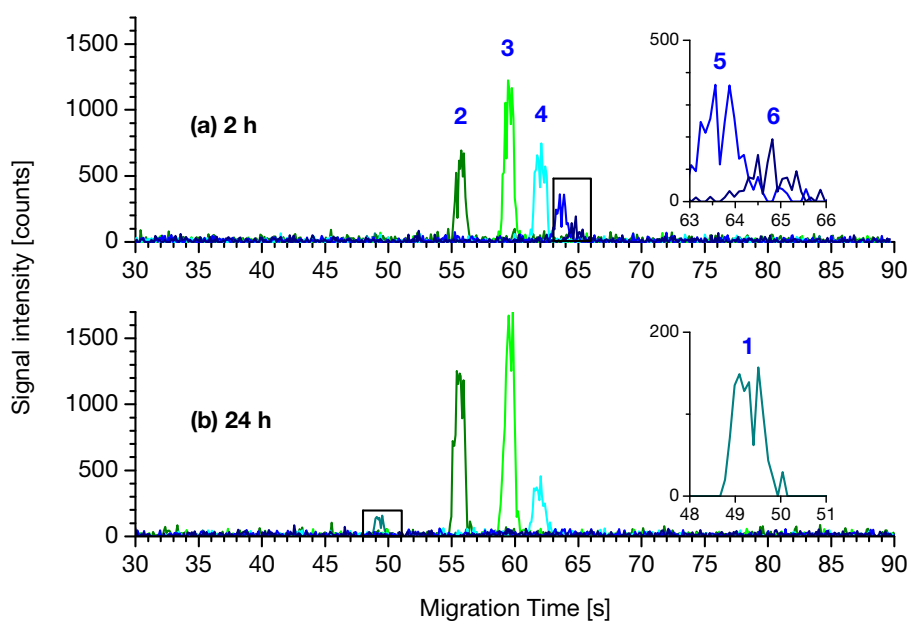


Fig. 30: CE-MS of hyaluronan digests after 2 h (a) and 24 h (b) digestion periods. Samples were diluted 1:10 prior to analysis. BGE was 25 mM NH_4OAc adjusted with ammonia to pH 8.5. Separations were conducted at 35 kV in a 28 cm \times 15 μm capillary (corresponding to 1.25 $\text{kV}\cdot\text{cm}^{-1}$). Signals 1, 5 and 6 were identified from their exact m/z values.

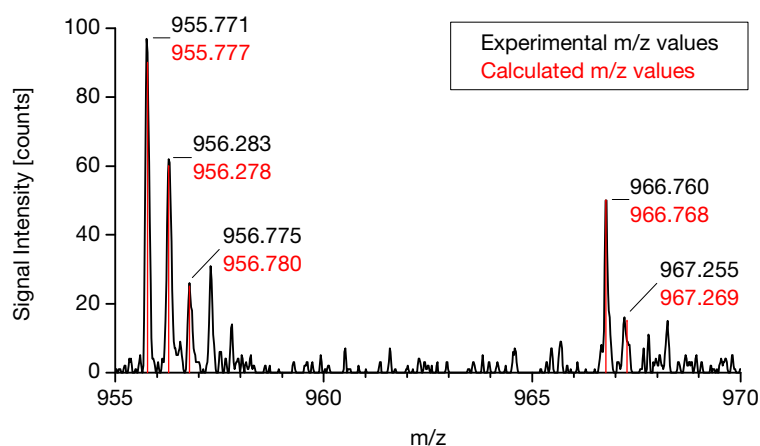


Fig. 31: Example of unknown substance identification. Experimental mass spectrum of compound 5 (Fig. 30) is shown (black), as well as theoretical (calculated) m/z values (red).

4.2.6 Application to the Analysis of a Complex Sample

Using this CE-MS method, it was possible to identify a large number of different hyaluronan oligomers in a complex mixture which is commercially marketed as “Hyalo Oligo 10,000”. Fig. 32 shows the density plot of a fast CE-MS separation after injecting a sample of high concentration.

By comparing their individual mass spectrum with calculated values, it was possible to identify 58 species, forming ten different homologous series. The charge states observed ranged from -1 to -4 . When subtracting species that were found in two different charge states, 51 distinct substances were found.

Apart from the standard oligomers ranging from $n = 2$ to 20, singly ethylated oligomers from $n = 2$ to 14, doubly ethylated oligomers from $n = 4$ to 7, and oligomers with one additional glucuronic acid unit from $n = 7.5$ to 10.5 were identified.

The advantage of combining a highly efficient separation method with high resolution mass spectrometric detection is highlighted when considering two different series of singly ethylated oligomers (migration time windows 45–59 s and 55–64 s, coloured light blue and dark blue, respectively) and two different series of doubly ethylated oligomers (40–47 s and 45–53 s, orange and red, respectively) that were found. While the compounds in each of the related series exhibit the same mass spectrum, they have a clearly distinct electrophoretic mobility. This suggests that the analytes only differ in the location of ethylation, a distinction that could not have been made with a mass spectrometric measurement alone.

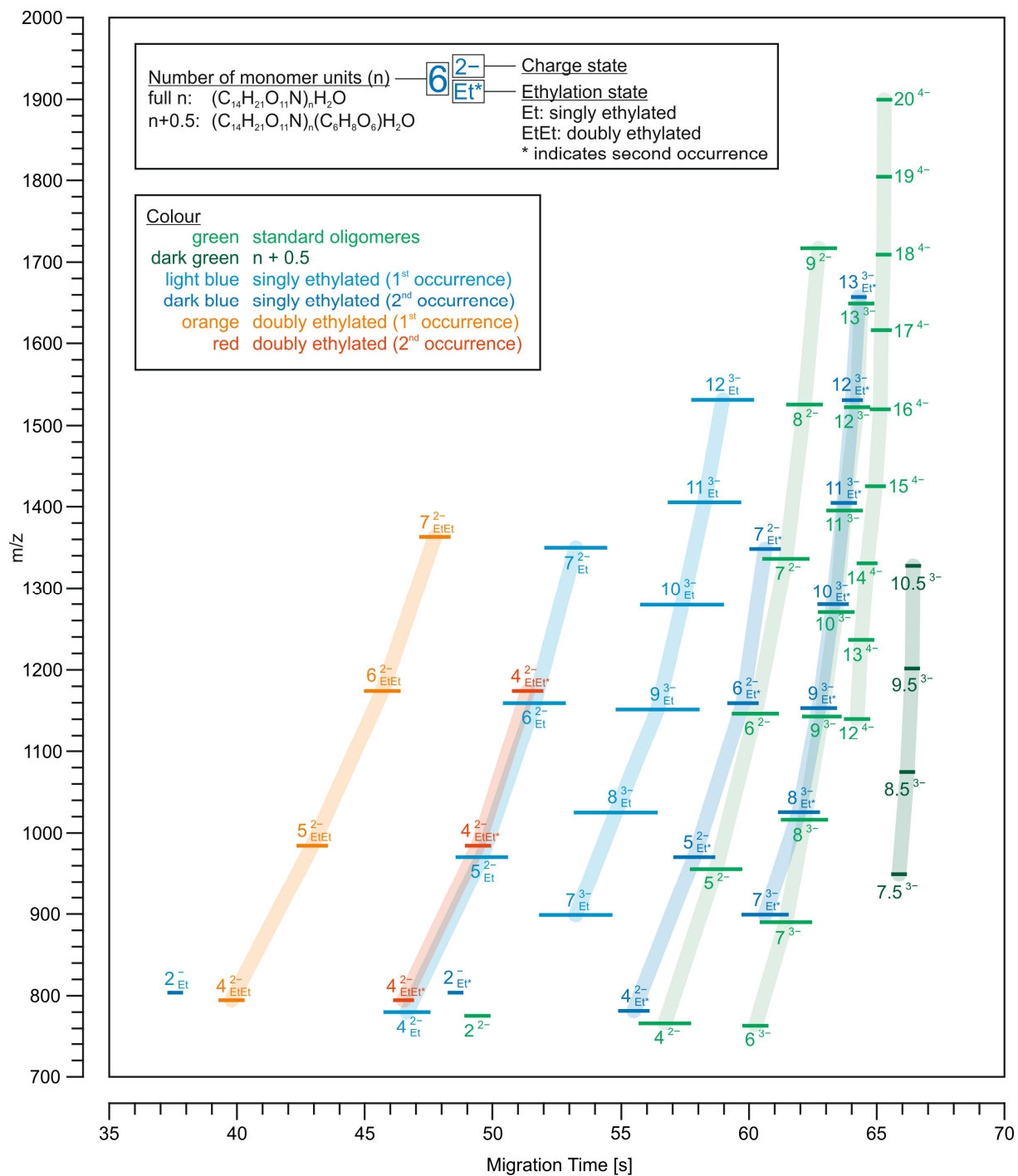


Fig. 32: Density plot of a CE-MS separation of a “Hyalo Oligo 10,000” sample. For clarity, only the identified signals are shown. Horizontal bars represent the identified signals in their respective position and horizontal extension. The different homologous series that were observed are indicated by bold connecting lines. Individual signal intensities cannot be inferred from this graph. The appendix (section 9.2, pg. 106) includes this graph as raw data as well as raw data with the identified signals overlaid.

4.2.7 Conclusions

By applying the fast CE-MS methodology to the analysis of hyaluronan, counter-electroosmotic separation conditions could be studied. It was found that fast and efficient CE-MS analyses could be completed in about one minute, when using short length fused silica capillaries in conjunction with high electrical field strengths. This is in stark contrast to established CE methods [64, 65] for these analytes, which require more than an hour to complete a single analysis. CE-MS runs were completed in 65 s and a sample throughput of about 35 samples per hour could be achieved, including sample change and a manual sample injection protocol.

High separation efficiency in combination with fast migration times could be achieved mainly by applying high electrical field strengths and capillaries of short length and small ID, as well as an optimised buffer composition. A capillary length of 28 cm is the shortest that can be applied to the CE-ESI-MS setup and allowed the application of a field strength of $1.25 \text{ kV}\cdot\text{cm}^{-1}$ at a separation high voltage of 35 kV. Surprisingly, a capillary ID of $15 \mu\text{m}$ showed the best analytical performance (both separation efficiency and signal intensity) for this separation situation, while analysis of catecholamines showed a significant loss of signal intensity for capillary ID smaller than $50 \mu\text{m}$. The optimal buffer composition was found to be 25 mM NH_4OAc adjusted with ammonia to pH 8.5.

The method could be successfully applied to hyaluronan digest samples, and additional experiments showed no deteriorating effects when injecting protein-containing samples. Therefore, only minimal sample pretreatment (filtration and dilution) is necessary.

This method has also been used in fast live kinetic studies of hyaluronidases. Further detailed studies of related enzymes regarding activity and breakdown products are planned.

4.3 Application to Organotin Speciation

This section details the development of a method for fast CE–MS of four organotin compounds (for details, see section 1.6.3, pg. 14). The buffer composition for the separation of the organotin compounds was established using a commercial CE–UV system. A non-aqueous BGE was employed for the separation of these compounds and its suitability for fast CE–MS tested.

4.3.1 CE–UV Method Development

A CE–UV method was developed for the determination of organotin compounds using an ammonium acetate/acetic acid (100 mM and 1 M) buffer system in acetonitrile/methanol (80:20). Various parameters were optimised for the separation of the organotin compounds. It was observed that an increase in the ratio of methanol to acetonitrile results in increased migration times, while a decrease leads to a decreased resolution. Therefore, an optimum ratio of 80:20 of acetonitrile/methanol was used for all further experiments. Replacing methanol with isopropanol caused the migration time to increase; however, separation efficiency remained unchanged. This can be attributed to the higher viscosity of isopropanol as compared to methanol. The effect of the ammonium acetate concentration on the separation was also studied and it was observed that at lower concentrations DBT co-migrates with TBT, while the separation time increases with the ammonium acetate concentration. The optimal concentration was found to be 50 mM. Fig. 33 shows a separation under optimised conditions. Table 6 summarizes the analytical characteristics of the final method.

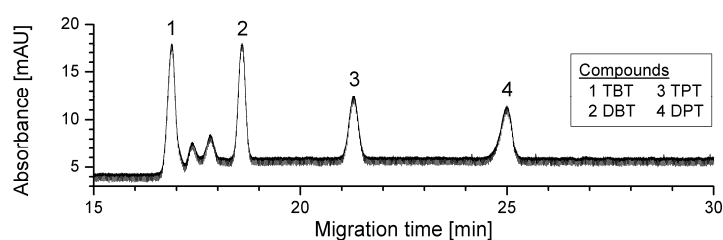


Fig. 33: Separation of the four analytes on a CE–UV system. A non-aqueous buffer consisting of acetonitrile and methanol (80:20, v/v) with 1 M HAc and 50 mM NH₄Ac was used.

Table 6: Analytical parameters of the CE-UV method.

	TBT	DBT	TPT	DPT
Calibration range		$5 \cdot 10^{-5} - 5 \cdot 10^{-3} \text{ M}$		
Regression coefficient	0.998	0.998	0.999	0.998
Limit of detection (S/N = 3) [10^{-6} M]	2.5	3.3	1.3	5.0
RSD of peak height (50 μM; n = 3) [%]	3.5	3.2	3.0	3.6
Migration time [min]	16.9	18.6	21.3	25.0
RSD of migration time (n = 3) [%]	3.5	3.2	3.0	3.6

4.3.2 Optimisation of MS Parameters

The general approach for TOF-MS method development has already been laid out in section 3.6 (pg. 31). The organotin compounds, however, required a more detailed investigation.

The mass spectrometer was tuned to work with highest sensitivity in the mass range of 250 to 700 m/z, where any species of the compounds studied were expected. For mass trace selection, individual standard solutions were injected without applying any separation voltage to the capillary. The signal clusters with typical tin isotope pattern were evaluated as to whether they can be attributed to any possible species (monomer or dimer, with different adducts). An additional set of mass spectra was then recorded under separation conditions for each compound in order to rule out solvent-dependant adduct formation due to the different solvent composition in analyte stock solution and CE buffer. For the species identified, mass spectra were simulated and compared to the experimentally obtained data. Calculated and recorded mass spectra for DPT and TPT are shown in Fig. 34. While both DPT and DBT showed two species with different adducts each (formate and acetate), TPT and TBT exhibited a tendency to form complex dimers in addition to simple molecular ions. The good agreement between theoretical and experimental m/z values allowed for the use of narrow mass windows ($\pm 0.01 \text{ m/z}$) for calculation of the extracted ion traces, effectively lowering the signal-to-noise ratio. Only singly charged ions were observed under the ionisation conditions applied.

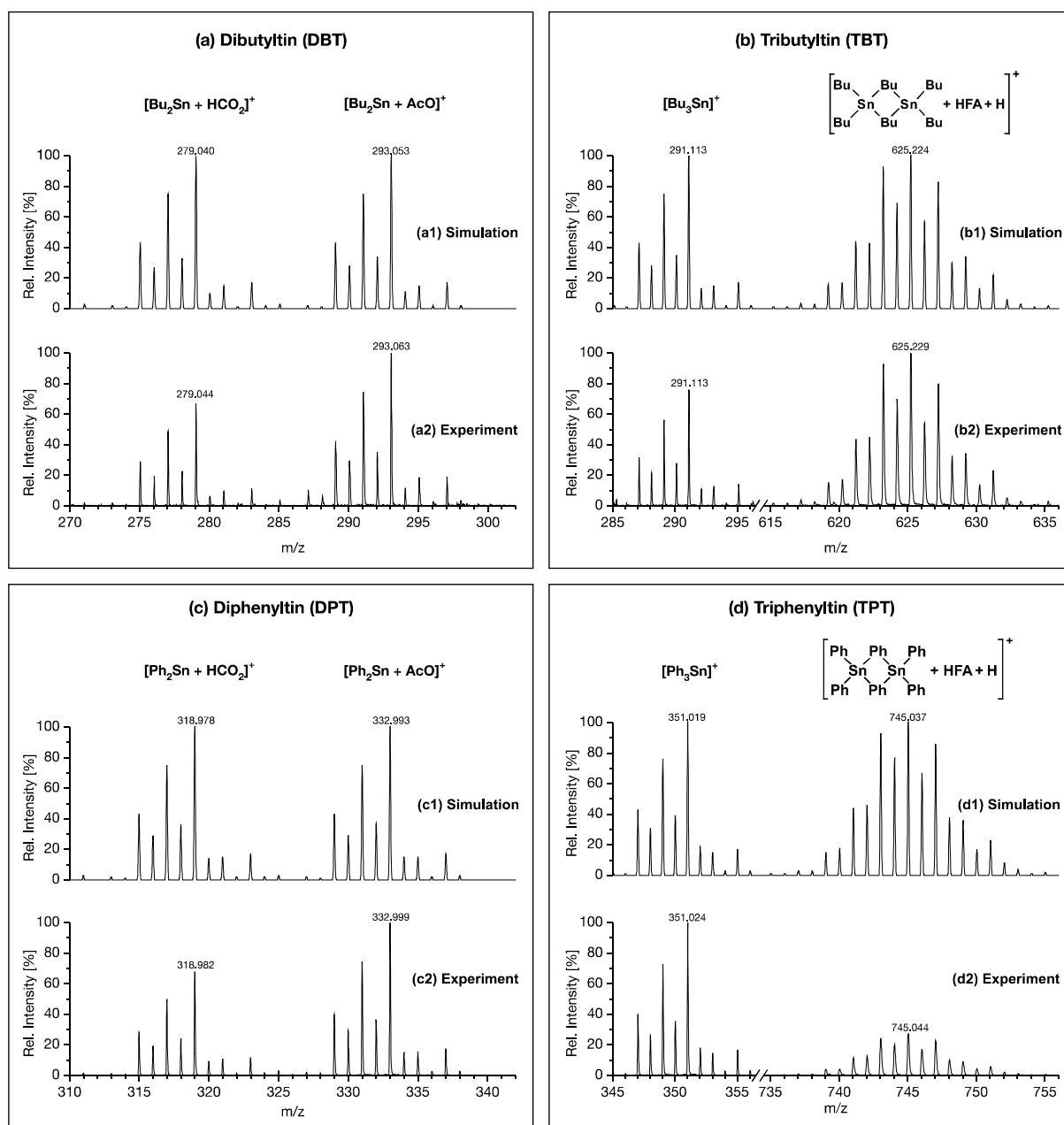


Fig. 34: Calculated and recorded mass spectra for DBT (a), TBT (b), DPT (c), and TPT (d). The proposed structures for the species found, as well as the m/z value of the base peak of each species are given.

Due to tin's complex isotope pattern, selection of m/z -signals for the calculation of extracted ion traces requires careful deliberation as to the S/N ratio obtained. While it would be possible to include all major isotope signals (intensity greater than 5% of the most abundant isotope; hence 7 signals for monomers and 13 for dimers), there would not only be an increase in sensitivity, but also in the baseline noise of the corresponding trace. For this reason, only those five individual m/z -signals with the highest intensity of a given species were used to calculate extracted ion traces, totalling 10 signals per trace.

4.3.3 CE-MS Method Development

The separation method was subsequently transferred to CE-MS, using the final CE-UV conditions as starting point. Injection times corresponding to an injection plug of 1.5% of the capillary length were used. This value was found to be the optimum regarding signal intensity and peak broadening, with higher injection times leading to increased band broadening while not considerably gaining signal intensity. For a capillary of 50 cm length, this corresponded to an injection time of 5 s.

Compared to the CE-UV system, the experimental setup for CE-MS allows for the use of shorter capillaries. Fig. 35 shows the effect of decreasing the capillary length from the initial 75 cm to 65 and 50 cm, while working at 35 kV. Both total separation time and resolution decreased. The shorter analysis times of only 2.5 min in a 50 cm capillary, however, was seen as more valuable than achieving baseline separation.

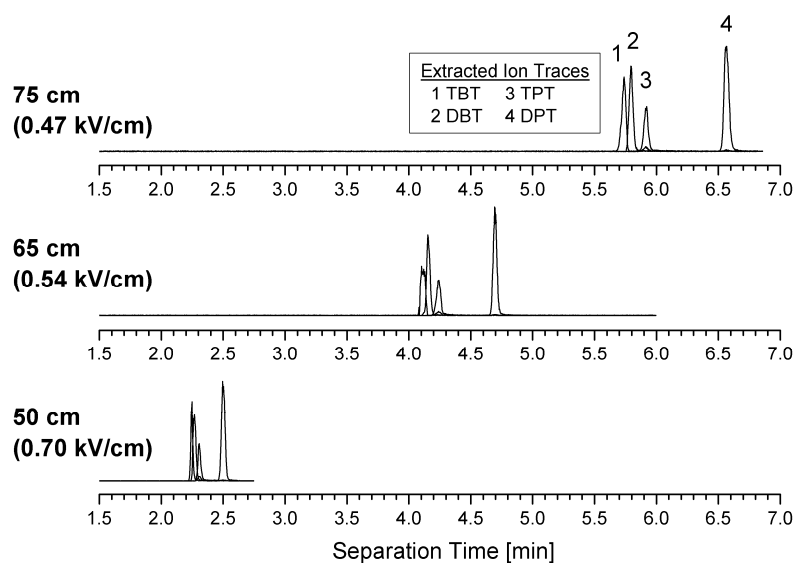


Fig. 35: CE-MS separations of four organotin species using capillaries with different lengths. The buffer composition was the same as described in Fig. 33.

In another set of experiments, the influence of high voltage field strengths (0.4 to $0.7 \text{ kV}\cdot\text{cm}^{-1}$) was evaluated, working with a capillary length of 50 cm. It was found that the decrease of resolution with increasing field strength is negligible compared to the shorter analysis times. A capillary length of 50 cm and a separation voltage of 35 kV ($0.7 \text{ kV}\cdot\text{cm}^{-1}$) were chosen for all further experiments.

4.3.4 CE-MS Method Evaluation

Calibration curves for the four analytes were recorded using the final CE-MS method. They were found to be linear over the concentration range investigated ($3 \cdot 10^{-7}$ – $3 \cdot 10^{-5}$ M).

Table 7 details the analytical parameters. The different sensitivity of the method for the four compounds studied can be attributed to different ionisation efficiencies on the one hand, and to different noise intensities of the extracted ion traces on the other hand. The limits of detection are about two orders of magnitude lower than those obtained using UV detection.

Table 7: Analytical parameters of the final CE-MS method. A series of five solutions with concentrations in the calibration range ($3 \cdot 10^{-7}$, $1 \cdot 10^{-6}$, $3 \cdot 10^{-6}$, $1 \cdot 10^{-5}$, and $3 \cdot 10^{-5}$ M) was analysed three times to evaluate linearity and repeatability. Linear regression was performed on the logarithmic plot without weighing of the data points.

	TBT	DBT	TPT	DPT
Calibration range		$3 \cdot 10^{-7}$ – $3 \cdot 10^{-5}$ M		
Regression coefficient	0.998	0.99994	0.9990	0.9997
Limit of detection (S/N = 3) [10^{-7} M]	8.1	3.9	2.4	0.98
RSD of peak height ($3 \cdot 10^{-5}$ M; n = 3) [%]	12	6	14	8
Migration time [min]	2.24	2.27	2.31	2.50
RSD of migration time (n = 3) [%]	3.9	4.0	4.0	4.7

4.3.5 Application to River Water Samples

River water samples were collected and subjected to the extraction procedure detailed in section 3.4.1 (pg. 22). Fig. 36 shows electropherograms of extracts from blank and spiked samples. The blank samples showed no detectable signal for any of the analytes under investigation. No other compounds with tin isotope pattern could be found in the extracts. When subjected to CE-UV analysis, the samples showed a number of signals in the migration time range of the analytes. Inspection of the corresponding migration intervals in the CE-MS analysis, however, clearly proved these to result from matrix components, emphasizing the need for mass spectrometric detection.

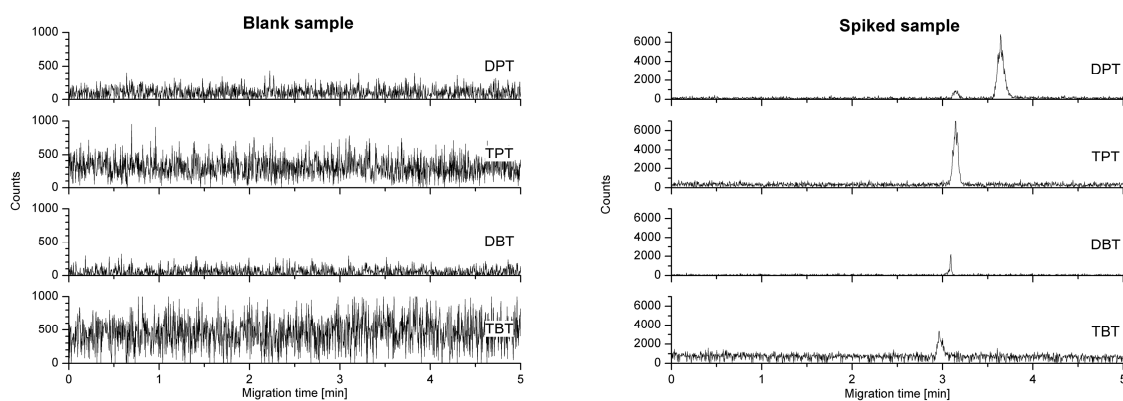


Fig. 36: Fast CE-MS separations of extracts obtained from blank and spiked river water samples. Spiked concentrations were $1.8 \cdot 10^{-8}$ M. Extracted ion traces are shown singly.

Table 8 summarizes the analytical characteristics of the extraction protocol. Recoveries vary for the different organotin compounds, with tri-substituted species showing better retention on the SPE cartridge than di-substituted ones as well as phenyl-substituted analytes showing better retention than butyl-substituted ones. With an SPE preconcentration factor of 113 and recoveries between 44 and 77%, effective preconcentration factors between 49 and 87 were achieved for spiked river water samples.

Table 8: Analytical characteristics of the SPE extraction protocol. 450 mL of river water were spiked to a concentration of $1.8 \cdot 10^{-8}$ M for all four compounds, extracted on a C18 cartridge and eluted in 4 mL of CE buffer. The extractions were carried out in triplicate.

	TBT	DBT	TPT	DPT	
Recovery [%]	66.0	43.9	77.4	52.1	
RSD of recovery (n = 3) [%]	5.7	16	2.5	7.3	
Effective preconcentration factor	74	49	87	59	
Limit of detection in conjunction with CE-MS method (S/N = 3)	[10^{-9} M]	11	7.9	2.7	1.7
	[$\mu\text{g} \cdot \text{L}^{-1}$]	3.2	1.8	0.94	0.46

4.3.6 Conclusions

A fast CE–MS method for the determination of four organotin compounds was developed. A method developed for CE with UV detection was transferred to the experimental setup for fast CE–MS. The use of a non-aqueous BGE with the fast CE–MS setup proved successful. Separations can be achieved in less than three minutes. The LODs of the method are between 1 and $8 \cdot 10^{-7}$ M (S/N = 3).

In addition, a solid phase extraction protocol was developed for the determination of the four analytes in water samples. Using spiked river water, recoveries from 44 to 77% with relative standard deviations between 2.5 and 16% could be obtained. LODs of the overall analytical method (extraction and analysis) were found to be between 1.7 and $11 \cdot 10^{-9}$ M.

Using time-of-flight mass spectrometry as the detection method proved particularly useful when analysing real samples. It allowed the unambiguous differentiation between analytes and matrix components, a common problem when using a non-specific detection method like UV/VIS.

4.4 Application to Organoarsenic Speciation

The development of a fast CE–MS method for the determination of four organoarsenic compounds (see section 1.6.4, pg. 14) is shown in this section. This set of analytes can be analysed with both an aqueous and a non-aqueous BGE. Separations using these two very different BGEs are evaluated and compared. Only relevant aspects of the method development are detailed.

4.4.1 Comparison of Aqueous and Non-aqueous BGEs

The suitability of an aqueous and a non-aqueous BGE were evaluated for the analysis of the analytes. As can be seen in Fig. 37, the separation under non-aqueous conditions takes longer and produces an AsB signal with considerable tailing.

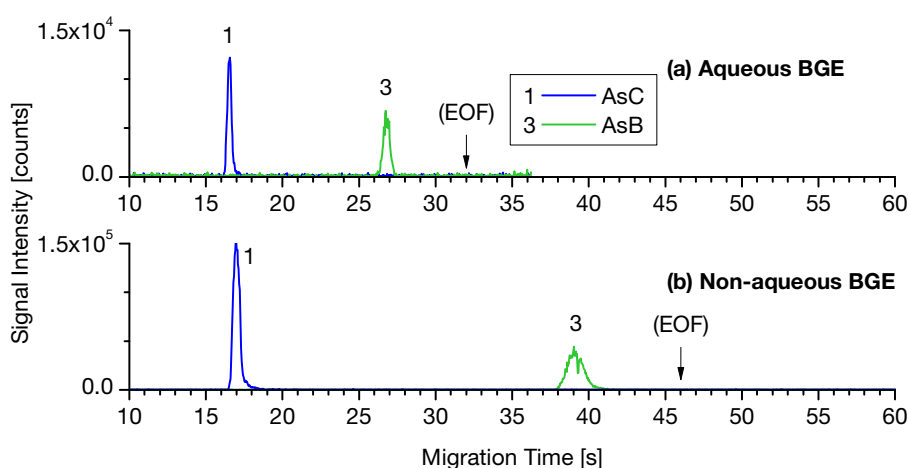


Fig. 37: Fast CE–MS separations of arsenocholine and arsenobetaine under aqueous (a; 0.05 M FA adjusted to pH2.8) and non-aqueous BGE conditions (b; 1 M acetic acid and 10 mM ammonium acetate in acetonitrile). Separations were conducted in a 50 μm \times 28.5 cm capillary with a separation high voltage of 35 kV.

4.4.2 Pressure-assisted (Very) Fast CE–MS

The limits of achievable separation speed with the simple CE–MS setup were investigated by applying additional pressure to the buffer vial shortly after the separation has been started. To accomplish this, the buffer vial was sealed and made airtight directly after injection, the separation high voltage was applied, and air was injected into the buffer vial through a syringe and tubing to yield a pressure of approx. 1 bar.

Fig. 38 shows very fast CE–MS separations using this protocol under aqueous and non-aqueous BGE conditions. The non-aqueous separation conditions proved to be of advantage here for two reasons. Firstly, the lower viscosity of the acetonitrile-based BGE resulted in a

higher increase in separation speed than usage of the aqueous BGE. Secondly, the analyte signals are narrower as compared to aqueous BGE conditions, even though the opposite was true for separations without additional pressure applied. The reason for this might again be the lower viscosity and, hence, different laminar flow profile of the acetonitrile-based BGE. Even though the pressure application protocol seems simple, migration time repeatability for these experiments was surprisingly good with RSD values of 7%.

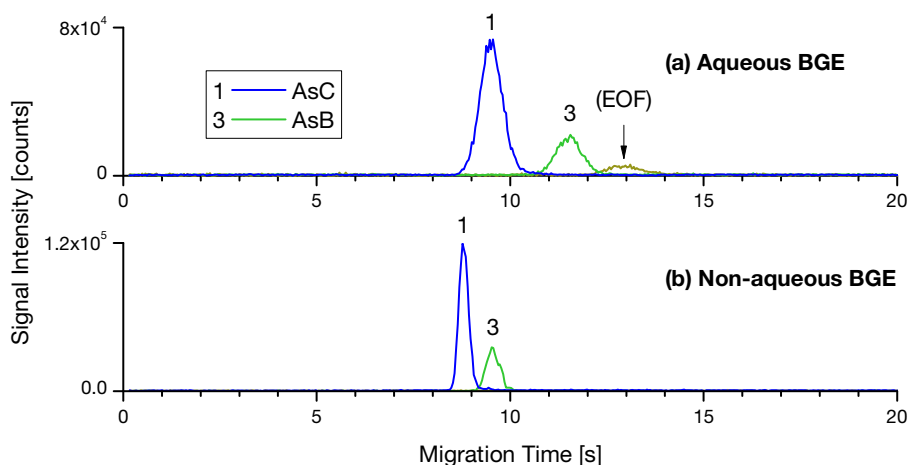


Fig. 38: Very fast CE-MS separations using an aqueous (a) and non-aqueous BGE (b). Approx. 1 bar of pressure was applied to the buffer vial 5 s after switching on the separation high voltage. BGE compositions and other parameters were as in Fig. 37.

4.4.3 BGE Optimisation

For further experiments, two more analytes (glycerol- and sulphate oxoarsenosugars) were included in method development. The focus was put on the aqueous BGE, since injections using the non-aqueous BGE proved to be more challenging and did not offer any advantage at this stage.

Fig. 39 compares the initial and optimised BGE conditions. Increasing the BGE pH from 2.4 (0.1 M formic acid) to 2.8 (0.1 M formic acid, pH-adjusted using ammonia solution) resulted in sharper signals and, most significantly, a better separation of analyte (4) from neutral components. While the overall separation time increased, all analytes are almost equally spread out over the migration time window. Since the analyte signals are very narrow with large migration time gaps in between, the situation shown in Fig. 39 (b) illustrates the optimal starting point for the development of a faster separation method. By using a setup that allows the use of shorter separation capillaries, it is conceivable that CE-MS

separations of these compounds could be finished in less than one minute, with all analytes being baseline separated.

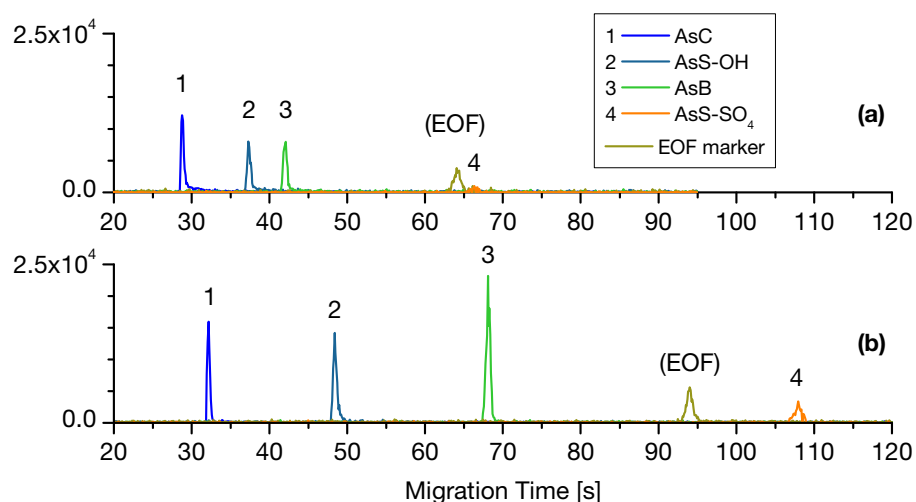


Fig. 39: Optimisation of the composition of the aqueous BGE. The BGE was formic acid of 0.1 M (a) and 0.1 M adjusted to pH 2.8 (b). Separations were carried out in a $50\ \mu\text{m} \times 29.5\ \text{cm}$ capillary at 35 kV.

It should be noted that the final CE-MS method is unusual in the fact that both cationic and anionic species (traveling co-electroosmotically and counter-electroosmotically) are separated in a *single* run, using only one simple BGE (as opposed to different leading and tailing BGEs in a single CE run, or two runs with different BGEs).

4.4.4 Conclusions

Two fast CE-MS methods were developed for the analysis of four organoarsenic compounds. Initial method development compared an aqueous and a non-aqueous BGE and showed that both are suitable. CE-MS separations in 10 s of the two single most common organoarsenic compounds, AsB and AsC, were achieved using a pressure-assisted approach.

Further method development focused on the aqueous BGE. The BGE pH was found to have a strong influence on the separation. Optimal separation conditions for further downscaling and faster separations were discussed. The method was successfully applied to the analysis of real-world samples, in which different arsenosugars could be identified.

5 Capillary Batch Injection

This section details the development of the CBI setup from initial tests to the evaluation of the final setup. All CE-MS experiments shown are separations of the catecholamine model system (see section 1.6.1, pg. 12)

5.1 Initial Tests

Some initial tests with a simple setup (see section 3.7.1, pg. 34) were carried out to evaluate the importance of a number of parameters surrounding the injection process.

5.1.1 Injection Environment

Tests showed that it is not possible to achieve successful injections by bringing the sample delivery capillary and the separation capillary in close contact inside a sleeve. Two kinds of failed injections can be distinguished. Air present between the capillaries, albeit only small amounts, creates a barrier that inhibits sample solution from reaching the separation capillary. This results in a separation with no sample present. Due to the suction pressure from the electrospray interface, the prolonged exposure to air can also lead to the injection of air into the separation capillary, leading to a breakdown of the CE high voltage circuit.

It was therefore found necessary to have the injection region filled with a solution during injections, and being able to insert the separation capillary in such a way that no air is trapped between the two capillaries. For further initial experiments, a setup was devised, which featured a small but constant flow of a flush solution through the sleeve.

5.1.2 Delivery of Sample Solution

The separation capillary exhibits a constant laminar flow into the mass spectrometer. Experiments were conducted to find out whether this suction is large enough to inject sample into the separation capillary. Fig. 40 compares the resulting separations after injecting sample either pressure-free or pressure-assisted. In Fig. 40 (a), the sample solution in the sample vial was kept level with the flush solution in the injection sleeve, and pressure compensation between the sample vial and the outside was achieved, resulting in a zero net flow through the sample delivery capillary. In Fig. 40 (b), additional pressure was applied to the sample vial, resulting in a forced flow of sample solution out of the sample delivery capillary.

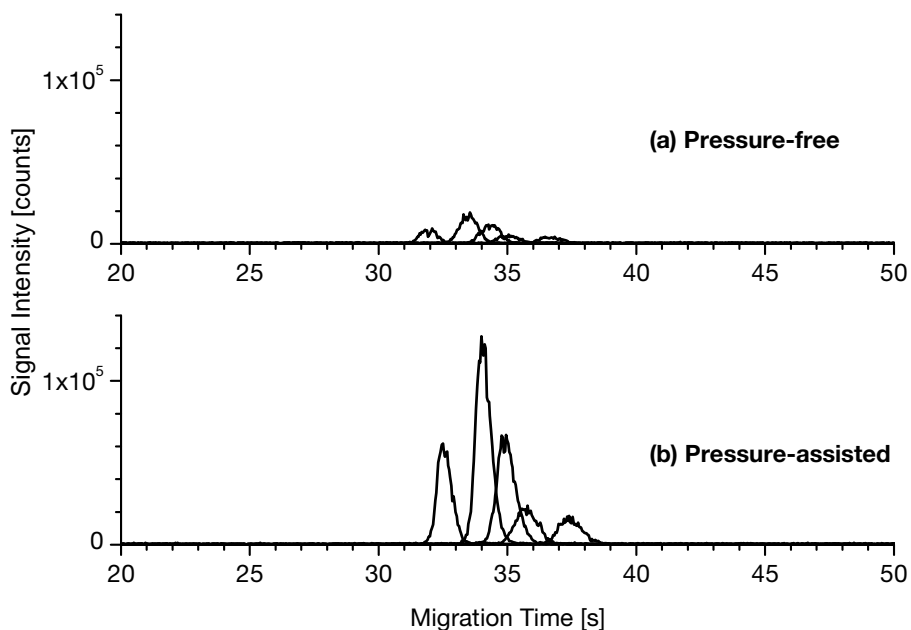


Fig. 40: Comparison of two CE-MS separations of the catecholamine model system after injections with pressure compensation (a), and pressure application (b) to the sample delivery capillary.

There is an almost ten-fold difference in the resulting signal intensities, suggesting that the hydrodynamic situation at the point of injection is not sufficient to selectively draw sample solution out of the sample delivery capillary into the separation capillary. With additional pressure applied, the signal intensities are not significantly lower than those achieved using a standard vial injection.

It appears that a successful injection process requires both the flow out of the sample delivery capillary and the flow into the separation capillary.

5.1.3 Alignment of Capillaries

During the experiments it was found that the precise alignment of sample delivery capillary and separation capillary had a strong influence on the injection result. Bad alignment would lead to lower signal intensities; whilst good alignment would yield signal intensities similar to those achieved using a standard vial injection procedure. Therefore, the small lateral freedom of the capillaries in the injection area (Fig. 9, pg. 35) was still large enough to account for substantially different injection conditions, largely depending on precise manual alignment.

In addition, these experiments and the result of the previous section suggested that a near-perfect alignment of the capillary faces can lead to a situation in which it would be possible

to almost seal them off from the surrounding flush liquid. This finding led to the idea of creating a seal on top of a capillary, the experimental details of which are outlined in section 3.4.5 (pg. 28), and its use for CBI injections is presented in section 5.5 (pg. 86).

5.2 General Considerations for the Injection Process

The largest conceptual difference between traditional injection in CE and CBI is the role of the separation capillary. In the former, the separation capillary is moved between a location for separation and a location for injection, whereas in the latter, it is kept in a fixed position, in an injection cell filled with BGE. This requires the sample to be brought to the separation capillary and not vice versa. An auxiliary capillary, the injection capillary, takes over sampling, transport and injection of sample solution. The injection procedure consists of three steps: Firstly, sample solution is drawn up into the injection capillary. Secondly, the injection capillary is moved to the injection cell and positioned in front of the separation capillary. Thirdly, sample solution is expelled onto or into the separation capillary.

During this last step, the actual injection, two processes take place: Firstly, sample solution is expelled from the injection capillary as a plume onto the separation capillary. Secondly, sample solution from this plume is drawn into the separation capillary. It is important to note, however, that these two processes happen simultaneously rather than consecutively. As soon as sample solution has been expelled from the injection capillary, diffusion with the surrounding BGE solution will lead to its dilution. While this effect can be beneficial in some circumstances, it is mostly undesirable.

In the experimental setup used for this study, the main contributor to a flow of liquid into the separation capillary is a constant laminar flow, caused by the ESI-MS interface. The magnitude of this flow depends on a number of parameters, such as the capillary position in the electrospray interface, nebulizer gas pressure, sheath liquid flow rate, capillary length, capillary inner diameter, and BGE viscosity. It is, however, constant for a given set of experimental conditions and can be determined by a flow injection-type experiment. It is further assumed that a comparably small amount of sample solution present in the separation capillary does not change this flow rate significantly.

With these characteristics of the system, as well as the results of the initial test in mind, the best approach for an injection can be devised. The most practical approach to control an injection seems to be to focus on the time during which freshly expelled sample solution is present in front of the separation capillary. The flow rate into the separation capillary as well as the time during which sample is drawn into it, define the injected sample volume. This approach eliminates any diffusion-induced dilution and also paves the way for a

further increase in injection efficiency: The flow rate, by which sample solution is expelled from the injection capillary, has to be only slightly larger than the flow rate into the separation capillary.

5.3 Sequence of Events for an Injection Process

Table 9 illustrates the order and kind of steps necessary to perform an injection. This sequence can be cycled, i.e. after completing one injection (and the corresponding CE separation), the next injection starts by performing the first step; there are no intermediate steps, other than switching the separation high voltage off.

Table 9: Steps and parameters for an optimised injection process.

Step	Instrument	Parameters ^a	Explanation
1	syringe pump	+200 nL, 50 nL/s	Flushing of injection capillary
2	x-motor	go to position "sample vial 1"	Movement to sampling position
3	z-motor	go to position "sample"	
4	syringe pump	-50 nL, 20 nL/s	Uptake of sample
5	syringe pump	+35 nL, 20 nL/s	Change of direction of plunger
6	z-motor	go to position "up"	Movement to injection position
7	x-motor	go to position "injection"	
8	z-motor	go to position "injection"	
9	syringe pump	+10 nL, 1 nL/s	Expulsion of sample
10	stirrer	stir for 1 s	Stirring
11	hv source	25 kV, initiate TOF-MS data acquisition	Start of separation and data acquisition
12	z-motor	go to position "up"	Movement out of injection cell

^a Negative syringe pump volumes indicate solution uptake into the injection capillary, positive values indicate sample expulsion.

After moving to the sampling position (which is a vial containing sample solution in the case of these experiments), sample solution is drawn into the injection capillary. Due to a backlash when reversing the direction of the syringe plunger, a small volume of sample is expelled into the sample container. This procedure ensures that any following sample expulsion is precise. For the microliter syringe employed in this setup, the corresponding "reversal volume" has been determined to be ca. 30 nL. The backlash itself can be attributed

to plunger bending, plunger seal compression as well as leadscrew/nut backlash in the syringe pump.

The injection capillary, containing sample solution, is then moved to the injection position. An investigation of optimal injection positions is discussed in the next section. The injection starts with sample solution being expelled from the injection capillary and simultaneously being drawn into the separation capillary. It is not entirely terminated by the end of sample expulsion since there is surplus sample solution present. To avoid continued injection of increasingly diluted sample solution (and hence tailing signals in the following separation), the stirrer and separation high voltage are switched on at the same time. This also marks the beginning of the separation and data acquisition.

Following the injection, the injection capillary is withdrawn from the injection cell. This prevents an unwanted EOF of BGE into the injection capillary. While the far end of the injection capillary is not intentionally grounded, the potential difference between the injection capillary's ends is still large enough to cause a noticeable EOF.

The separation can either be terminated manually by the user or automatically after a given time period has elapsed.

5.4 Optimisation of Injection Process

Clearly, the most critical step of the injection procedure is the delivery of sample solution into the separation capillary. Surrounding this, there are four parameters, which govern the process. Their impact on the injection has been determined and optimal values are discussed in the following. These parameters are; sample expulsion speed and volume, capillary alignment, capillary distance, and stirring. Fig. 41 shows microphotographs of the injection process, where the sample solution is dyed blue.

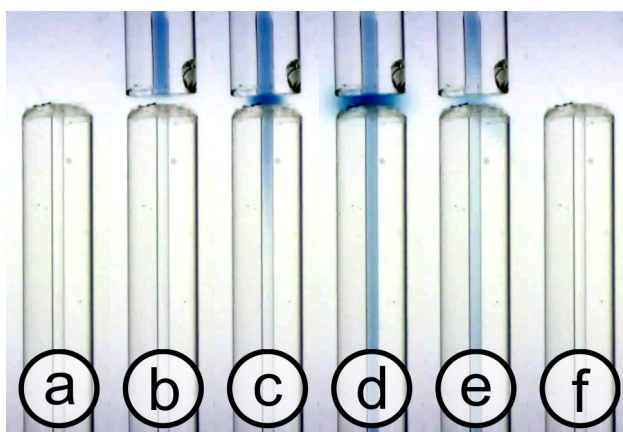


Fig. 41: Microphotographs of an injection process. The steps shown are; (a) before injection process, (b) arrival of injection capillary, (c) start of injection, (d) end of injection, (e) stirring/start of separation, (f) after removal of injection capillary.

Sample expulsion speed and volume. As discussed earlier, the sample expulsion flow rate needs to be larger than the flow rate of BGE into the separation capillary. The injected volume itself is usually optimised as part of the CE method and has to be considered invariable in term of injection procedure optimisation. The injected volume, in turn, is controlled by the time, during which sample solution is present at the separation capillary. That also excludes this expulsion time from optimisation, allowing only combinations of sample expulsion flow rate and volume, which lead to the expulsion time required. Following the initial goal of minimizing the sample volume necessary for an injection, the sample expulsion flow rate should be as low as possible. For the experiments in this study, this minimal flow rate was determined visually and found to be 1 nL/s. It can be seen that most expelled sample solution enters the separation capillary while only a small surplus amount accumulates between both capillaries. The ratio of injected sample solution to sample solution expelled from the injection capillary (v/v) is 80% for this example.

Capillary Alignment. Axial alignment of the capillaries (x,y-plane, excluding capillary distance) can be adjusted using the x,y-positioner installed atop the injection cell. It was found that an offset of up to 50 μm did not have any negative impact on the injection. The larger-than-necessary flow rate of sample solution being expelled from the injection capillary can adjust for this spatial difference. This is in contrast with the results obtained during the initial tests, owing to the fact that the expulsion of sample solution is much better controlled here than it was then.

Capillary Distance. Capillary distance (z distance) was initially expected to have a large influence on the injection. It was found, however, that a noticeable decrease of signal intensity with increasing capillary distance only starts from a distance of 50 μm between the capillaries. It is reasonable to again explain this with the larger-than-necessary flow rate of sample solution being expelled from the injection capillary. It is further conceivable that a larger flow rate would be able to compensate for an even larger capillary distance. At the other end of the spectrum, it is also possible to make use of this effect by deliberately diluting sample solution at the point of injection. This can be desirable as a very simple form of sample pretreatment of otherwise raw samples. Fig. 42 shows the dependence of signal intensity on capillary distance.

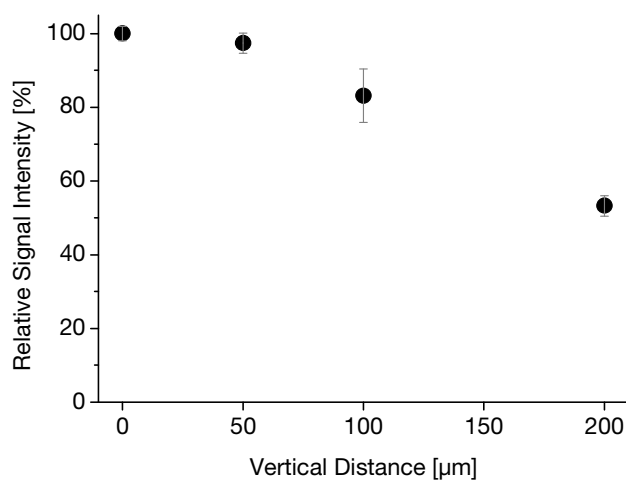


Fig. 42: Dependence of signal intensity on capillary distance. Error bars represent standard deviation for $n = 3$ consecutive runs.

Stirring. At the end of the injection, i.e. after expulsion of sample solution from the injection capillary stops and separation high voltage is applied, there is still surplus sample solution present at the separation capillary. Fig. 43 illustrates the significance of removing this excess sample solution by stirring. Failure to do so results in a slow post-injection

inflow of increasingly diluted sample solution, which leads to significant peak tailing. This will have a particularly negative impact on fast CE experiments or separations with a large number of analytes, where high separation efficiency is needed.

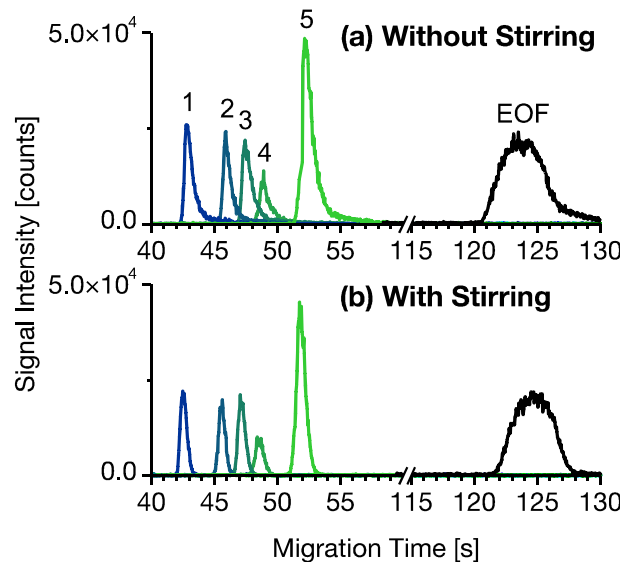


Fig. 43: Comparison of the resulting CE-MS separation after injections with (a) and without (b) stirring.

5.5 100% Injection Efficiency

The procedure detailed so far allows injections with efficiencies of up to 80% with no adverse effects on the separation. These injections are based on creating a small and undiluted sample “cloud” in front of the separation capillary, into which sample is drawn either electrokinetically or due to a laminar flow. Excess sample solution, albeit very small, is diluted in the large amount of BGE present in the injection cell.

For a number of reasons it would seem beneficial to inject the sample directly *into* (rather than *onto*) the separation capillary. Firstly, such a method could achieve an injection efficiency of 100%, since no more sample solution has to be expelled from the injection capillary than enters the separation capillary. Secondly, such a method would not release any sample solution into the BGE, and hence allow a drastic size reduction of the injection cell, which would allow for a quick change of BGE. Finally, such a method would allow flushing and conditioning of the separation capillary without the need for disassembling the setup. Particularly this last benefit is of crucial importance when developing an automated system that can run without user supervision and interaction.

In order to inject from the injection capillary into the separation capillary, both have to form a seal in mid-solution with sufficient pressure resistance. This was achieved by coating the tip of one capillary with a half-torus shaped seal made from silicone elastomer. Section 3.4.5 (pg. 28) details the experimental details for the creation of this seal. It was found that the seal coating is preferably applied to the separation capillary, since the movement of the injection capillary through the capillary guide causes mechanical stress which can lead to the seal’s deterioration.

Fig. 44 illustrates an injection process where sample solution is forced directly into the separation capillary. In contrast to a normal injection (as shown in Fig. 41, pg. 83), no sample solution is present in the BGE at any point before, during, or after injection takes place.

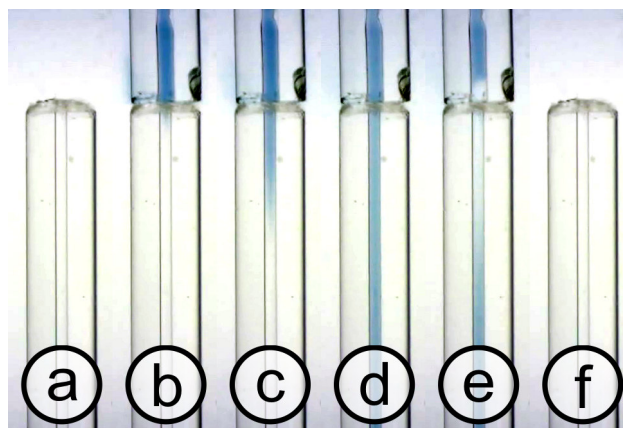


Fig. 44: Microphotographs of a seal injection process. The steps shown are; (a) before injection process, (b) arrival of injection capillary, (c) start of injection, (d) end of injection, (e) start of separation, (f) after removal of injection capillary.

A further advantage of this sealed injection is an increase in speed. The flow rate at which a solution is forced into the separation capillary can be substantially higher than flow rates achieved with electrokinetic injection or the laminar flow caused by the electrospray interface. While this is beneficial in many cases, it becomes even more important when using separation capillaries with smaller inner diameters.

It should be noted that this experimental approach allowed for the repeated sealed connection between two capillaries in mid-solution, precise to less than $10\ \mu\text{m}$ of lateral displacement, without any guidance for approx. 5 mm in either direction.

5.6 Analytical Characterisation

In order to evaluate the performance of the injection process developed, it was compared to the manual sample injection technique used in fast CE–MS studies of the same model system (section 4.1, pg. 46). Comparisons were performed such that all parameters relating to the separation were kept unchanged (e.g. capillary dimensions, BGE composition, sample composition, ESI–MS parameters). Importantly, the injected sample amount was kept constant at 2% of the capillary length.

No negative impact on peak shape, such as tailing or widening, was observed. Repeatability of CBI injections and CBI seal injections was better than with manual injections (RSD of peak heights for $n = 7$: 6.0%, 8.3% and 10%, respectively). Injection efficiency increased from below 0.1% for manual injections to 80% and 100% for CBI injections and CBI seal injections, respectively.

5.7 Very Fast CE–MS

An additional benefit of the CBI setup lies in the fact that the separation capillary is fixed in position. This allows for the use of shorter separation capillaries than with any other CE–MS setup. In addition to about 12 cm of capillary length, which are inside the electrospray interface, only 3 cm of capillary is needed to fix the capillary in the injection cell. The use of a 15 cm long capillary together with the high voltage source employed in this setup enables separations at high electric field strengths of up to 2 kV/cm.

Such high electric field strengths lead to a considerable increase of the electrophoretic current, negatively influencing separation efficiency or rendering CE separations impossible. To compensate for this, the capillary inner diameter of the separation capillary was decreased from 50 to 25 μm . This, in turn, allowed for an increase of BGE concentration from 0.1 to 1.0 M. Fig. 45 shows a separation of the catecholamine model system in a 15 cm \times 25 μm capillary. Analytes migrate between 8 and 12 s, with peak widths at half height between 0.11 s and 0.15 s, the EOF is recorded after only 20 s.

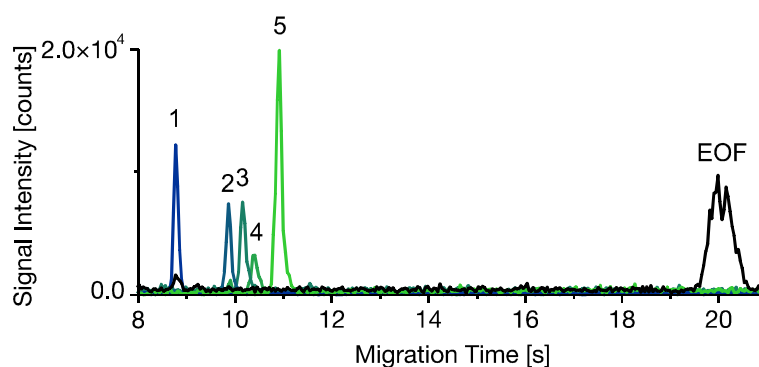


Fig. 45: Fast CE–MS separation after CBI. The separation was conducted at 1.7 kV/cm in a 15 cm \times 25 μm capillary filled with 1 M aqueous formic acid as BGE.

5.8 Conclusions

Efficient sample usage is of key importance in many bioanalytical questions for which a CE–MS separation is sought. The concept of injection efficiency highlights the current lack of development towards sample-efficient injection methods for CE–MS. Out of the concepts that strive to increase injection efficiency in CE, CBI seems to be the most versatile one, since it inherently combines sampling and sample injection in one setup.

The CBI system developed here is automated and of small footprint, but provides enough experimental freedom to both optimise the injection process and implement future applications.

The ability to seal off injection and separation capillary in the injection cell makes injections with 100% injection efficiency possible. More importantly, though, it allows flushing and conditioning of the separation capillary without the need for manual user interaction. Future developments based on this setup could include an automated routine which, when the electrophoretic current breaks down during the separation, automatically flushes the capillary and starts a new separation.

Using the CBI setup, CE–MS separations are possible with capillaries shorter than in any other setup. The capillary lengths employed here mark the limit of what can be achieved using current commercial electrospray interfaces for MS. The main advantage of separations in short capillaries lies in maintaining high separation efficiency while drastically decreasing migration times down to a few seconds.

Future work with the CBI setup will be directed towards applications. The areas of microdialysis, (in-capillary) kinetics, cell culture probing, and single-cell analysis are envisioned.

6 Summary

6.1 Fast Capillary Electrophoresis–Mass Spectrometry

Measurements with capillary electrophoresis (CE) coupled to mass spectrometry (MS) are desirable when both the high separation efficiency of capillary electrophoresis and the identification capabilities of mass spectrometry are required. With current instrumentation, analyses require between 10 min and more than one hour to complete. Fast CE–MS measurements are generally preferable; however, they become mandatory when a high sample throughput is required.

Using an experimental setup of simple and straightforward design, a methodology to separate analytes with CE–MS both fast and efficiently has been developed, which successfully employs both aqueous and non-aqueous background electrolytes (BGEs). High electric field strengths of up to $1.25 \text{ kV}\cdot\text{cm}^{-1}$ and the use of short-length capillaries were found to be key in achieving fast separations.

Hyphenation of CE and MS was accomplished using a coaxial sheath liquid electrospray ionisation interface. Its commercial availability and simple experimental design aid in the rapid implementation of fast CE–MS methodology by other researchers and laboratories. The influence of parameters inherent to this interface was studied in more detail as to its effects on both separation and detection, including suction pressure and dilution. It was shown that parameter settings different from those routinely recommended have to be used in order to achieve highly efficient separations. General conclusions could be drawn from these findings, which allow rapid method development for fast CE–MS.

The influence of the capillary inner diameter (ID) on separations was investigated. In addition to standard capillaries of 75 and 50 μm ID, separations in capillaries with IDs of 25, 15, and 5 μm have been successfully applied to this setup. The analytical performance is compared over this range of capillary dimensions and both advantages and disadvantages are discussed. Usage of reduced ID capillaries allows for the analysis of sub-nL samples, the use of high conductivity BGEs, and can eliminate problems arising from certain parameter combinations in CE–MS experiments based on non-aqueous BGEs. Most significantly, it could be shown that reducing the separation capillary ID can have great potential in improving the separation efficiency.

The often-cited assumption of increased dilution at the ESI interface (and, hence, decreased signal intensity) with decreased separation capillary ID was found to be far less dramatic. Together with the increase in separation efficiency and the correspondingly sharper analyte signals, this dilution effect either was not present at all, or was considerably lower than what would be expected from the volumetric ratio of separation capillary outflow to sheath liquid flow rate.

The fast CE–MS methodology has been successfully applied to the separation of cationic and anionic analytes (co- and counter-electroosmotic separation conditions, respectively), namely catecholamines, hyaluronan oligomeres, organoarsenic compounds, and organotin compounds. For relevant sets of analytes, it could be shown that matrix-containing samples can be injected with only minimal sample pretreatment, with no negative effect on the CE–MS method. Most of these analytes could be separated in less than one minute; using a pressure-assisted approach, a separation within 10 s was possible.

While the injection process employed here was manual, it could be easily automated. At the time of writing, work towards an automated setup for fast CE–MS is being conducted in the same working group.

6.2 Small Samples

Efficient sample usage is of key importance in many bioanalytical questions for which a CE–MS separation is sought. The concept of injection efficiency is introduced to give a figure of merit to the injection process in analytical systems. It represents the ratio of injected sample and the amount of sample needed for carrying out the injection process (v/v). Typical values for the injection efficiency in CE range from 10^{-3} to 10^{-7} .

Based on the concept of capillary batch injection (CBI), the development of an automated system is presented. This device is capable of running true multi-sample measurement series, using minimal sample volumes in the lower nL range and delivering an injection efficiency of up to 100%. It is compatible with both aqueous and non-aqueous background electrolytes. Design and specifications of the injection device are shown, and all parameters relevant for achieving both high injection efficiency and high separation efficiency are discussed. These parameters include liquid handling of sample volumes with the injection

capillary, relative positioning of injection and separation capillary, and convection effects in the injection cell.

Furthermore, a procedure is presented to coat the tip of a fused silica capillary with a silicone elastomer acting as a seal between two capillaries in mid-solution. This allows for the injection of sample solution from the injection capillary directly into the separation capillary.

As an additional benefit, very short separation capillaries down to 15 cm in length can be used with this device. CE-MS separations of a catecholamine model system in capillaries of only 15 cm length under conditions of high electric field strength could be completed in 20 s with high separation efficiency.

7 Zusammenfassung

7.1 Schnelle Kapillarelektrophorese–Massenspektrometrie

Die Kopplung von Kapillarelektrophorese (CE) und Massenspektrometrie (MS) ist immer dann von Vorteil, wenn sowohl die hohe Trenneffizienz der CE als auch die Identifikationsstärke der MS benötigt werden. Bei Einsatz gängiger Instrumentierung dauern Messungen zwischen 10 min und über einer Stunde. Schnelle CE–MS-Messungen sind generell wünschenswert, werden aber unumgänglich, wenn ein hoher Probendurchsatz erzielt werden soll.

Mithilfe des hier eingesetzten einfachen experimentellen Aufbaus wurde eine Methodik entwickelt, um Analyte mittels CE–MS sowohl schnell als auch effizient zu trennen. Wässrige und nicht-wässrige Hintergrundelektrolyte (BGE) wurden erfolgreich eingesetzt. Der Verwendung kurzer Trennkapillaren und der Einsatz hoher elektrischer Feldstärken von bis zu $1.25 \text{ kV} \cdot \text{cm}^{-1}$ waren die Hauptfaktoren, um schnelle Trennungen zu erreichen.

Die Kopplung von CE und MS erfolgte über ein koaxiales sheath-liquid Elektrospray-Interface. Da es kommerziell verfügbar ist und einen einfachen experimentellen Aufbau erlaubt, wird die Übernahme der schnellen CE–MS-Methodik durch andere Forscher und Arbeitsgruppen erleichtert. Der spezifischen Parameter dieses Interfaces wurden detailliert auf ihre Einflüsse in Trennung und Detektion, einschließlich Saugdruck und Verdünnung, hin untersucht. Es konnte gezeigt werden, dass andere als die üblicherweise verwendeten Parametereinstellungen gewählt werden müssen, um Trennungen mit möglichst hoher Trenneffizienz zu ermöglichen. Aus diesen Untersuchungen konnten allgemeine Schlussfolgerungen abgeleitet werden, die eine rasche Methodenentwicklung für schnelle CE–MS erlauben.

Der Einfluss des Innendurchmessers (ID) der Trennkapillare wurde untersucht. Zusätzlich zu üblicherweise eingesetzten Kapillaren mit 75 und 50 μm ID konnten solche mit 25, 15 und 5 μm ID erfolgreich für Trennungen mit dem experimentellen Setup eingesetzt werden. Die analytische Leistung wird über diesen Bereich verglichen und Vor- und Nachteile werden diskutiert. Die Verwendung von Trennkapillaren mit kleineren ID erlaubt die Analyse von sub-nL Proben und die Verwendung von BGE mit höherer Leitfähigkeit. Zudem können dadurch Probleme behoben werden, die durch bestimmte

Parameterkombinationen in der nicht-wässrigen CE-MS verursacht werden. Vor allem aber konnte gezeigt werden, dass die Verringerung des Kapillar-ID großes Potential bei der Verbesserung der Trenneffizienz zeigt.

Häufig wird angenommen, dass eine Verringerung des Kapillar-ID zwangsläufig zu einem größeren Verdünnungseffekt am ESI-Interface (und damit kleineren Signalen) führt. Es konnte jedoch gezeigt werden, dass diese Verdünnung deutlich kleiner ist als vermutet. Die erhöhte Trenneffizienz und die entsprechend schärferen Signale führten dazu, dass es entweder zu keiner Signalverringerng kam oder aber diese deutlich geringer ausfiel, als vom Verhältnis der Flussraten aus der Trennkapillare und des sheath-liquid zu erwarten wäre.

Die Methodik der schnellen CE-MS konnte erfolgreich auf die Analyse kationischer und anionischer Spezies (co- und counter-elektroosmotische Trennbedingungen) angewandt werden. Eingesetzte Analyte waren Catecholamine, Hyaluronsäureoligomere, Organoarsenverbindungen und Organozinnverbindungen. Für entsprechend relevante Analyte konnte gezeigt werden, dass matrixbelastete Proben nach nur minimaler Probenvorbereitung injiziert und analysiert werden konnten, ohne negative Auswirkungen auf die Bestimmungsmethode zu haben. Die Analyte konnten i. A. in weniger als einer Minute getrennt werden. Durch Druckbeaufschlagung während der Trennung konnten sogar CE-MS-Trennungen in nur 10 s erreicht werden.

Der hier angewandte Injektionsprozess ist manuell, kann aber leicht automatisiert werden. Zum Zeitpunkt der Schriftlegung wird in derselben Arbeitsgruppe bereits an einem Aufbau zur automatisierten schnellen CE-MS gearbeitet.

7.2 Kleine Probemengen

Der effizienten Probennutzung kommt v. a. in solchen bioanalytischen Fragestellungen eine Schlüsselrolle, in denen Bestimmungen mit CE-MS durchgeführt werden. Das Konzept der Injektionseffizienz wird eingeführt, um dem Injektionsprozess in Analysensystemen eine Güteziffer zu geben. Die Injektionseffizienz bezeichnet das Verhältnis von injizierter Probe zu der Menge an Probe, die für die Durchführung des Injektionsprozesses notwendig ist (v/v). Typische Werte für CE-MS liegen im Bereich von 10^{-3} bis 10^{-7} .

Basierend auf dem Konzept der Kapillar-Batch-Injektion (CBI) wird die Entwicklung eines automatisierten Systems vorgestellt. Es ist in der Lage, Messreihen unterschiedlicher Proben durchzuführen, wobei nur minimale Probenvolumina im unteren nL-Bereich benötigt werden und eine Injektionseffizienz von bis zu 100% erreicht werden kann. Es kann sowohl für wässrige als auch nicht-wässrige Elektrolytsysteme verwendet werden. Aufbau und Spezifikationen des Gerätes werden vorgestellt und alle Parameter, die für das Erreichen hoher Trenn- und Injektionseffizienzen relevant sind, werden diskutiert. Diese Parameter umfassen u. a. Handhabung von Probenvolumina mit der Injektionskapillare, relative Positionierung von Injektions- und Trennkapillare sowie Konvektionseffekte in der Injektionszelle.

Weiterhin wird eine Prozedur vorgestellt, mit der das Ende einer Quarzglas- kapillare mit einem Silikonelastomer beschichtet werden kann. Damit kann zwischen zwei Kapillaren in Lösung eine reversible dichtende Verbindung geschaffen werden. Dies erlaubt die direkte Injektion von Probelösung in die Trennkapillare hinein.

Ein weiterer Vorteil des entwickelten Aufbaus besteht darin, dass sehr kurze Trennkapillaren von nur 15 cm Länge eingesetzt werden können. CE-MS-Trennungen eines Catecholamin-Modellsystems konnten in einer 15 cm langen Kapillare unter hoher Feldstärke in nur 20 s mit hoher Trenneffizienz durchgeführt werden.

8 References

- 1 Foret F, Krivánková L, Boček P (1993) Capillary zone electrophoresis. VCH, Weinheim
- 2 Engelhardt H, Beck W, Schmitt T (1994) Kapillarelektrophorese. Vieweg, Braunschweig
- 3 Kuhn R, Hofstetter-Kuhn S (1993) Capillary electrophoresis. Springer, Berlin
- 4 Grossmann PD (ed) (1992) Capillary electrophoresis. Academic Press, San Diego
- 5 Khaledi MG (ed) (1998) High performance capillary electrophoresis. Wiley, New York
- 6 Jandik P, Bonn G (1993) Capillary electrophoresis of small molecules and ions. VCH, New York
- 7 Shintani H (ed) (1997) Handbook of capillary electrophoresis applications. Blackie Academic and Professional, London
- 8 Hjerten S, Valtcheva L, Elenbring K, Liao JL (1995) Electrophoresis 16:584–594
- 9 Hutterer KM, Jorgenson JW (1999) Anal Chem 71:1293–1297
- 10 Palonen S, Jussila M, Porras SP, Hyötyläinen T, Riekkola ML (2001) J Chromatogr A 916:89–99
- 11 Palonen S, Jussila M, Porras SP, Hyötyläinen T, Riekkola ML (2002) Electrophoresis 23:393–399
- 12 Vandaneer IV WR, Pisas-Farmer SA, Fischer DJ, Frankenfeld CN, Lunte SM (2004) Electrophoresis 25:3528–3549
- 13 Zhong M, Lunte S (1996) Anal Chem 68:2488–2493
- 14 Müller O, Minarik M, Foret F (1998) Electrophoresis 19:1436–1444
- 15 Matysik FM (2006) Electrochem Commun 8:1011–1015
- 16 Matysik FM, Neusüß C, Pelzing M (2008) Analyst 133:1764–1766
- 17 Opekar F, Coufal P, Štulík K (2009) Chem Rev 109:4487–4499
- 18 Plenert ML, Shear JB (2003) Proc Natl Acad Sci USA 100:3853–3857
- 19 Lemmo AV, Jorgenson JW (1993) Anal Chem 65:1576–1581

- 20 Hooker TF, Jorgenson JW (1997) *Anal Chem* 69:4134–4142
- 21 Wätzig H, Kaupp S, Graf M (2003) *Trends Anal Chem* 22:588–604
- 22 Baeuml F, Welsch T (2002) *J Chromatogr A* 961:35–44
- 23 Matysik FM (2010) *Anal Bioanal Chem* 397:961–965
- 24 Wallingford RA, Ewing AG (1988) *Anal Chem* 60:1975–1977
- 25 Olefirowicz TM, Ewing AG (1990) *Anal Chem* 62:1872–1876
- 26 Chien JB, Wallingford RA, Ewing AG (1990) *J Neurochem* 54:633–638
- 27 Olefirowicz TM, Ewing AG (1990) *J Neurosci Meth* 34:11–15
- 28 Kristensen HK, Lau YY, Ewing AG (1994) *J Neurosci Meth* 51:183–188
- 29 Kennedy RT, Oates MD, Cooper BR, Nickerson B, Jorgenson JW (1989) *Science* 246:57–63
- 30 Hogan BL, Yeung ES (1992) *Anal Chem* 64:2841–2845
- 31 Blasco S, Kortz L, Matysik FM (2009) *Electrophoresis* 30:1–6
- 32 Lapainis T, Rubakhin SS, Sweedler JV (2009) *Anal Chem* 81:5858–5864
- 33 Lin Y, Trouillon R, Safina G, Ewing AG (2011) *Anal Chem* 83:4369–4392
- 34 Hommerson P, Khan AM, de Jong GJ, Somsen GW (2011) *Mass Spec Rev* 30:1096–1120
- 35 Hernández-Borges J, Neusüß C, Cifuentes A, Pelzing M (2004) *Electrophoresis* 25:2257–2281
- 36 Zamfir AD (2007) *J Chromatogr A* 1159:2–13
- 37 Maxwell EJ, Chen DDY (2008) *Anal Chim Acta* 627:25–33
- 38 Jussila M, Sinervo K, Porras SP, Riekkola ML (2000) *Electrophoresis* 21:3311–3317
- 39 Siethoff C, Nigge W, Linscheid M (1998) *Anal Chem* 70:1357–1361
- 40 Kubáň P, Hauser PC (2011) *Electrophoresis* 32:30–42
- 41 Pantůčková P, Gebauer P, Boček P, Křivánková L (2011) *Electrophoresis* 32:43–51
- 42 Ramautar R, Mayboroda OA, Somsen GW, de Jong GJ (2011) *Electrophoresis* 32:52–65

- 43 Haselberg R, de Jong GJ, Somsen GW (2011) *Electrophoresis* 32:66–82
- 44 Somsen GW, Mold R, de Jong GJ (2010) *J Chromatogr A* 25:3978–3991
- 45 Lazar IM, Lee ED, Rockwood AL, Lee ML (1998) *J Chromatogr A* 829: 279–288
- 46 Kubáň P, Engström A, Olsson JC, Thorsén G, Tryzell R, Karlberg B (1997) *Anal Chim Acta* 337:117–124
- 47 Tůma P, Opekar F and Jelínek I (2000) *J Chromatogr A* 883:223–230
- 48 Fang ZL, Liu ZS, Shen Q (1997) *Anal Chim Acta* 346:135–143
- 49 Fang ZL, Fang Q (2001) *Fresenius J Anal Chem* 370:978–983
- 50 Fu CG, Fang ZL (2000) *Anal Chim Acta* 422:71–79
- 51 Cao XD, Fang Q, Fang ZL (2004) *Anal Chim Acta* 513:473–479
- 52 Dawson RMC, Elliott DC, Elliot WH, Jones KM (1959) *Data for Biochemical Research*. Clarendon Press, Oxford
- 53 Tuckerman MM, Mayer JR, Nachod FC (1959) *J Am Chem Soc* 81:92–94
- 54 Drayton CJ (1990) *Comprehensive Medical Chemistry Vol. 6*. Pergamon Press, Oxford
- 55 Asari A (2005) *Glycoforum*
(<http://www.glycoforum.gr.jp/science/hyaluronan/HA12a/HA12aE.html>)
- 56 Chen WY, Abatangelo G (1999) *Wound Repair Regen* 7:79–89
- 57 Noble PW (2002) *Matrix Biol* 21:25–29
- 58 Day AJ, De la Motte CA (2005) *Trends Immunol* 26:637–643
- 59 Boregowda RK, Appaiah HN, Siddaiah M, Kumarswamy SB, Sunila S, Thimmaiah KN, Mortha K, Toole B, Banerjee S (2006) *J Carcinog* 5:2–10
- 60 Stern R (2005) *Pathol Biol* 53:372–382
- 61 Stern R (2008) *Semin Cancer Biol* 18:275–280
- 62 Grimshaw J, Kane A, Trocha-Grimshaw J, Douglas A, Chakravarthy U, Archer D (1994) *Electrophoresis* 15:936–940
- 63 Grimshaw J, Trocha-Grimshaw J, Fisher W, Rice A, Smith S, Spedding P, Duffy J, Mollan R (1996) *Electrophoresis* 17:396–400

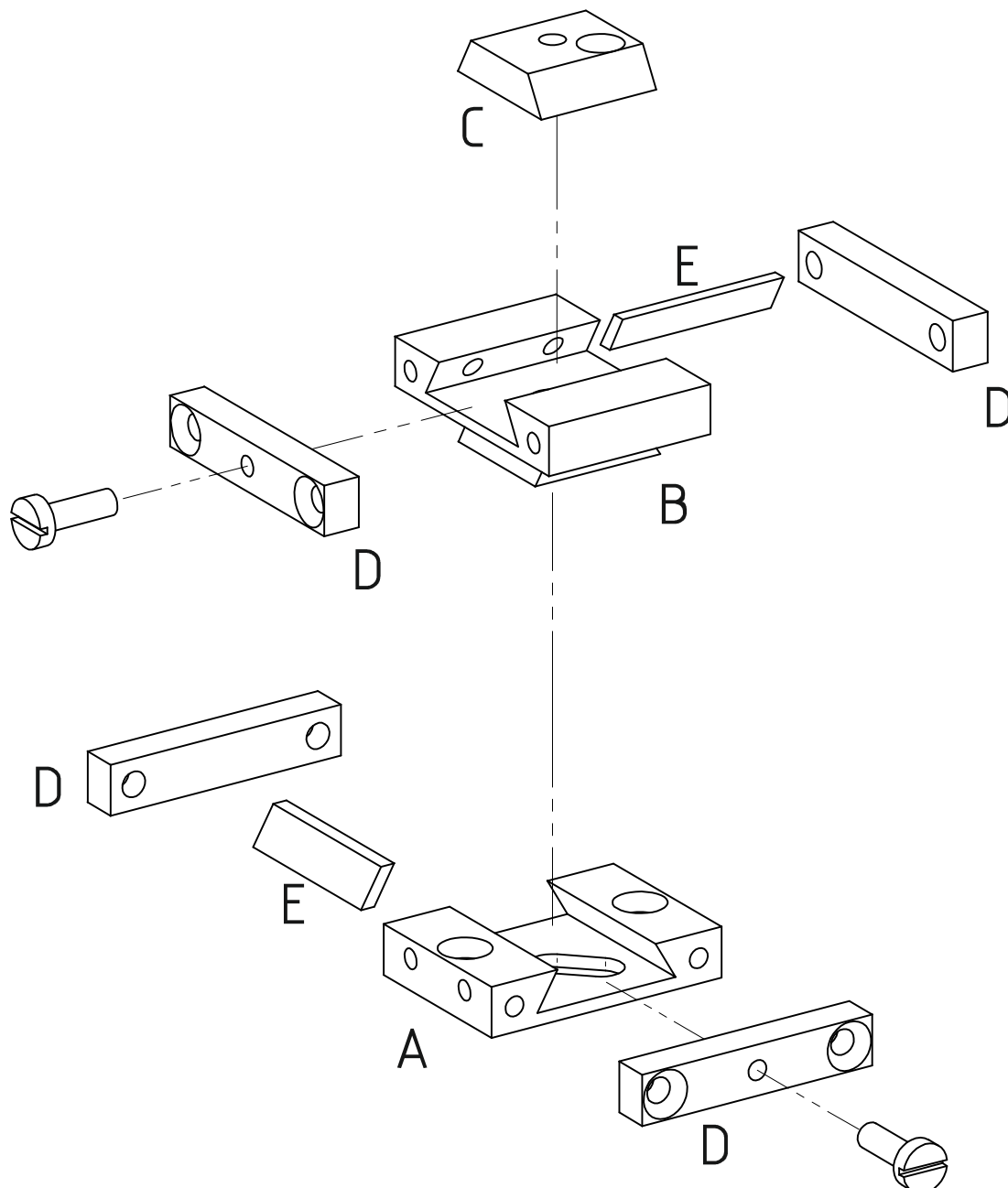
- 64 Hofinger ESA, Bernhardt G, Buschauer A (2007) *Glycobiology* 17:963–971
- 65 Hofinger ESA, Hoechstetter J, Oetl M, Bernhardt G, Buschauer A (2008) *Glycoconj J* 25:101–109
- 66 Hascall VC, Laurent TC (1997) *Glycoforum*
(<http://www.glycoforum.gr.jp/science/hyaluronan/HA01/HA01E.html>)
- 67 Evans CJ, Karpel S (1985) *Organotin compounds in modern technology*, Elsevier
- 68 Hoch M (2001) *Appl Geochem* 16:719–743
- 69 Craig PJ (2003) *Organometallic compounds in the environment*, J. Wiley
- 70 Fent K (1996) *Crit Rev Toxicol* 26:1–117
- 71 Fent K (2004) *Toxicology* 205:223–240
- 72 Feldmann J, Krupp EM (2001) *Anal Bioanal Chem* 399:1735–1741
- 73 Wei C, Li W, Zhang C, van Hulle M, Cornelis R, Zhang X (2003) *J Agric Food Chem* 51:5176–5182
- 74 Niegel C, Matysik FM (2010) *Anal Chim Acta* 657:83–99
- 75 Kennedy RT (1999) *Anal Chim Acta* 400:163–180
- 76 Landers JP (ed) (2008) *Capillary and microchip electrophoresis and associated microtechniques*. CRC Press, Raton CA
- 77 Garcia CD, Carrilho E (2010) *Instrumentation for CE and microchip-CE*. Wiley-VCH, Weinheim
- 78 Henry CS, Dressen BM (2008) in: Landers JP (ed) *Capillary and microchip electrophoresis and associated microtechniques*. CRC Press, Raton CA
- 79 Kitagawa F, Otsuka K (2011) *J Pharmaceut Biomed* 55:668–678
- 80 Jankowski JA, Tracht S, Sweedler JV (1995) *Trends Anal Chem* 14:170–176
- 81 Kennedy RT, Watson CJ, Haskins WE, Powell DH, Strecker RE (2002) *Curr Opin Chem Biol* 6:659–665
- 82 Perry M, Li Q, Kennedy RT (2009) *Anal Chim Acta* 653:1–22
- 83 Hogan BL, Lunte SM, Stobaugh JF, Lunte CE (1994) *Anal Chem* 66:596–602
- 84 Bowser MT, Kennedy RT (2001) *Electrophoresis* 22:3668–3676

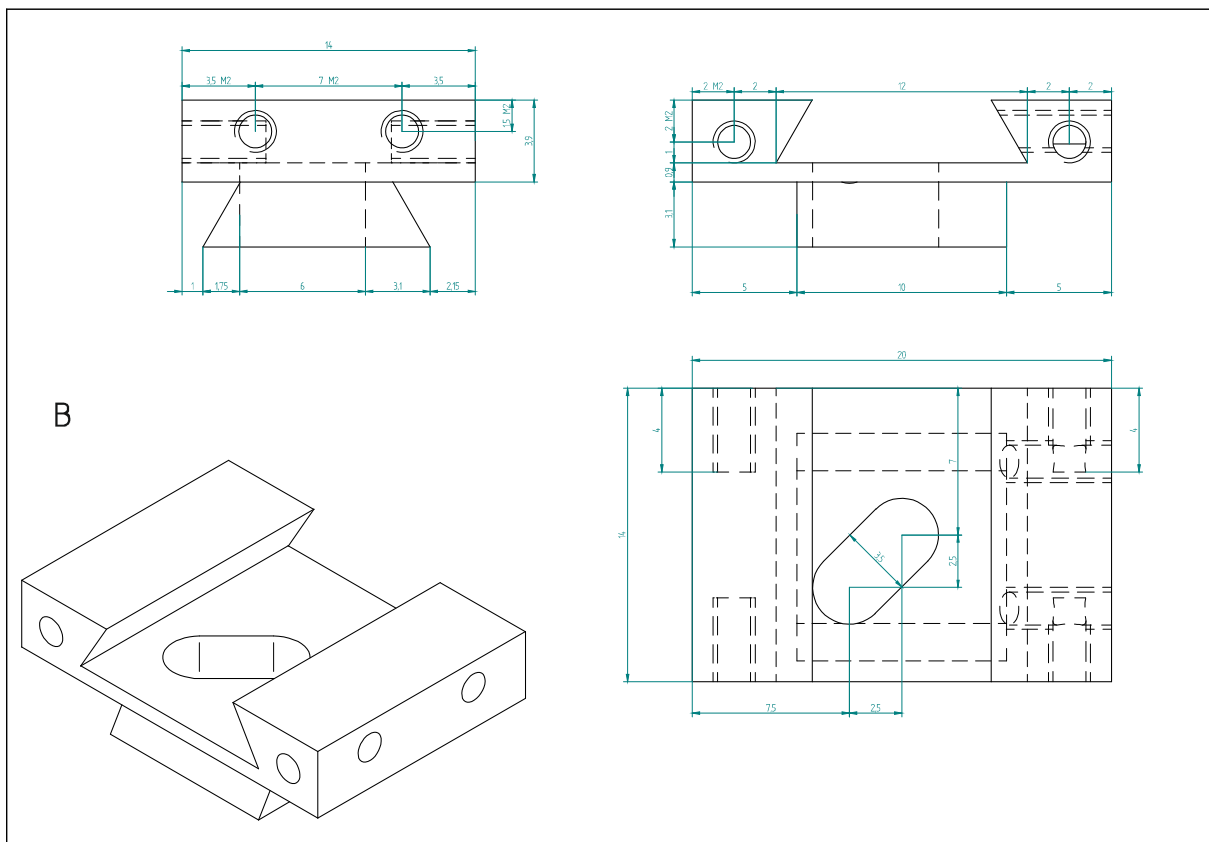
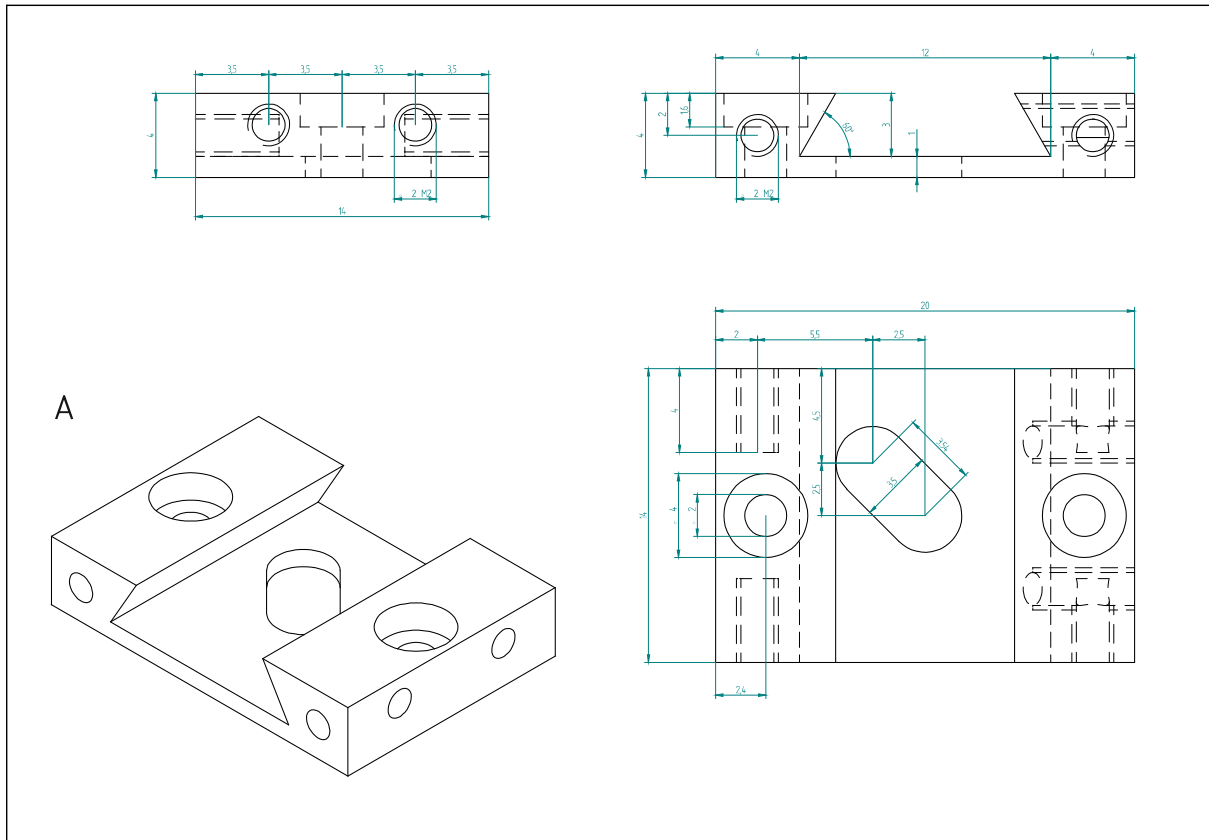
- 85 Lapainis T, Sweedler JV (2008) *J Chromatogr A* 1184:144–158
- 86 Coursey JS, Schwab DJ, and Dragoset RA (2003) *Atomic Weights and Isotopic Compositions* (version 2.3.1). [Online] Available: <http://physics.nist.gov/Comp> [2004, February 26]. National Institute of Standards and Technology, Gaithersburg, MD.
- 87 Fecher P, Schuffenhauer C (2003) Poster presentation, GDCh Jahrestagung Chemie 2003, Munich
- 88 Reissig JL, Strominger JL, Leloir LF (1955) *J Biol Chem* 217:959–966
- 89 Muckenschnabel I, Bernhardt G, Spruss T, Dietl B, Buschauer A (1998) *Cancer Lett* 131:13–20
- 90 Mokaddem M, Gareil P, Belgaied JE, Varenne A (2008) *Electrophoresis* 29:1957–1964
- 91 Matysik F, Werner G (1993) *Analyst* 118:1523–1526
- 92 Pittman JL, Schrum KF, Gilman SD (2001) *Analyst* 126:1240–1247
- 93 König S, Fales HM (1999) *J Am Soc Mass Spectrom* 10:273–276
- 94 Ohnesorge J, Neusüß C, Wätzig H (2005) *Electrophoresis* 26:3973–3987
- 95 Smith AD, Moini M (2001) *Anal Chem* 73:240–246
- 96 Kirby DP, Thorne JM, Götzinger WK, Karger BL (1996) *Anal Chem* 68:4451–4457
- 97 Mokaddem M, Gareil P, Belgaied JE, Varenne A (2009) *Electrophoresis* 30:1692–1697
- 98 Corradini D, Spreccacenero L (2003) *Chromatographia* 58:587–596
- 99 Vuorensola K, Sirén H, Kostianen R, Kotiaho T (2002) *J Chromatogr A* 979:179–189
- 100 Peterson ZD, Collins DC, Bowerbank CR, Lee ML, Graves SW (2002) *J Chromatogr B* 776:221–229
- 101 Charles L (2003) *Rapid Commun Mass Spectrom* 17:1383–1388
- 102 Enke CG (1997) *Anal Chem* 69:4885–4893

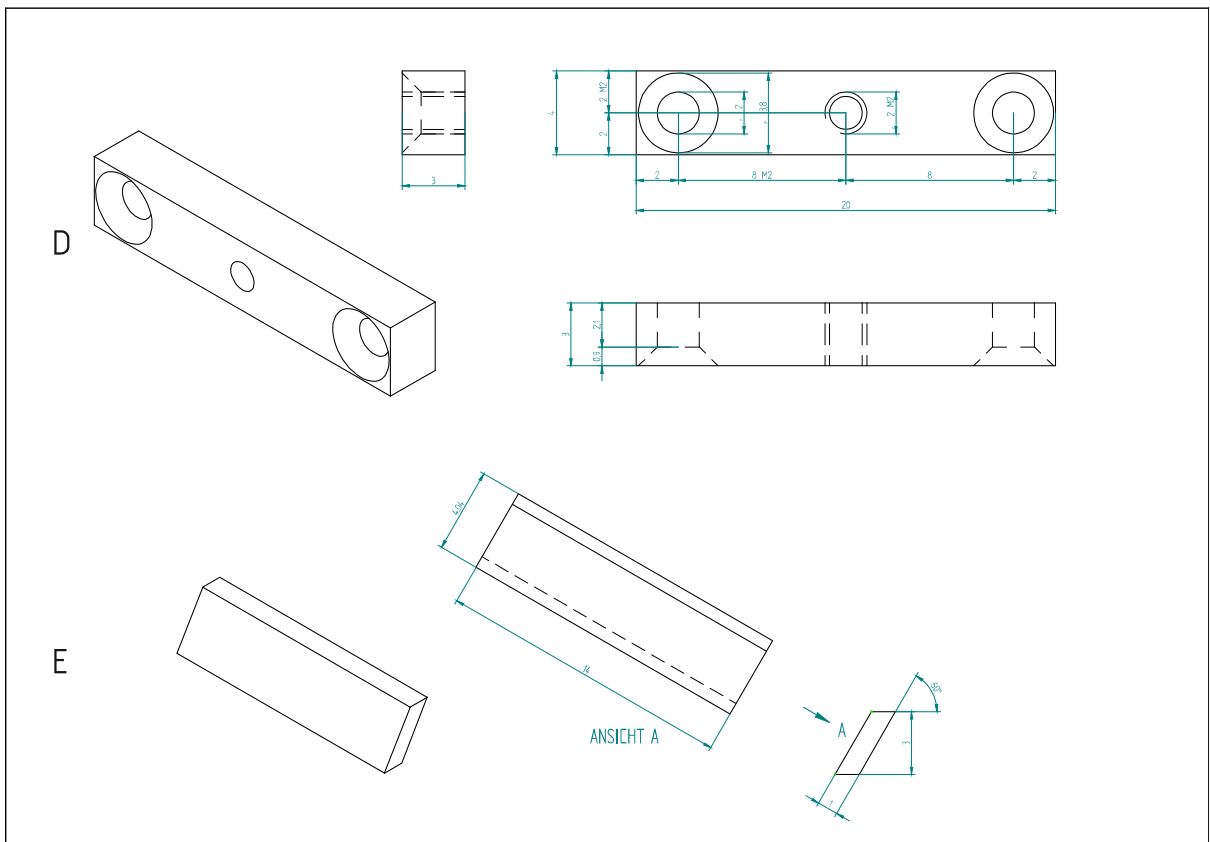
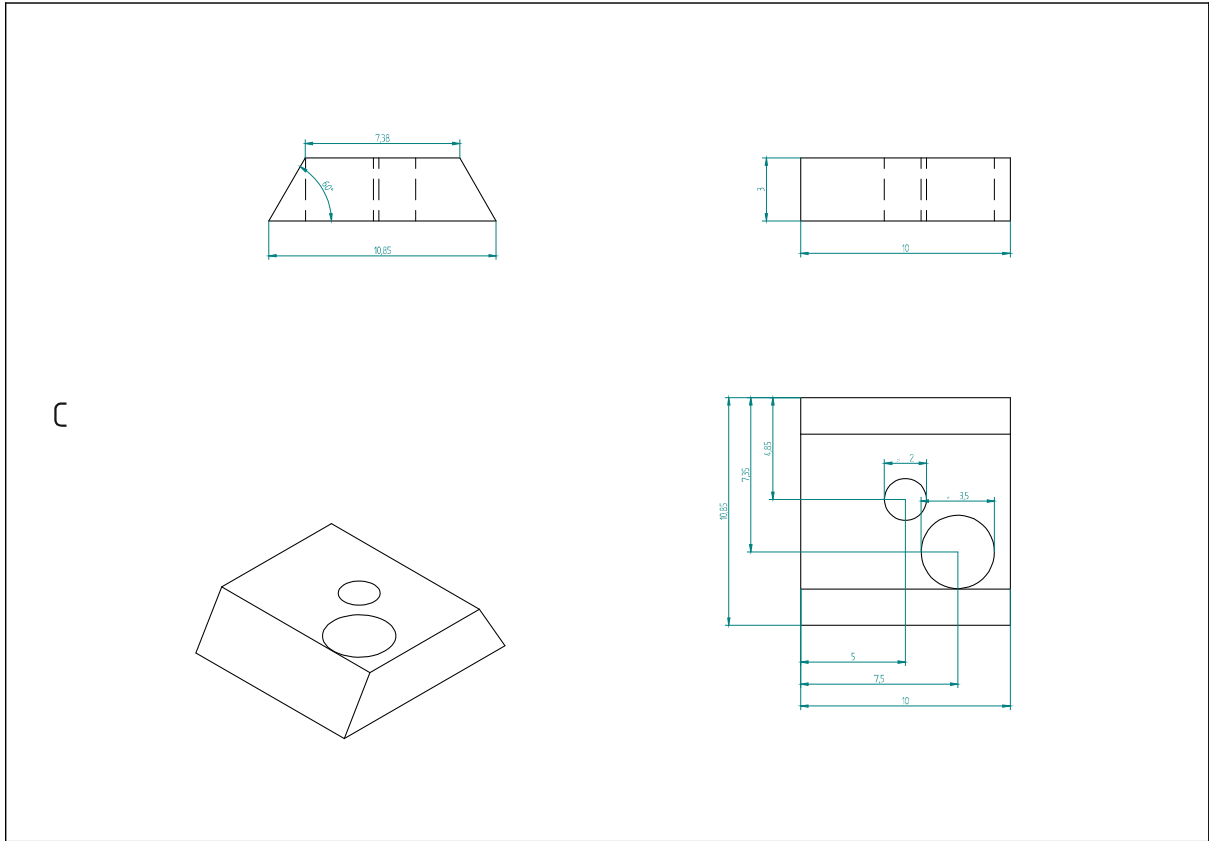
9.1.2 x,y-Positioner

Capillary alignment in CBI required a micropositioning device on top of the injection cell. It had to be of low profile in order to minimise the injection capillary's vertical movement. It was therefore undesirable to use a stack of two single-axis positioning devices. Instead, an integrated x,y-positioner was designed.

Since the positioner was located in close vicinity to the high voltage electrode, all components had to be fabricated from non-metallic materials. PEEK was chosen for all parts except the screws, which were made from nylon.







9.2 Complex Hyaluronan Sample

Raw data (this page) as well as raw data with the identified signals overlaid (next page) in addition to Fig. 32 (pg. 64). Darker colours indicate higher signal intensity. Picture contrast and brightness levels have been adjusted in order to visualise as many signals as possible. Therefore, signal colours can only be correlated to relative, not absolute, signal intensities.

